Alma Mater Studiorum – Università di Bologna

Dottorato di Ricerca in Oncologia, Ematologia e Patologia

Ciclo XXXII

Settore Concorsuale: MALATTIE DEL SANGUE ONCOLOGIA E REUMATOLOGIA

Settore Scientifico disciplinare: MED 15/ MALATTIE DEL SANGUE

SETD2 loss of function as a new marker of advanced disease in systemic mastocytosis: biological and clinical implications

Presentata da: Dott.ssa Michela Rondoni

Coordinatore Dottorato

Chiar. Mo Prof. Pier-Luigi Lollini

Supervisore

Dr. ssa Simona Soverini

Esame finale anno 2020

INDEX

1. ABSTRACT

This project stems from the results of a whole exome sequencing analysis of a rare case with a progressive, KIT mutation-negative form of advanced systemic mastocytosis (SM) termed mast cell leukemia (MCL), that identified biallelic inactivating mutations of the SETD2 gene. SETD2 encodes a histone methyltransferase responsible for trimethylation of histone H3 at lysine 36 (H3K36) and is a tumor suppressor whose loss of function is implicated in solid tumors and acute leukemias, but previously unreported in SM. We thus moved to investigate 1) the prevalence, the underlying mechanisms, the pathogenetic role and the 'druggability' of SETD2 loss of function in SM, and 2) its clinical relevance. Screening of a validation cohort of 57 patients with various forms of SM for H3K36 trimethylation levels as a surrogate marker for SETD2 loss of function by Western Blotting showed that H3K36 trimethylation is reduced or absent in all cases with SM. Median SETD2 and H3K36 trimethylation levels resulted to be significantly lower in neoplastic mast cells of patients with advanced SM as compared to patients with indolent SM. Thus, SETD2 impaired/loss of function can be considered a general phenomenon in SM, with the extent of SETD2 down-modulation and H3K36 trimethylation deficiency correlating with the aggressiveness of the disease. Interestingly, we uncovered that in the great majority of SM patients, SETD2 loss of function is accomplished via a novel post-translational mechanism of hyperubiquitination and enhanced degradation of the protein, and that inhibition of proteasome-mediated degradation is able to rescue SETD2 expression and function. We identified MDM2 as the major ubiquitin E3 ligase responsible for SETD2 hyperubiquitination, and demonstrated that phosphorylation by Aurora kinase A is the main trigger. We also found that SETD2 loss of function disrupts the p53 checkpoint and correlates with increased DNA damage as a result of reduced recognition of double strand breaks by the homologous recombination machinery. We then tested *in vitro* in cell

lines and primary patient cells novel therapeutic approaches aimed to revert SETD2 non genomic loss of function: the proteasome inhibitor bortezomib; the MDM2 inhibitor SP-141; the Aurora kinase inhibitor danusertib. We also found that the clinical activity of midostaurin (a multi-target kinase inhibitor recently approved for the treatment of advanced SM) relies not only in KIT tyrosine kinase inhibition, but also in the partial inhibition of Aurora A, and that SETD2 loss of function may serve as a biomarker of response to midostaurin. Finally, we investigated the clinical significance of SETD2 loss of function in a cohort of 88 patients with various forms of SM assessing the prognostic value of SET2 and H3K36 trimethylation levels in the context of other relevant clinical and laboratory variables, and found that reduced SETD2 and H3K36 trimethylation levels significantly correlate with shorter overall survival.

2. INTRODUCTION

2.1 Systemic mastocytosis

Mastocytosis results from a clonal proliferation of morphologically and immunophenotypically abnormal mast cells. For many years, mastocytosis was believed to be a disease of the skin. A first description of the typical (pigmented) skin lesions was provided by Nettleship and Tay in 1869. A few years later, the term urticaria pigmentosa was coined, and following Paul Ehrlich's description of MCs in 1879, the presence and accumulation of MCs in urticaria pigmentosa lesions was recognized by Unna in 1887. However, in 1949, Ellis described a first case of systemic mastocytosis. Over time since this observation, systemic mastocytosis has become a well-recognized diagnostic entity, although other patients were found to have urticaria pigmentosa without systemic involvement[1].

Normal MCs play an important role in the regulation of immunoglobulin E (IgE)–mediated allergic responses, inflammation, and the innate and adaptive immune responses to infection[1]. Abnormal activation and accumulation of MCs can lead to mediator symptoms and organ damage. Following activation and degranulation, mast cells secrete and generate a host of mediators that contribute to allergic inflammation. The disease manifestations exhibited in mastocytosis are a consequence of increased mast cells present in tissue and the degree of release of mast cell mediators. The clinical features associated with mast cell mediators are pruritus, flushing, urticaria,fatigue, weight loss, cachexia, hypotension, swelling, gastritis, intestinal cramping, osteoporosis, bronchoconstriction. Mast cell mediator release causes both local tissue and distal inflammation as they are released into the bloodstream. Clinically, the most significant mediator is histamine but also prostaglandin D2 and leukotriene C4, interleukin-3 (IL-3), IL-16 and tissue necrosis factor-α (TNF-α)[2]. The clinical presentation is heterogeneous, ranging from skin-limited disease

(cutaneous mastocytosis [CM]), particularly in children, to varying degrees of extracutaneous involvement (systemic mastocytosis [SM]), generally seen in adults[1]. The World Health Organization (WHO) included Mastocytosis from 2008, and recognizes several SM variants[3]. Indolent SM (ISM) is predominantly characterized by symptoms related to mast cell degranulation/mediator release and/or allergies or anaphylaxis[3,4]. In contrast, advanced mastocytosis variants (aggressive SM, mast cell leukemia and SM with associated hematologic neoplasm) are characterized by organ dysfunction related to mast cell infiltration[4,5]. Some mastocytosis patients present concurrently with, or subsequently develop, an associated clonal hematological non mast cell lineage disease, generally a myeloid neoplasm[6]. Most adult mastocytosis patients, regardless of disease subtype, harbor the KITD816V mutation, which has pathogenetic and diagnostic relevance[3].

2.1.1 Epidemiology of Systemic mastocytosis

A prevalence of mastocytosis of 1 in 10000 inhabitants has been reported, but underdiagnosis is assumed.

There were no epidemiologic studies defining the precise incidence, point prevalence, or cumulative prevalence of mastocytosis in the general population until the last two decades. In fact firm criteria for the diagnosis of mastocytosis have only been defined in 2001 and after this diagnosis has become more recognized[7,8]. The European Competence Network on Mastocytosis (ECNM) attempts to ensure a good quality of diagnosis by defining reference and excellence centres for mastocytosis. When the number of patients in several competence centres were analyzed, a steep increase in the number of SM patients was noted from 1998 to 2010, which is very likely the result of increased experience and recognition of the disease in this area during

these years. At the consensus meeting of mastocytosis experts in Boston 2010, a general cumulative prevalence of approximately 1 in 10,000 persons was estimated[8,9].

Mastocytosis can occur in children and adults. Although mastocytosis can occur at any age, the onset of mastocytosis is in the first 2 years of life in 50% or more of cases. In adults, most patients are diagnosed in middle age between 20 and 50 years of age[10]. Because of a chronic nature and low regression rate of adult-age mastocytosis the cumulative prevalence of adult patients of mastocytosis rises with age. Gender distribution is approximately equal[11].

2.1.2 Classification of Systemic mastocytosis

The first attempt to classify the mastocytoses was made in 1979 by the pathologists Lennert and Parwaresch of Kiel, Germany[12]. After various modifications, in 2000 an international group of experts agreed on the categorization that was then adopted by the WHO in 2001[8].

The updated WHO classification of 2016 divides cutaneous mastocytosis into maculopapular cutaneous mastocytosis (MPCM), also known as urticaria pigmentosa, diffuse cutaneous mastocytosis (DCM), and localized mastocytoma of skin. Specific criteria of cutaneous mastocytosis have been defined and published by the consensus group[13-15]. Most patients with cutaneous mastocytosis are children. In contrast, in most adult patients, systemic mastocytosis is detected. The major criterion of systemic mastocytosis is the multifocal accumulation and clustering of MCs (at least 15/ cluster) in the bone marrow or another extra-cutaneous organ[7,8,13,14]. Minor systemic mastocytosis criteria confirm the clonal (neoplastic) nature of the disease and include an abnormal MC morphology (spindling), expression of CD2 and/or CD25 in MCs in extracutaneous organs, expression of an activating mutation in codon 816 of KIT (usually

KIT D816V) in extra-cutaneous cells, and a basal serum tryptase level exceeding 20 ng/mL (Table 1).

Major and Minor WHO Criteria of Systemic Mastocytosis (SM criteria)*

Major criterion:	Multifocal dense infiltrates of mast cells (>15 mast cells in aggregates) in bone marrow biopsies and/or in sections of other extracutaneous organ(s)
Minor criteria:	
	a. >25% of all mast cells are atypical cells (type I or type II) on bone marrow smears or are spindle-shaped in mast cell infiltrates detected on sections of visceral organs
	b. *KIT* point mutation at codon 816 in the bone marrow or another extracutaneous organ
	c. Mast cells in bone marrow or blood or another extracutaneous organ expresses CD2 or/and CD25
	d. Baseline serum tryptase concentration >20 ng/ml (in case of an unrelated myeloid neoplasm, d. is not valid as an SM criterion)

If at least one major and one minor or three minor criteria are fulfilled
→ the diagnosis is systemic mastocytosis = SM

*SM criteria have been defined by the WHO in 2001 and confirmed in 2008 and 2016.

Table 1. *Diagnostic criteria for Systemic mastocytosis (SM)*

Systemic mastocytosis is further divided into indolent systemic mastocytosis (ISM), smoldering systemic mastocytosis (SSM), systemic mastocytosis with an associated hematologic (non-MC-lineage) neoplasm (SM-AHN), aggressive systemic mastocytosis (ASM), and MC leukemia (MCL) [16,17]. The provisional variant termed isolated bone marrow mastocytosis (BMM) have been described where the disease is essentially restricted to the bone marrow and the tryptase level is low or normal[18,19].

The extent of organ infiltration and subsequent organ damage serve as a basis for the WHO classification of SM as indolent SM or advanced SM (AdvSM). Diagnosis of SSM requires two or more “B” findings, that include BM biopsy showing >30% mast cell infiltration and/or serum tryptase >200 ng/mL; signs of dysplasia or myeloproliferation in non-mast cell lineages with normal blood counts; hepatomegaly without impairment of liver function, and/or splenomegaly without hypersplenism, and/or lymphadenopathy on palpation or imaging. On the other hand, ASM is defined by the presence of at least one “C”-finding, such as: one or more cytopenia(s) in absence of non-mast cell hematopoietic malignancy; hepatomegaly with impairment of liver function; splenomegaly with hypersplenism; malabsorption with weight loss due to gastrointestinal mast cell infiltrates; large osteolytic lesions and/or pathological fractures[20].

A distinct entity that does not belong to the SM is the Monoclonal mast cell activation syndrome (MMAS), that is described in patients with anaphylaxis and clonal mast cells expressing the D816V mutation in KIT and expressing the a-chain of the interleukin-2 receptor CD25, but without the full set of criteria needed to diagnose mastocytosis[21]. The frequency of MMAS varies among different study groups between 6% and 27%.

Cutaneous mastocytosis (CM)
- Maculopapular CM (MPCM) = urticaria pigmentosa (UP)
- Diffuse CM (DCM)
- Mastocytoma of skin
Systemic mastocytosis (SM)
- Indolent SM (ISM)
- Smoldering SM (SSM)
- SM with associated hematologic neoplasm (AHN)[a]
- Aggressive SM (ASM)
- Mast cell leukemia (MCL)
Mast cell sarcoma (MCS)

[a]The previous term SM-AHNMD (systemic mastocytosis with clonal hematologic non-mast cell–lineage disease) and the new term AHN can be used synonymously.

Table 2. *WHO classification of Mast Cell Disease*

2.1.3 Prognosis of disease and new prognostic score

The life expectancy of patients affected by SM, when considered as a group, appears to be shorter as compared to age-matched and gender-matched controls, with the excess deaths in this group occurring within the first 3-5 years after diagnosis (Figure 1)[22]. The WHO classification is most widely used for prognostication and has been validated in multiple studies: although indolent mastocytosis is generally not fatal, other forms (e.g. MCL and ASM) usually have a rapidly devastating outcome.

It is commonly believed that most patients with initial ISM had a normal life expectancy. This is derived from data published in 2009 from Mayo Clinic, where in a retrospective study of 342 consecutive adult patients with SM seen between 1976 and 2007, 159 patients were indolent (46%)(Figure 1)[22].

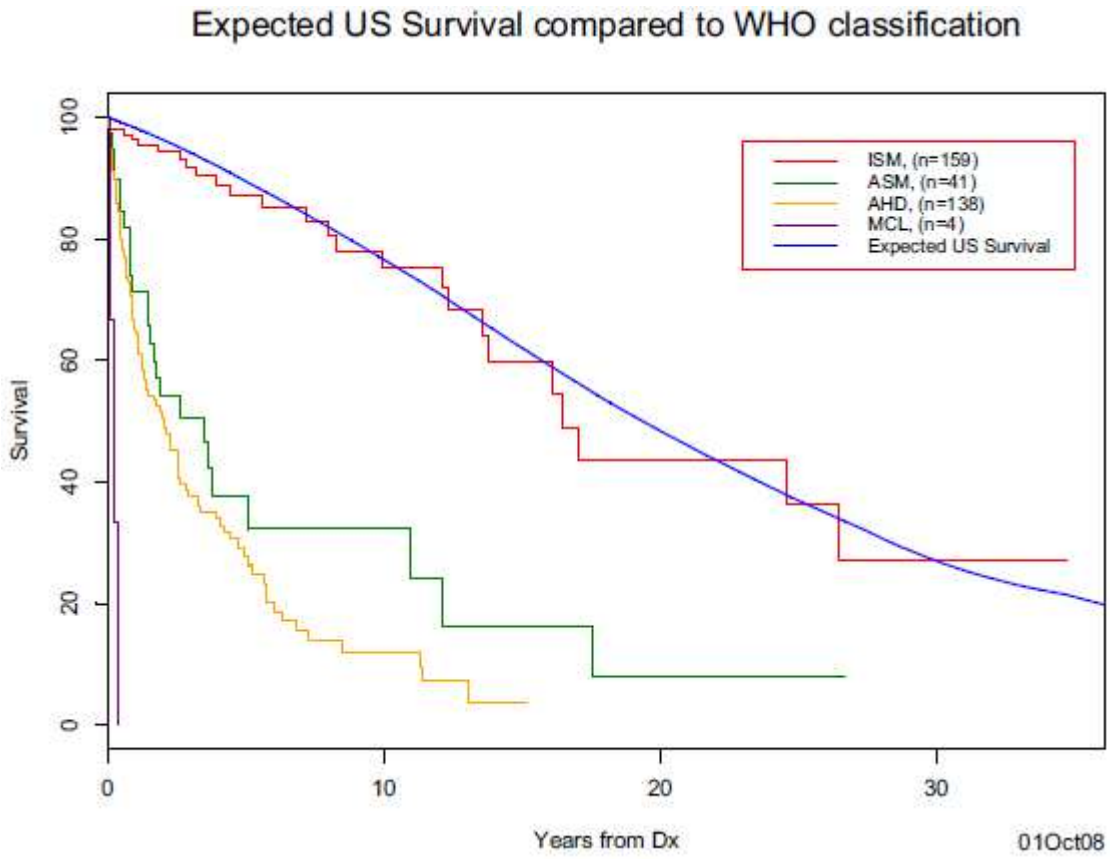

Figure 1. *Survival of systemic mastocytosis patients in the retrospective analysis of Mayo Clinic(1976-2007)*

The prognosis of patients with adult ISM has been studied in a long-term follow-up of 145 consecutive adult patients observed for a median of 147 months by the Spanish group of REMA[23]. The results show that the disease was stable in most patients. There were signs for biologic progression indicating an increased proliferation of mast cells, such as an increase in serum tryptase greater than 200 ng/mL, osteoporosis, or organomegalies in 27% of patients. Only five patients (3%) showed progression from ISM to a more advanced form of SM, and a cumulative probability of disease progression in ISM of 1.7% in 10 years. The REMA group have recently updated the case studies and reported 14 of 200 ISM patients that has progressed after a median follow-up of 9 years[24]. They investigated the frequency and prognostic impact of variants in 18 genes, found to be altered in advSM, and detected genetic variants in 55 of 322 (17%) patients.

Mutated ISM cases, particularly those carrying ASXL1, RUNX1, and/or DNMT3A (A/R/D) with a high variant allele frequencies (VAFs) ≥30%, exhibited significantly shortened progression-free survival (PFS) and overall survival (OS). Multivariate analysis showed that serum b2-microglobulin levels > 2.5 mg/mL, together with a KIT D816V VAF ≥1% in bone marrow and pathogenic variants of A/R/D, were the best combination of independent predictors for PFS. Based on these variables, 2 scoring systems were constructed for risk stratification of ISM at diagnosis with significantly different 10-year PFS (100%, 91%, 0% for scores of 0, 1, ≥2, respectively) and OS (100% and 50% for scores of 0 and 1) rates[24]. The authors suggest that multilinear KIT, together with mutations in genes other than KIT, might provide the genetic background required for disease progression and death but the data are still limited about the frequency and potential prognostic impact of mutations in genes other than KIT in ISM.

Several prognostic scoring system have been recently proposed to improve risk stratification in advSM[25-28]. Clinical and genetic informations have been combined. The somatic mutations in addition to KIT D816V (eg, in ASXL1, CBL, JAK2, RUNX1, SRSF2, EZH2 or TET2), being present in more than 60% of patients with AdvSM have been included in the molecular characterization of patients.

In the study of Jawhar et al. a spleen volume > 450 mL on magnetic resonance imaging and an elevated level of serum alkaline phosphatase (AP) were both associated with inferior survival in a multivariate analysis[25]. In this series of 108 patients with indolent (n = 41) and advanced systemic mastocytosis (advSM, n = 67) they distinguished a 3-year OS of 100, 77, and 39%, respectively (P<0.0001), for patients with 0 (low risk, n = 37), 1 (intermediate risk, n = 32) or 2 (high risk, n = 39) parameters. For advSM patients with fully available clinical and molecular data (n = 60), univariate analysis identified splenomegaly ≥ 1200 ml, elevated AP and mutations in the SRSF2/ASXL1/RUNX1

(S/A/R) gene panel as significant prognostic markers. In multivariate analysis, mutations in S/A/R and elevated AP remained predictive adverse prognostic markers for OS. The 3-year OS was 76 and 38%, respectively (P = 0.0003), for patients with 0–1 (intermediate risk, n = 28) or 2 (high risk, n = 32) parameters[25].

The MARS score combined clinical and molecular parameters in a study that included 383 patients with AdvSM: in multivariable analysis, the risk factors identified as being associated with OS were age greater than 60 years, anemia (hemoglobin , 10 g/dL), thrombocytopenia (platelets , 100 > 10^9/L), presence of one high molecular risk gene mutation (SRSF2, ASXL1, and/or RUNX1), and presence of two or more high molecular risk gene mutations. By assigning hazard ratio–weighted points to these variables, the following three risk categories were defined: low risk (median OS, not reached), intermediate risk (median OS, 3.9 years; 95% CI, 2.1 to 5.7 years), and high risk (median OS, 1.9 years; 95% CI, 1.3 to 2.6 years; P <001). The mutation-adjusted risk score (MARS) was independent of the WHO classification and was confirmed in the independent validation set. During a median follow-up time of 2.2 years (range, 0 to 23 years), 63 (16%) of 383 patients experienced a leukemic transformation to secondary mast cell leukemia (32%) or secondary acute myeloid leukemia (68%)[26-27].

The Mayo prognostic score was elaborated on the total of the 580 patients seen at the Mayo Clinic between 1968 and 2015 combining the clinical and genetic characteristics (diagnosis of SM was per WHO criteria, karyotype and next-generation sequencing data were available in a subset of patients) of the patients with SM. Multivariable analysis of clinical variables identified age >60 years, advanced SM, thrombocytopenia <150 x 10^9/L, anemia below sex-adjusted normal, and increased alkaline phosphatase (AP) as independent risk factors for survival. In addition, ASXL1, RUNX1, and NRAS mutations were independently associated with inferior survival[28].

To date, the independent prognostic value of most variables and proposed risk scores has been derived from relatively small sets of patients, and they have not been confirmed or validated.

2.2 Advanced Systemic Mastocytosis

AdvSM includes patients with SM and an associated hematologic neoplasm (SM-AHN), aggressive SM (ASM), and mast cell leukemia (MCL)[7,29-31]. In contrast to indolent SM, AdvSM has a poor prognosis[32]. The overall survival (OS) of patients with AdvSM ranges from a few months to several years, with a median OS of approximately 4 years[33].

2.2.1 Aggressive Systemic Mastocytosis

ASM was the third most common subgroup (n = 41; 12%) in series of Lim et al[22]. In ASM , organ systems typically involved with C-findings are the BM, with severe anemia (Hb <10 g/dL; 24%) or thrombocytopenia(platelets $<100\times10^9$/L; 27%), liver (hepatomegaly, ascites, increased liver enzymes), spleen (50%), bones (osteolysis, pathologic fractures), and the gastrointestinal tract (malabsorption, weight loss). Patients frequently displayed constitutional symptoms (60%), lymphadenopathy (30%) and markedly elevated serum tryptase levels (>200 ng/mL; 40%)[34]. An important aspect of ASM is that the disease can presents as slowly progressing ASM (similar to SSM but with C-findings) or rapidly progressing ASM. Overall median survival in ASM was 41 months[31].

2.2.2 Systemic Mastocytosis with an Associated Hematologica Neoplasia (SM-AHN)

SM-AHN (70% to 80% of all patients with AdvSM) is the most heterogeneous and clinically challenging subtype of AdvSM. The AHN usually resembles a myeloid neoplasm (eg, chronic myelomonocytic leukemia, myelodysplastic/myeloproliferative neoplasm unclassifiable, chronic eosinophilic leukemia, or myelodysplastic syndrome). Histopathologic evaluation of SM-AHN merits special consideration because of its associated diagnostic complexity and potential impact. In the Mayo series, the median OS of SM-AHN patients was 2 years[22]. Although the prognosis of SM-AHN frequently relates to the AHN component, marked heterogeneity in outcomes exists between AHN subtypes (ie, average survivals of 31, 15, and 13 months for SM-MPN, SM-CMML, and SM-MDS, respectively)[22-35].

In the vast majority of patients, the phenotypically most important somatic mutation (ie, KIT D816V) is detectable in the clonal mast cell compartment and in cells derived from the AHN[36,37].

2.2.3 Mast cell leukemia

Mast cell leukemia (MCL) is a rare form of systemic mastocytosis characterized by leukemic expansion of mostly immature mast cells, organ damage, drug-resistance, and a poor prognosis. In a recent retrospective analysis a median OS survival of 9.4 moths is reported, with 42.9% of patients alive at 12 months, 23.2 patients alive at 36 months and 16.% alive at 5 years. These data are very different from what was thought before, maybe influenced by the therapies[38]. In the series of Mayo Clinic of 2009 the median OS for MCL was < 4 months[22].

In patients with MCL, KIT mutations are detected less frequently then in the other forms. Here neoplastic MCs display KIT D816V in only 50-70% of the cases. In the remaining MCL cases, other KIT mutations or no KIT mutations are found. in most patients with MCL, most MCs in BM smears are immature, tryptase level is quite low, and more frequently the skin is undamaged. The cell

surface phenotype of MCs in MCL is quite similar when compared to the cell surface membrane phenotype of MCs in other variants of SM. The new entity of Chronic Mast cell leukemia has been proposed by Valent, characterized by relatively long survival and specific morphological features (a majority of all MCs have a more mature morphology)[39].

2.2.4 Therapy of AdvSM

Therapeutic options for patients with newly diagnosed ASM, SM-AHN, and MCL are represented today by Midostaurin, Cladribine, Interferon and Allogeneic hematopoietic stem cell transplantation[40]. Clinical trials are ongoing with Avapritinib, a KIT and PDGFRα inhibitor specifically designed to inhibit KITD816V. Early results from a Phase 1 trial suggest that avapritinib has potent antineoplastic activity in AdvSM, extending to patients who failed midostaurin, and clinical trials are ongoing in several centers. Midostaurin has been approved for all 3 AdvSM subtypes, irrespective of KIT mutation status in 2017 by Food and Drug Administration and in 2018 by European Medicines Agency. For patients with SM-AHN, a determination must first be made regarding whether treatment is needed and which component requires more immediate therapy (the SM component or the AHN). Cladribine and [pegylated]–interferon-a with or without prednisone have been used on an off-label basis for all 3 advSM variants; Cladribine (2-chlorodeoxyadenosine [2-CdA]) is a synthetic purine analog cytoreductive treatment, whose efficacy is mostly reported in advanced SM. Standard administration consists of 5 days of 0.14 mg/kg infusion or subcutaneous administration, repeated until 9 courses. The reported overall response rate was 72%, with clinical improvement in mediator release, mast cell infiltration (including urticaria pigmentosa) and serum tryptase levels decrease. It is preferred in patients requiring rapid debulking of disease, whereas interferons are preferred in slow progressors[34].

Imatinib is approved for the rare ASM patients who are KIT D816V mutation negative or whose KIT mutation status is unknown. For patients with eosinophilia, rule out FIP1L1-PDGFRA positivity, because such neoplasms are very sensitive to imatinib. Allogeneic hematopoietic stem cell transplantation (HSCT) may be considered as initial therapy for ASM or SM-AHN. Bone marrow transplantation is recommended as frontline treatment of MCL, but it may be considered for individuals achieving substantial clinical benefit with midostaurin, cladribine, or a clinical trial drug[31,42]. Multiagent chemotherapy as initial treatment of MCL is not recommended today. Corticosteroids may be used on a short-term basis for rapidly progressive SM-related organ damage. Symptom-directed treatment should be considered in all SM patients, also during cytoreductive therapy. Anti- mediator therapies for SM are directed at MC degranulationsymptoms (eg, pruritus, urticaria, angioedema, flushing, nausea, vomit-ing, abdominal pain, diarrhea, episodic anaphylactoid attacks), symptomatic skin disease (eg, urticaria pigmentosa) and/or osteope-nia/osteoporosis/pathologic fractures[31].

The most attractive therapy is Midostaurin, for its peculiar mechanism of action, that potently target activation loop mutants of KIT receptor, cementing the view that KITD816V represents the driver mutation for SM. Midostaurin was originally termed PKC412, and is a semi-synthetic derivative of the alkaloid staurosporine, a well-known inhibitor of PKC (Figure 2)[41]. Although initially considered a rather specific pharmacologic inhibitor of PKC, midostaurin interacts with a broad spectrum of clinically relevant kinase-targets, including KIT and other KIT mutants, FLT3, platelet-derived growth factor receptor alpha (PDGFRA), PDGFRB, vascular endothelial growth factor receptor KDR, and the Aurora kinasi A and B (Table 3)[41].

In the global Phase 2 CPKC412D2201 trial, 116 patients with advanced SM were enrolled; the primary efficacy population comprised of 89 patients (16 with ASM, 57 with SM-AHN, and 16 with

MCL); patients were treated with PKC412 at 100 mgBID[83]. The ORR per conventional criteria was 60% with 45% having a major response and 15% having a partial response. The response rate was 75% in ASM patients, 58% in SM-AHN patients and 50% in MCL patients. After a median follow up of 26 months (range 12-54), the median duration of response was not reached in ASM or MCL patients and was 12.7 months in SM-AHN patients. Responses occurred regardless of KITD816V status. The median OS for ASM, SM-AHN and MCL subgroups was not reached, 20.7 months and 9.4 months, respectively[43].

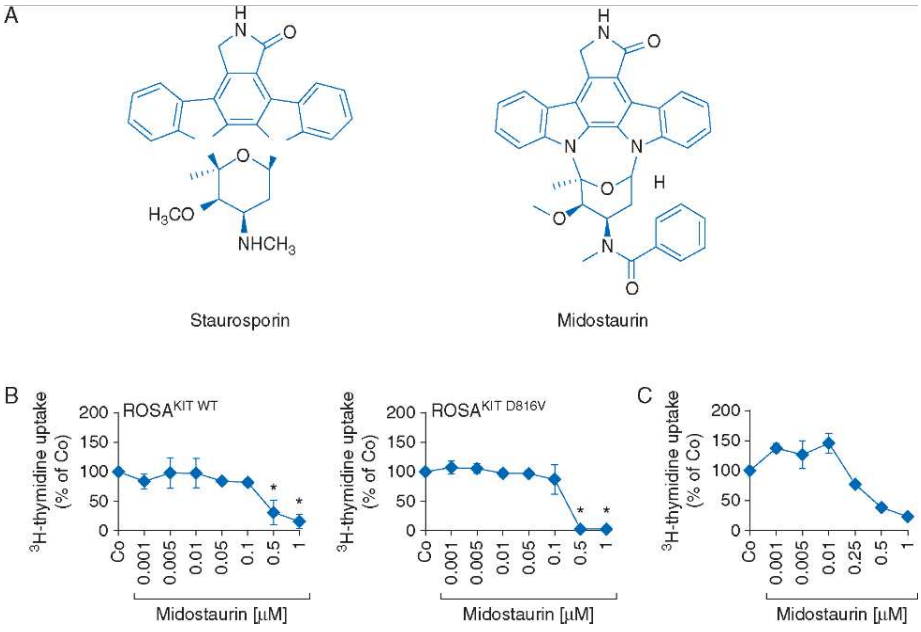

Figure 2. *Chemical structure and anti-neoplastic effects of midostaurin. (A) Chemical structure of staurosporin and its derivative midostaurin. (B) anti-neoplastic effects of midostaurin on the human mast cell lines ROSA$^{KIT\ WT}$ (left panel) and ROSA$^{KIT\ D816V}$ (right panel) (C) anti-neoplastic effects of midostaurin on primary mast cells of a patient with ASM.*

Molecular target[a]	Major target cell populations and disorders
KIT wt	Mast cells, AML blasts, GIST cells
KIT D816V	Mast cells in SM, AML blasts, GIST cells
KIT V560G	Mast cells in SM, GIST cells
KIT K509I	Mast cells in CM
FES	Mast cells in KIT D816V+ SM
	(KIT D816V-downstream-signaling)
FLT3 wt	Myeloid (progenitor) cells
FLT3 ITD	AML blasts
FLT3 D835H	AML blasts
FLT3 D835Y	AML blasts
FLT3 N841I	AML blasts
PDGFRA wt	Fibroblasts, mesenchymal stem cells
FIP1L1-PDGFRA (F/P)	Eosinophils, CEL, MPN-eo
F/P mutant forms	Eosinophils, CEL, MPN-eo
PDGFRB wt	Fibroblasts, mesenchymal stem cells
PDGFRB mutant forms	Eosinophils, CEL, MPN-eo
JAK2	Myeloid cells, MPN cells
JAK3	Various immune cells

Molecular target[a]	Major target cell populations and disorders
AAK1	Notch adaptor in neoplastic cells
SYK	IgE-R+ cells, IgE-R-downstream signaling
AURKA	Mitosis regulator in various neoplastic cells
AURKB	Mitosis regulator in various neoplastic cells
MARK3	Oncogenic molecule in hepatocellular cancer
PKN1	Wnt/β-catenin repressor in cancer cells
FGFR3	B cells, multiple myeloma cells
FGFR3 TDII (K650E)	B cell lymphoma cells, multiple myeloma cells
TEL-FGFR3	T cell lymphoma cells, MPN, AML blasts

Table 3. *Molecular targets of Midostaurin*

2.3 Genomic landscape of mastocytosis

The mechanisms involved in the development of mastocytosis are mainly unknown. The presence of gain-of-function mutations involving the tyrosine kinase domain of c-kit is used as diagnostic criteria, and activation of kinase pathways (i.e. D816V mutation of *KIT*) have previously been shown to be relevant for development of disease. In adult patients, the frequency of the D816V *KIT* mutation varies from 75% to virtually all cases. Mastocytosis may occur also in absence of mutations in the oncogene KIT, indicating that the molecular reasons behind this disease are variable, they do not depend on a single mutation or oncoprotein, and they could have both genetic and epigenetic basis. Further molecular knowledge are arising today, but given the heterogeneous clinical behavior it seems quite likely that more than one pathway are altered in

the disease and the identification of others genetic alterations or mechanisms concurring to disease presentation are warranted. Studies of gene expression profile have identified differentially expressed genes in patients affected by indolent systemic mastocytosis compared with healthy controls. They involve the ubiquitin-mediated proteolysis, MAPK signaling pathway, Jak-STAT signaling, and p53 signaling pathway, with influence on transcription, cell cycle, protein transport, and signal transduction[44]. The studies by Garcia-Montero showing that the *KIT* mutation is present not only in mast cells but also in myeloid and lymphoid cell lineages seems to be relevant to establish the prognosis of patients with indolent mastocytosis[45], with important implications on therapeutic approach to these patients.

2.3.1 c-kit

Molecular pathogenesis of mastocytosis involves acquisition of *c-KIT* mutations, particularly D816V, which is present in a majority of all patients with SM, irrespective of WHO SM subtype, including ISM, ASM, or MCL[24,46,47]. Type III RTKs consist of a glycosylated extra-cellular ligand-binding domain (ectodomain) connected to a cytoplasmic region by means of a single transmembrane helix. The cytoplasmic region of KIT is composed of an auto-inhibitory juxta-membrane region (JMR) and a protein tyrosine kinase (PTK) that is subdivided into proximal and distal lobes separated by an insert sequence of variable length (70–100 amino acids). In human KIT, the 77-amino acid kinase insert domain (KID) possesses phosphorylation sites and provides an interface for the recognition of pivotal signal transduction proteins. KIT is notably expressed by MC, hematopoietic progenitor cells, germ cells, melanocytes, and interstitial cells of Cajal in the gastrointestinal tract [48]. KIT expression is down regulated during differentiation of hematopoietic progenitors into mature cells of all lineages, but MCs retain high levels of cell surface KIT

expression. Binding of SCF to KIT leads to receptor dimerization, intermolecular auto-phosphorylation of specific tyrosine residues and PTK activation. The activation process involves a large rearrangement of the activation loop (A-loop, ,20–25 residues) of PTK. Conformational switch of A-loop from an inactive packed position to an active extended form releases access for Mg2+ -ATP and protein substrate(s) to the kinase catalytic site[49]. A variety of mutations of KIT were found in different types of human cancer, in gastrointestinal stromal tumors (GISTs), acute myeloid leukemia (AML), mast cell leukemia (MCL) and human germ cell tumors, among others and they induce the activation of tyrosine kinases. Longley et al. early proposed a classification of KIT gain-of-function mutations according to their structural and functional locations[50]. The JMR mutations, frequently found in GISTs, are considered regulatory as they disrupt the auto-inhibitory mechanism which negatively regulates the activity of the protein. The PTK mutations are considered catalytic as they directly affect the configuration of the enzymatic site probably by stabilizing the A-loop extended conformation. To this category belongs the mutation D816V found in mastocytosis, that also confer resistance to Imatinib treatment[51]. Other somatic KIT mutations were identified in adult SM, even if they are less common (<5%): D815K, D816Y, insVI815-816, D816F, D816H, and D820G. All these mutations mapped in exon 17 of KIT, that corresponds to the activation loop region; other point mutations, as V560G, are mapped in exon 8 or exon 9 of KIT, in the juxtamembrane region of the receptor. Mutations described primarily in pediatric cases with cutaneous mastocytosis (CM) are located in exon 7, 9 and exon 11 : C443Y, S451C, S476I, D572A and frequently the molecular alterations are represented in these cases by insertions, deletion and Internal Tandem duplication (ITD). (Figure 3)

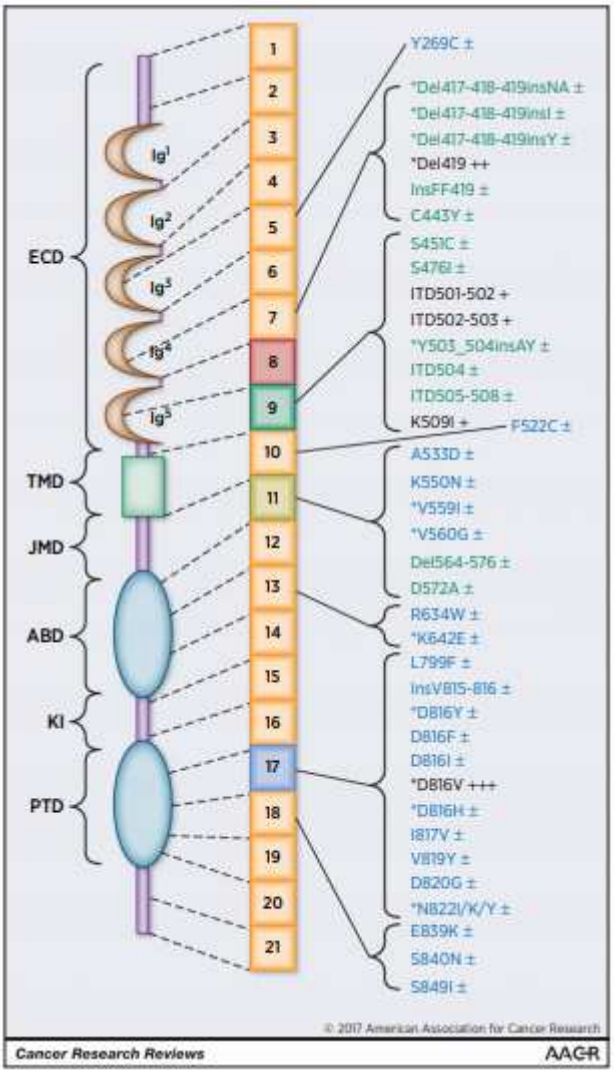

Figure 3. *Overview of KIT mutations described in patients with mastocytosis. ABD, ATP-binding domain; Del, deletion; ECD, extracellular domain; Ins, insertion; ITD, internal tandem duplication; JMD, juxtamembrane domain; KI, kinase insert; PTD, phosphotransferase domain; TMD, transmembrane domain. The asterisk denotes KIT mutations that have also been described in other neoplasms such as GIST, acute myeloid leukemia (AML), lymphomas, or seminomas.*

Several observations suggest that KIT D816V alone is not a fully transforming oncoprotein. While activating KIT mutations are frequently associated with human mastocytosis, they do not occur universally, and the different natural history of childhood- and adult-mastocytosis, with the former often exhibiting skin-limited disease that spontaneously regresses with age; in contrast, the latter

characterized by persistent multi-organ involvement, often with second non-MC hematologic neoplasm, should be related to different biological pattern, but experimental data with regard to this issue have not been conclusive[52].

2.3.2 Myeloid mutations

Schwaab et al. for the first time reported on the identification of a variety of additional mutations in 89% of patients with advanced KIT D816V positive SM. The most frequently affected genes were TET2, SRSF2, ASXL1, RUNX1 and CBL. (Blood, 2013)[53]. Subsequent studies addressed the issue of the presence of additional mutations, and their role as prognostic factors. Hence, recent studies based on relatively limited gene panels have shown that advanced forms of SM, including 177 of 284 SM-AHN cases, 28 of 284 ASM cases, and 8 of 284 MCL cases, often carry mutations in genes previously reported to be altered in other myeloid neoplasms, in addition to the KIT mutation[36,53-55]. However, relatively limited information exists about the frequency of mutations in those genes in diagnostic subtypes of SM other than SM-AHN (eg, ISM and smoldering SM in addition to ASM and MCL). Also, these mutations have been found in the other hematological neoplasm component of the disease but not always in the MC compartment[35]. In addition, it remains unknown whether the occurrence of such mutations in an early hematopoietic precursor would also confer a worse prognosis to SM patients, as demonstrated by Jawhar et al for SM-AHN cases and previously reported for KIT D816V[55].

2.4 Next generation sequencing technologies

Driven by incredibly rapid technological advances, medicine, genetics and molecular biology have indeed witnessed in recent years a deluge of new experimental methods for interrogating different properties of a cell on a genome-wide scale. Each technology offers a unique, although complementary, view of genome organization and cellular functions and therefore allows the identification of specific molecular alterations of tumor cells, such as aberrant gene expression profile signatures, driver mutations, structural genomic rearrangements, novel gene fusions and methylation patterns. Next Generation Sequencing (NGS) technologies, overcoming the limited scalability of traditional Sanger sequencing, are recently revolutionizing genomics and transcriptomics by providing a cost-efficient and single base resolution tool for a unified deep analysis of tumor complexity[56]. Systemic Mastocytosis, an uncommon disease with heterogeneous clinical presentation and different prognosis, with the unique known genetic lesion involved in the pathogenesis represented by specific KIT mutation, may constitute an exciting field of application for these techniques.

2.5 The index case

A 65-year-old Caucasian woman presented to emergency department because of flushing and hypotensive shock. She did not show serum biochemistry alterations, except for serum total tryptase levels of 2255 *n*g/mL (normal value: <13.0), haemoglobin 10.2 g/dL, total white blood cell count (WBC) 15980 × 10^9/L, and platelets 319000 × 10^9/L. She was referred to the hematology unit some days later and the high serum tryptase level was confirmed. She had 50–60% infiltration of atypical MCs on bone marrow smears and 70–80% on biopsy. Neoplastic MCs showed bright expression of CD117, positivity of CD2, and negativity of CD25 antigen; the morphological examination of peripheral blood smear showed <1% of MCs, so she was diagnosed as aleukemic

variant of MCL. Direct sequencing of the entire KIT gene on bone marrow and peripheral blood tested negative for the KIT D816V mutation and for any other mutation (primers are reported). Due to the asymptomatic presentation, she was given antihistamine alone for five months. Then, the appearance of anemia (9.7 g/dL), with serum tryptase level steadily around 2000 ng/mL, prompted starting therapy with imatinib 400 mg/die, that was indicated on the basis of the absence of KIT mutations. The patient maintained a stable disease for twelve months when on imatinib, then imatinib had to be stopped due to increasing anemia and no substantial response. The subsequent therapy with dasatinib did not have any effect and the patient died due to haemorrhagic stroke in disseminated intravascular coagulation, three weeks after dasatinib initiation and twenty-four months after initial symptoms.

We undertook an integrated molecular genetic study of this KIT gene mutation-negative MCL case. After having obtained written informed consent, we extracted genomic DNA and total RNA from purified mast cells (MCs) isolated from bone marrow at diagnosis and at progression, as well as DNA from saliva, and performed whole exome sequencing (WES) and RNA-seq on an HiSeq1000 (Illumina, San Diego CA). Among the mutated genes detected in MCs but not in saliva by WES, SETD2 stood out among others because two loss-of-function mutations: a nonsense mutation in exon 15 (NM_014159:c.G6753T:p.Glu2234Ter) and a frameshift insertion of a C in exon 20 (NM_014159:c.7595_7596insC: p.Gly2515ArgfsTer5). Both were validated by Sanger sequencing (Figure 4a). The first mutation was predicted to result in a truncated protein lacking 330 amino acids at the C-terminal whereas the second mutation was predicted to result in a truncated protein lacking 46 amino acids at the C-terminal (Figure 4b). The result was the inactivation of both alleles of the gene. Western Blotting (WB) confirmed the expression of the truncated SETD2

isoform (tSETD2) resulting from the nonsense mutation. tSETD2 was predicted to lose the highly conserved WW and SRI domains and its ability to bind and tri-methylate histone H3 (Figure 4c).

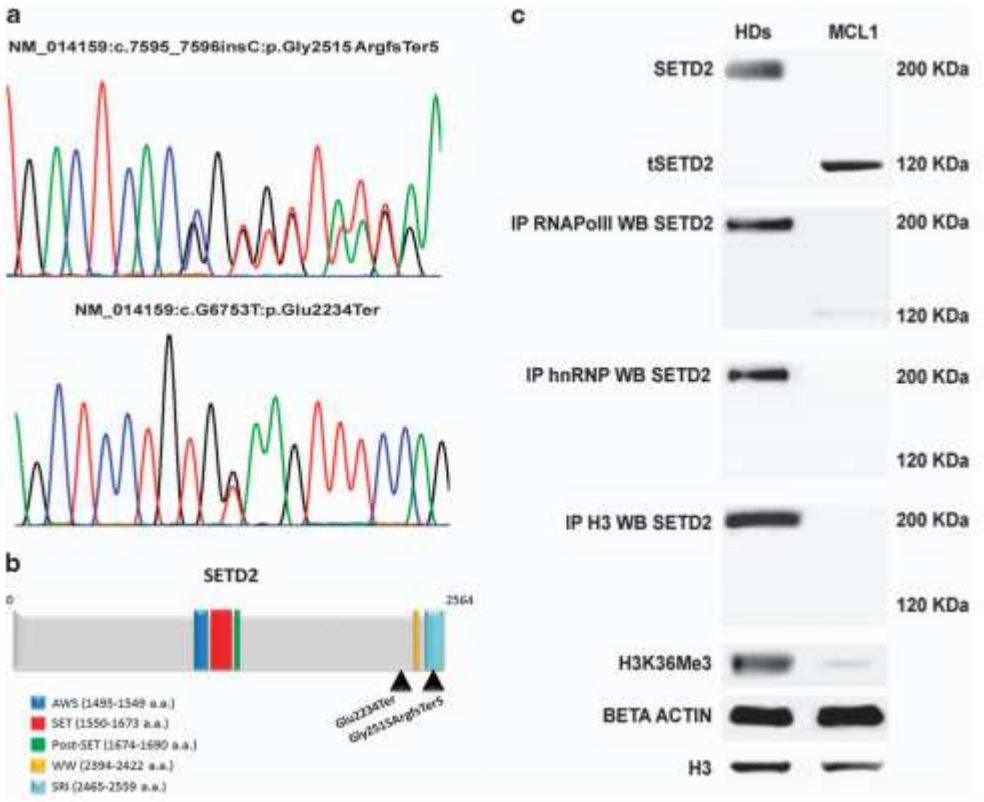

Figure 4. *SETD2 loss of function mutations in the index MCL case (MCL1). (a) Sanger sequencing chromatograms with the frameshift (top) and nonsense (bottom) mutations identified by whole-exome sequencing. (b) Localization of the mutations with respect to the key functional domains of the SETD2 protein. The SRI domain is necessary for histone H3 lysine 36 trimethylation (H3K36Me3) and mediates SETD2 interaction with the phosphorylated C-terminal domain of the RNA polymerase II large subunit (RNA pol II) and with the heterogeneous nuclear ribonucleoprotein-L (HnRNP), thus coupling H3K36Me3 with transcription elongation and splicing. (c) from top to bottom: western blotting (WB) showing the truncated SETD2 (tSETD2) protein as compared to full-length SETD2 detectable in a pool of proteins from mononuclear cells of healthy donors; co-*

immunoprecipitation experiments performed by using: an anti-RNA pol II, an anti-hnRNP and an antihistone H3, respectively, to isolate the proteins of interest and then an anti-SETD2 as primary antibody to label the PVDF membrane on which the immunoprecipitates were transferred; WB for H3K36Me3. Histone H3 and actin were used as loading controls.

2.6 SETD2 gene

The human SETD2 gene is located at the cytogenetic band p21.31 of chromosome 3, a region frequently targeted by copy number loss in various tumors . *SETD2* encompasses a genomic region of 147Kb, and the 21 exons encode an 8,452nt transcript. The SETD2 protein consists of 2,564 amino acids and has a molecular weight of 287.5 KD. Three conserved functional domains have been identified in the SETD2 protein: the triplicate AWS-SET-Post SET domains, a WW domain and a Set2 Rpb1 interacting (SRI) domain (Figure 5). The SETD2 gene encodes a histone methyl-transferase responsible for trimethylation of Lysine 36 of Histone H3 (H3K36Me3)[57], a key hystone mark associated not only with active chromatin but also with transcriptional elongation, alternative splicing, DNA replication and repair[58]. SETD2 has indeed a key role in maintaining the integrity of the genetic information at the DNA and transcript level, and specifically in: i) preventing aberrant transcription through binding to the C-terminal domain of the RNA polymerase II (PolII)[59]; ii) regulating splicing through association with the large subunit of the heterogeneous nuclear ribonucleoprotein complex (hnRNP-L)[60]; iii) participating both in Homologous Recombination (HR) repair after a double strand break (DSB) has occurred[61] as well as in Mismatch Repair (MMR) during DNA replication[62] vi) activating p53-dependent cell cycle checkpoint (Figure 6)[62,63].

In recent years, *SETD2* has attracted a lot of interest as a gene whose inactivation is involved in tumor initiation and progression.

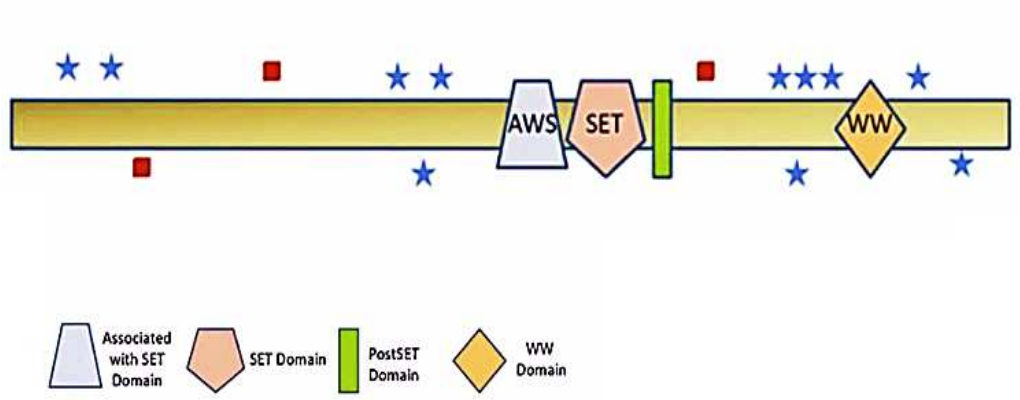

Figure 5. *Structure of SETD2protein*

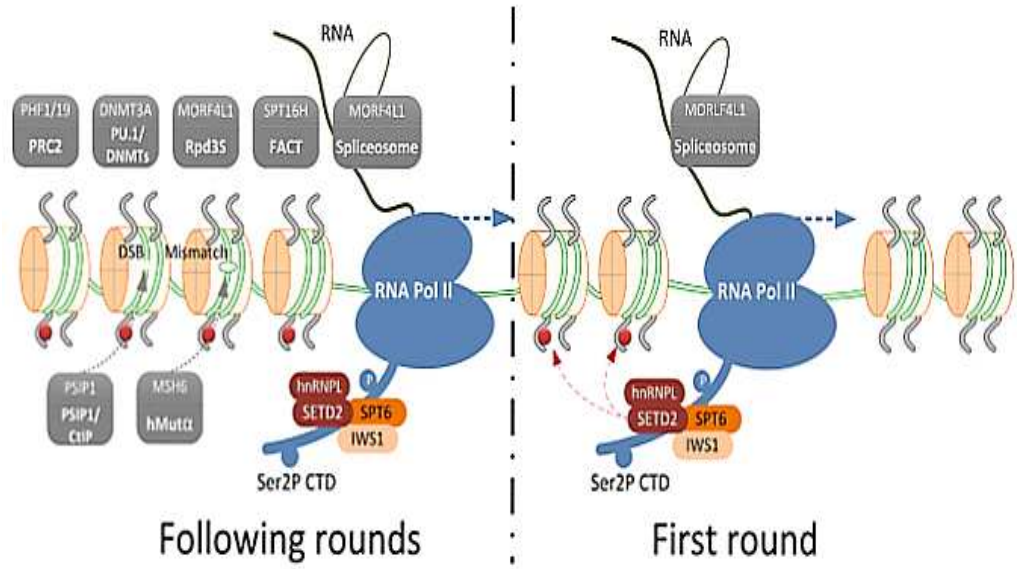

Figure 6. *Schematic representation of SETD2-mediated trimethylation of H3K36 and an overview of the H3K36me3 readers that define its role in various biological processes.*

2.6.1 Mutations of SETD2 gene

The first report on *SETD2* mutations in cancer dates from 2010 when Dalgliesh *et al* identified inactivation mutations in ccRCC[64,65]. This bi-allelic inactivation of SETD2 was the first clue that the gene might be a tumor suppressor gene. Two large cohort studies revealed an overall frequency of *SETD2* mutations of approximately 11% in clear-cell Renal cell carcinoma (ccRCC). Still, whole-exome sequencing studies did reveal somatic *SETD2* mutations in various types of cancer including lung, breast, skin and brain cancers, and this can be seen as an indication that SETD2 inactivation plays a role in the development of other tumors, albeit with low frequencies in most of them. Moreover, the majority of somatic *SETD2* mutations were missense mutations for which the functional consequences are often unclear. In renal cell carcinomas, SETD2 loss of function mainly results from large monoallelic deletions or CN-LOH at chromosome 3p, followed by mutation of the remaining allele.33 In acute leukemias, it rather derives from biallelic missense or truncating mutations. This is illustrated by the study of Zhu *et al* [66] of 241 cases of leukemia (134 acute myeloid leukemia and 107 acute lymphcytic leukemia) in which only 8 of the 19 somatic SETD2 mutations identified in 15 patients were truncating. Bi-allelic mutations were detected in only 4 patients. It cannot be excluded that in ALL, and possibly in other tumors as well, *SETD2* haploinsufficiency does lead to a disease phenotype. *SETD2* mutations appeared to be most frequent in leukemias that carried a *MLL* gene rearrangement[66,67]. Loss of function of the SETD2 tumor suppressor gene, which encodes the only histone methyltransferase that can catalyze H3K36Me3, and global loss of H3K36Me3 have been observed to be associated with worse prognosis or advanced cancer stage. In gliomas, *SETD2* mutations were predominantly seen in high-grade (16 out of 178 cases) but not in low-grade cases (0 out of 45 cases)[68]. Further evidence supporting a role of SETD2 inactivation in progression of tumors comes from a recent study performed by Ho *et al* [69]. Using immuno-histochemical approaches, Ho *et al* observed a decrease

in H3K36me3 levels in metastatic ccRCC as compared to primary ccRCC[69]. Either acquired *SETD2* mutations or alternate mechanisms may be the cause of this, suggesting that a decreased level of H3K36me3 is correlated with progression. Using whole exome sequencing and H3K36me3-staining of tissue sections, they identified different *SETD2* mutations in different regions of the same primary tumor in three cases. This suggested that loss of SETD2 can be a late event that provides a selective advantage to tumor cells[70].

2.6.2. Methylation and cancer

Cancer is characterized by uncontrolled cell growth and acquisition of metastatic properties. In most cases, activation of oncogenes and/or deactivation of tumor suppressor genes lead to uncontrolled cell cycle progression and inactivation of apoptotic mechanisms. There are different mechanisms by which these genetic and cellular changes occur. The canonical mechanisms are mutation, chromosomal translocation or deletion, and dysregulated expression or activity of signaling pathways. The role of epigenetics in carcinogenesis is less well defined. Recent studies suggest that epigenetic alteration may be another hallmark of cancer due to its role in the generation of cancer progenitor cells and subsequent initiation of carcinogenesis. Epigenetic changes can induce pro-cancer characteristics in even mutation-free cells producing alterations in gene expression, independent of changes in DNA sequence. Many epigenetic modifications, such as DNA methylation and hydroxymethylation, histone acetylation and methylation, and changes in small noncoding RNAs, have profound effects on gene expression. DNA methylation at CpG islands has been shown to silence gene expression by interfering with transcriptional machinery. Many other epigenetic changes, such as hypomethylation of oncogenes, hypermethylation of tumor suppressor genes, depletion of hydroxymethylation, changes of histone acetylation and

methylation patterns, and miRNA expression level variations, are known to be associated with many cancers. Epigenetic silencing of tumour suppressor genes promotes tumour progression via inhibition of apoptosis in cancer cells. Apoptosis is a highly regulated process of cell death in the development and maintenance of a normal cell population in mature organisms. Deregulation of apoptosis pathways is thus a key feature of carcinogenesis, because the inhibition of natural cell death mechanisms plays an important role in tumour progression by permitting abnormal cell growth. However, the dynamic nature of epigenetic modification leaves the door open to the reversal of cancer-related epigenetic changes by drugs that permit re-expression of pro-apoptotic and pro-autophagy tumour suppressors or cell-cycle regulators[71].

3. AIM OF THE STUDY

The overall aim of this project is to assess the prevalence, the underlying mechanisms and the effects of SETD2 reduced/loss of function in SM; provide some new elements that can help to understand the heterogeneity of the disease from Indolent to the more aggressive forms, with the aim of identifying new possible therapeutic targets.

3.1 AIM 1: Study of SETD2 gene inactivation and function in SM

We identify a new nonsense mutation in the SETD2 gene in a case of MCL negative for any KIT gene mutation, and a consequent reduction in its gene expression.

We hypothesized that the dowmodulation of SETD2 protein, and corresponding reduction of H3K36Me3, could also be observed in a more extensive cohort of cases of advanced SM, and

examined more cases of AdvSM and ISM to test this hypothesis. Also, we examined the gene alterations, changes in expression, function, interaction with other proteins and cellular consequences with functional validation studies conducted on patients' cell and cell lines models to test how this gene down modulation may afford an alternative mechanism of aggressiveness in SM.

3.2 AIM2: Clinical implication of SETD2 inactivation in SM

With our previous results we had demonstrated that MCL and ASM had significantly lower levels of SETD2 protein and H3K36Me3 as compared to ISM, with some exceptions. We therefore planned to extend the SETD2 evaluation to a greater number of cases of ISM and we collected all the clinical data useful to the prognostication of the cases. Once we established the strong association of inactivation of SETD2 with the aggressiveness of the disease, we wanted to verify which is the clinical impact of the SETD2 gene expression level OS. After identifying a SETD2 value that distinguishes indolent forms from other forms, we analyzed all the clinical features to correlate the impact of downmodulation of SETD2/H3K36Me3 on clinical presentation of disease.

4. MATERIALS AND METHODS

4.1 AIM 1 : Study of SETD2 gene inactivation and function in SM

4.1.1 Patients samples and cell lines

A total of 57 SM patients were included in the validation cohort based on sample availability (23 patients with ISM (three with SM-AHN), three with SSM, 20 with ASM (three with ASM-AHN) and 11 with MCL (two with MCL-AHN)) were diagnosed and classified according to WHO criteria[3,7,30].

Mononuclear cells isolated from BM and PB samples were used to extract DNA, RNA and proteins. The mononuclear cell fraction (MNC) from bone marrow and peripheral blood samples of patients were obtained by means of Ficoll-Hypaque gradient and subsequential centrifugation. Equal amounts of RNA and proteins from peripheral blood samples of 8 HDs were pooled to avoid individual differences in transcript and protein expression.

To identify molecular mechanisms involved in SETD2 loss of function we uses two different cell lines as in vitro models. HMC-1 cells were cultured in flasks with Iscove's basal medium plus stable glutamine, supplemented with 10% v/v FBS, 100 µM penicillin, 100 µg/ml streptomycin and incubated at 37 °C in a 5% CO2 atmosphere. Every three days, the cells were pelleted at 700 rpm for 5 min and the culture medium was changed. The cells were resuspended in a concentration of 2×106 cells/ml. HMC-1 cells derived from a mast cell leukemia patient and display two subclones: HMC 1.1 harboring V560G mutation and HMC 1.2 harboring both V560G and D816V mutations. ROSA cells are a stable stem cell factor (SCF) -dependent human MC line, ROSA(KIT WT), expressing a fully functional immunoglobulin E (IgE) receptor. Transfection with KIT D816V converted ROSA(KIT WT) cells into an SCF-independent clone [72-75].

4.1.2 Whole exome Sequencing

For the DNA sample obtained from CD117+ cells, 155 million reads were generated (coverage, 114x) with 99.84% mapped reads. For the DNA sample obtained from saliva, 197 million reads were generated (coverage, 147x) with 99.77% mapped reads.

Data analysis was performed following Genome Analysis ToolKit (GATK) best practice as described below. Briefly, raw data were inspected to detect low quality reads. Adapters were trimmed out when needed and resulting files were aligned to reference genome (hg19) with the Burrows-Wheeler Aligner (BWA). Picard tool was employed to mark duplicates and indels recalibration step was carried out in order to clean up artifacts produced in the initial mapping step. Base quality score recalibration (BQSR) was performed to get more accurate base qualities. Recalibrated BAM files were subjected to variant discovery by employing MUTECT and VARSCAN analytical tools for paired samples[76]. Variants obtained were filtered against genes known as sequencing artifacts and for hyper mutated and polymorphic genes[76]. A list of high confidence SNVs and indels was obtained and annotated for amino acid substitution and SIFT function predictive score[76].

4.1.3 Single Nucleotide Polymorphism (SNP)-Array analysis

Cytoscan HD arrays were processed by NEXUS analysis software to obtain segmented copy number variant (CNV) regions across the genome. CNVs smaller than 1kb were filtered out. CNVs were filtered against those annotated in the Database of Genomic Variants (DGV) and matching ones removed[76].

4.1.4 Loss-of-heterozygosity (LOH) analysis at 3p21.3

Characterization of the Copy Neutral (CN)-LOH region found by SNP-arrays in 10/13 SM patients of the validation cohort revealed that the minimal common region (MCR) of LOH included *SETD2* and nine additional genes (*CCDC12*, *NBEAL2*, *NRADDP*, *KIF9-AS1*, *KIF9*, *KLH18*, *PTPN23*, *SCAP*, *ELP6*). In order to screen for LOH specifically at 3p21.3 in the remaining patients of the validation cohort, nine SNPs with Minor Allele Frequency (MAF)>40% were selected in the MCR (rs11720139, rs2305634, rs2305635, rs1079276, rs2278963, rs6780013, rs1531875, rs4082155, rs6767907) and genotyped. Thirty nanograms of DNA was amplified by polymerase chain reaction (PCR), then the sequencing of PCR products was performed on an ABI PRISM 3730XL (Life Technologies).

4.1.5 Sanger sequencing

SETD2 mutations identified by WES in the index case were validated by Sanger sequencing at the genomic level[76].

In the HMC-1.1 and HMC-1.2 cell lines and in the 11 MCL cases of the validation cohort, the entire coding sequence of the *SETD2* gene (21 exons) was screened for mutations by Sanger sequencing on an ABI PRISM 3730XL (Life Technologies) using 30ng DNA and the primers reported in Duns et al(37 amplicons)[77]. In the remaining 46 samples of the validation cohort, *SETD2* mutation screening was performed by a high throughput approach based on library preparation with the Access Array technology (Fluidigm) and sequencing on a MiSeq Instrument (Illumina). The *SETD2* gene was targeted by 52 amplicons. Briefly, 80ng of DNA was used as input material for the Access Array, while exon 1 was amplified separately by PCR using a GC-rich enzyme (Roche Applied Science). *SETD2* was sequenced with a mean coverage of 1,898 for all amplicons and patients, the detection limit was set to 3%. The Sequence Pilot software version 4.2.2 Build 502 (JSI Medical

Systems) was used for alignment and variant calling. Gene mutations were annotated compared to the reference sequence based on the *SETD2* Ensembl Transcript ID ENST00000409792 (Ensembl release 74: Dec 2013). Analysis parameters were set according to manufacturer's default recommendation. Validity of called variants was checked against the publicly accessible COSMIC v73 database (http://cancer.sanger.ac.uk/cancergenome/projects/cosmic), ClinVar (v2015-08-06) (http://www.ncbi.nlm.nih.gov/clinvar/), and dbSNP database (http://www.ncbi.nlm.nih.gov/snp; Build 137). Functional interpretation was performed using SIFT 1.03 (http://sift.jcvi.org), PolyPhen 2.0 (http://genetics.bwh.harvard.edu/pph2) and MutationTaster 1.0 algorithms (http://www.mutationtaster.org). *SETD2* promoter was amplified using by PCR using a GC-rich enzyme (roche Applied Science) and the following primers: F, 5'-CGGTCTGGCCCACATCACT-3' and R, 5'- ATCGGGAGCGGCTGGAGA-3' and was sequenced separately by Sanger sequencing.

4.1.6 Quantitative RT-PCR

In the HMC-1.1 and HMC-1.2 cell lines and in the 57 samples of the validation cohort, SETD2 mRNA expression was assessed by quantitative RT-PCR. Total RNA (200 ng) was reverse transcribed to cDNA with the High-Capacity cDNA Reverse Transcription Kit (Thermo Fisher Scientific). Assays were performed in triplicate on the ABI 7900HT system (Applied Biosystems) using pre-designed TaqMan Gene Expression Assays (Thermo Fisher Scientific) for SETD2 (Hs01014784_m1) and TBP (Hs00427621_m1) as control gene. SETD2 mRNA expression levels were quantified using the Comparative Ct method, using a pool of healthy donors as calibrator[76].

4.1.7 Methylation analysis of the SETD2 promoter

Methylation status at the *SETD2* promoter was assessed in the validation cohort using EpiTect Methyl II PCR Assays (EPHS110216-1A; Qiagen) on an ABI PRISM 7900HT, according to manufacturer's instructions. A methylation sensitive (EPHS115450-1A) and methylation dependent (EPHS115451-1A) control assay were also run for all the samples analyzed[76].

4.1.8 Sequencing of recurrently mutated myeloid genes

Fifty-four genes frequently mutated in myeloid malignancies, including all those so far reported to be mutated in SM, were interrogated in 40 patients of the validation cohort for whom leftover DNA from SETD2 mutation screening was available, using the Trusight Myeloid Sequencing Panel (Illumina) on a MiSeq instrument (Illumina). The panel interrogated the full coding region of 15 genes: *BCOR*, *BCORL1*, *CDKN2A*, *CEBPA*, *CUX1*, *DNMT3A*, *ETV6/TEL*, *EZH2*, *KDM6A*, *IKZF1*, *PHF6*, *RAD21*, *RUNX1/AML1*, *STAG2* and *ZRSR2*, and exonic hotspots of 39 genes: *ABL1*, *ASXL1*, *ATRX*, *BRAF*, *CALR*, *CBL*, *CBLB*, *CBLC*, *CSF3R*, *FBXW7*, *FLT3*, *GATA1*, *GATA2*, *GNAS*, *HRAS*, *IDH1*, *IDH2*, *JAK2*, *JAK3*, *KIT*, *KRAS*, *KMT2A/MLL*, *MPL*, *MYD88*, *NOTCH1*, *NPM1*, *NRAS*, *PDGFRA*, *PTEN*, *PTPN11*, *SETBP1*, *SF3B1*, SMC1A, *SMC3*, *SRSF2*, *TET2*, *TP53*, *U2AF1* and *WT1* by 568 amplicons (length range: 225–275 bp). Amplicon libraries were prepared from 50 ng of DNA. Paired-end sequencing runs were performed on a MiSeq (Illumina, San Diego, CA) with reagent kit v3 according to manufacturer's instructions. Base-calling and sequence alignment were performed using MiSeq reporter software. VCF files were generated using Somatic Variant Caller and uploaded to Variant Studio v2.1, where variants were annotated, classified, and filtered for quality, coverage, read depth, allelic frequency, and significance[76].

4.1.9 Drug treatments, Aurora kinase A and mdm2 silencing

Bortezomib (10 nM) was used as proteasome inhibitor, to evaluate if SETD2 degradation was a proteasome-dependent or -independent mechanism. Danusertib (500nM) was used as Aurora Kinase inhibitor and SP141 (5 μM) as mdm2 inhibitor. Finally, midostaurin (PKC412) 4 μM was used to test its ability to inhibit AKA activity in a H3K36Me3-deficient context.

After 24 h exposure of HMC-1.1 and HMC-1.2 cells to the above mentioned drugs treatments apoptotic cell death was assessed by measuring the uptake of fluorescinated Annexin V and propidium iodide (PI, both from Roche). A FACsCantoII flow cytometer (Beckton Dickinson) set at 488nm excitation and 530nm wavelength bandpass filter for fluorescin detection or 580nm for PI detection, and a dedicated software (DIVA software, Beckton Dickinson) were used for analysis.

Drug cytotoxicity was evaluated in clonogenic assays in HMC1.1 and 1.2 cells and in primary cells derived from advanced SM patients. Drug specificity was evaluated using 2 healthy donors as control. Briefly, we evaluated the reduction of colony (generated in 0.9% methylcellulose supplemented with 30% fetal calf serum) number in the presence of increasing doses of bortezomib (0.25-1 nM) after 10-day incubation at 37°C in fully humidified atmosphere and 5% CO_2. Nonlinear regression analyses were used to calculate the lethal dose (LD_{50}) of the different drug.

Finally, to confirm AKA and mdm2 effects on setd2 deficiency, we transiently silenced AKA and mdm2 expression using a short interfering RNA approach. Briefly, we transfected in HMC1 cell line a selected siRNA able to inhibit AKA or mdm2 expression. RT-PCR to confirm reduced expression of the target genes, western blotting and immunoprecipitation assays to test silencing effects on setd2 were performed after 72 hrs from transfection.

4.1.10 Protein extraction, co-immunoprecipitation/immunoblotting and Western blotting

HMC 1 cells or primary SM patient cells were cultured for in standard medium alone or with 4 µM midostaurin (c-Kit inhibitor), 10 nM bortezomib (proteasome inhibitor), 500nM danusertib (AKA inhibitor), 5 µM SP141 (MDM2 inhibitor), followed by lysis and boiling for 10 min in SDS-PAGE loading buffer. Lysates were separated on 10% Tris-glycine gels, transferred, and blotted.

Briefly, western blotting analysis was performed using 70 µg of whole cell lysates. Co-immunoprecipitation (IP) and Immunoblotting were performed using 250 µg of whole cell lysates in the presence of Cyanogen bromide (CNBr)-activated sepharose 4B (GE Healthcare) conjugated with an anti-setd2 antibody (Abnova) raised against a synthetic peptide corresponding to an internal region of human setd2 maintained in the truncated isoform. The anti-setd2 antibody was added to a 50% protein G-sepharose bead slurry and incubated with rotation at 4°C overnight. The cleared cellular lysates were added to the anti-SETD2-bound protein G-sepharose and the incubation continued overnight at 4°C. Proteins or IP products obtained through overnight incubation with primary antibodies in IP buffer (250 mM NaCl, 15 mM MgCl2, 40 mM HEPES, 60 mM glycerophosphate supplemented with protease inhibitors) were resolved in SDS-polyacrylamide gel electrophoresis. Gels were then transferred onto PVDF membranes and labeled with primary and secondary antibodies in PBS buffer with 5% bovine serum albumin and 0.1% Tween 20. The following primary antibodies were used for Co-IP/immunoblotting and WB: anti-setd2, anti-H3K36Me3, anti-RNAPol II, anti-hnRNP, anti-AKA, anti-phospho-AKA(T288), anti AKB, anti-phospho-AKB(T232), anti-phosphoH3(S10), anti-p53, anti-p21, anti-p27, anti-bax, and anti-MDM2. Beta actin and Histone H3 were used as loading control. Immunoreactive proteins were visualized by probing with horseradish peroxidase-conjugated secondary antibodies and then

by enhanced chemiluminescence (ECL, Thermo Fisher Scientific). Signal intensities in single blots obtained from three individual experiments were quantified with the ImageJ software. Such software attributes a numerical value to signals of chemiluminescent substrates, thereby allowing a comparative analysis of protein levels across different samples.

4.1.11 SETD2 silencing in ROSA D816V cell line

To investigate cellular effects of SETD2/H3K36Me3 deficiency on DNA damage and genomic instability, we silenced SETD2 expression using a short interfering RNA approach. Briefly, we transfected in ROSA D816V cell line a selected siRNA able to inhibit SETD2 expression after 9 weeks exposure. The transfection was repeated every 4 days and SETD2 expression, both at transcriptional and at translational levels, was assessed by RT-PCR and WB.

To assess the activation and proficiency of HR, control and SETD2 siRNA-depleted cells was challenged with DNA damaging agents (UV and doxorubicine) and chased in fresh media at regular timepoints afterwards (2, 4, 6, 8, 24hrs). Phosphorylated H2AX and RAD51 expression were assessed by WB. Moreover P-H2AX and RAD51 foci as surrogate markers of active HR were evaluated by immunofluorescence (IF). An empty vector was transfected in Rosa cells and used as a negative control.

4.1.12 Immunofluorescence (IF) analyses

Cells set on poly-L-lysine-coated glass slides were fixed with 3% paraformaldehyde for 10’ at 37°C, washed with 0.1M glycine in phosphate-buffered saline (PBS), permeabilized in 70% ice-cold ethanol for 2’ at -20° C and incubated overnight at 4°C with primary anti-ɣH2AX antibody and anti RAD51 antibodies. Slides were then stained with a secondary anti-rabbit antibody conjugated with

Alexa Fluor 568 for 2 h at room temperature and a subsequent anti-mouse antibody fluoresceinated. 6-diamidino-2-phenylindole (DAPI) was used to stain the nuclear compartment. IF analyses were performed using an Axiovert 40 CFL microscope (Zeiss). Images were acquired with a 100X objective and analyzed with the AxioVision software.

4.1.13 Statistical analysis

Analysis of variance followed by Tukey post-hoc test was applied in order to detect differences in SETD2 and H3K36Me3 expression between groups. Statistical analysis were carried out by R.15 Spearman correlation index was calculated between SETD2 and H3K36Me3 level and disease subtype.

4.2 AIM2: Clinical implication of SETD2 inactivation in SM

4.2.1 Samples

A total of 88 SM patients were included in this part of the study. We prospectively added to our historical cohort (57 patients) the newly diagnosed patients with ISM from the participating centers (Azienda Ospedaliera Universitaria Integrata, Verona; IRCCS Policlinico San Matteo Foundation, Pavia; University of Bologna; IRCCS Ca' Granda Ospedale Maggiore Policlinico Foundation and University of Milan; Azienda Unità Sanitaria Locale, Romagna), with the intent to extend the group of the “non advanced” form, that we supposed having normal level of SETD2 and normal H3K36Me3. The diagnosis were: ISM (n=44), SSM (n=5), SM-AHN (n= 10), including ISM-AHN (n=2, one associated with indolent non Hodgkin Lymphoma and one with myelodisplastic/myeloproliferative neoplasm unclassified), ASM-AHN (n=5 , two cases associated with Myelomonocytic leukemia, two cases associated with myelodisplastic syndrome, and one

Acute myeloid leukemia), MCL-AHN (n=3, two cases associated with a myelodisplastic syndrome and one with Acute Myeloid leukemia), ASM (n=17), MCL(n=12).

All the data collected refer to the time of diagnosis, prior to any therapy performed.

4.2.2 Diagnosis

Diagnosis of systemic mastocytosis was based on the World Health Organization (WHO 2016) diagnostic criteria, and it was established when the major plus one minor criterion, or three minor criteria, were satisfied. All the patients were studied with bone marrow smears cytology, BM biopsy with immunohistochemistry staining for tryptase; serum tryptase levels; analysis of CD2/CD25 expression on mast cells by flow or immunohistochemistry ; genotyping of cKIT (D816V) mutation. Bone marrow biopsies were evaluated by local pathologist. Analysis for mutations in KIT were performed with reverse transcriptase polymerase chain reaction (RT-PCR) restriction fragment length polymorphism (RFLP) analysis , allele-specific ARMS-RT-qPCR, D-HPLC analysis followed by Sanger sequencing, direct Sanger sequencing, and/or Digital PCR according to center's policy.

The diagnosis of SSM was based on the presence of two or more "B" findings, that include BM biopsy showing >30% mast cell infiltration and/or serum tryptase >200 ng/mL; signs of dysplasia or myeloproliferation in non-mast cell lineages with normal blood counts; hepatomegaly without impairment of liver function, and/or splenomegaly without hypersplenism, and/or lymphadenopathy on palpation or imaging. The diagnosis of ASM was based on the presence of one or more C-findings (cytopenia with an absolute neutrophil count $<1 \times 10^9$ /l, hemoglobin <10 g/dl, platelets <100 × 109 /l, hepatomegaly with impaired liver function, palpable splenomegaly with signs of hypersplenism, malabsorption with significant hypoalbuminemia and/or significant

weight loss >10% over the past 6 months)[14,29]. Diagnosis of MCL was based on the presence of at least 20% MC in BM smears with or without C-findings. The diagnosis AHNMD was established by evaluating peripheral blood (for example, monocytosis, basophilia and/or eosinophilia, left shift and/or a prominence of myelocytes) and bone marrow smears by morphology, histology and immunohistochemistry using WHO criteria and a panel of standard markers, depending on the suspected AHN subtype.

4.2.3 Laboratory studies

D816V KIT mutation was evaluated locally according to center's policy, only selected cases that were negative were repeated with more sensitive Digital-PCR.

Setd2 and H3K36Me3 values were obtained by WB analysis, as previously described.

4.2.4 Clinical data

The clinical baseline characteristics we collected were: age, sex, diagnosis as for WHO2016, Hb (g/dL), WBC (x 10^9), platelets (x 10^9), serum tryptase level (ug/L), presence of skin lesions, presence of mediator related sympthoms (including pruritus, flushing, urticaria and angioedema; gastrointestinal, including diarrhea, nausea and vomiting; muscular pain; headache and dizziness, hypotension), history of severe allergic/anaphylactic episodes, palpable splenomegaly, presence of osteoporosis or osteopenia, serum alkaline phosphatase [ALP] (U/L), lactate dehydrogenase [LDH] (U/L), expression value of SETD2 protein and H3K36Me3.

All patients were studied for B and C findings using appropriate laboratory tests and ultrasound or CT scan. Osteoporosis was assessed by bone mineral density of lumbar spine and femur with Dual-

energy X-ray absorptiometry (DEXA) technique and defined as T score <-2.5 in at least one site. Osteosclerosis, fractures and lytic lesions were assessed with x-ray of skeleton or spine and pelvis, at minimum.

4.2.5 Statistical Analysis

All statistical analyses considered clinical and laboratory parameters obtained at the time of diagnosis or first referral to clinical care center, which, in most instances, coincided with time of BM biopsy and study sample collection. We summarized data by using mean ± standard deviation (SD) or median and range, as appropriate, for continuous variables and absolute frequencies and percentages for categorical variables.

Chi-square or Fisher's Exact test were used, as appropriate, for comparisons between categorical variables whereas the Student t-test or Wilcoxon rank-sum test were used for comparisons between a binary and continuous variable. In case of more than two categories the F test or the Kruskal Wallis test were used.

Correlation among variables was assessed using using Pearson correlation coefficients or the tetrachoric ones.

The identification of the cutoff for the expression of SETD2/H3K36me3 separating ISM from the other WHO subtypes was evaluated using receiver operating characteristic (ROC) and the Youden index criteria.

Overall survival (OS) was defined as the time since date of diagnosis to date of death from any cause and last visit. The Kaplan–Meier (KM) method and log-rank test were used to compare OS between groups of patients. Hazard ratios (HRs) and 95% confidence intervals (CIs) were estimated by means of the Cox proportional hazards regression model. The proportional hazard assumption was assessed graphically and through the test based on Schoenfeld residuals.

Multivariable survival analysis was performed using a stepwise forward algorithm for variable selection (the nominal value for variable selection was set to 0.10). Nevertheless, the set of candidate variables to consider for multivariable analysis took into account the results from the correlation analysis among variables and the knowledge (from the pertinent literature) about the prognostic significance of certain clinical and laboratory variables.

All statistical tests were two-sided, with $P < 0.05$ considered as statistically significant where not otherwise specified.

All statistical analyses were performed using STATA 15.1 statistical software (StataCorp, College Station, TX, USA) or with R, version 3.4 (R Core Team: Vienna, Austria).

5. RESULTS

5.1 AIM 1: Characterization of mechanisms involved in SETD2 down-modulation in SM

5.1.1 SETD2 and H3K36Me3 deficiency are recurrent events in SM and cluster in advanced disease

To investigate the frequency of SETD2 inactivation in a relatively large cohort of SM patients, we used a western blotting approach to assess H3K36Me3 levels as a surrogate marker of loss of SETD2 function and to screen for the expression of SETD2 full-length vs truncated isoforms. No evidence of abnormal isoforms was found. However, the SETD2 protein turned out to be reduced or not at all expressed in the great majority of patients examined (Figure 7). H3K36Me3 paralleled SETD2 expression and was reduced or absent accordingly (Figure 7). In one MCL, one ASM and two ISM patients, SETD2 and H3K36Me3 levels were assessed in total MNC fractions obtained from BM and in purified CD117+ cells in parallel and no differences were observed.

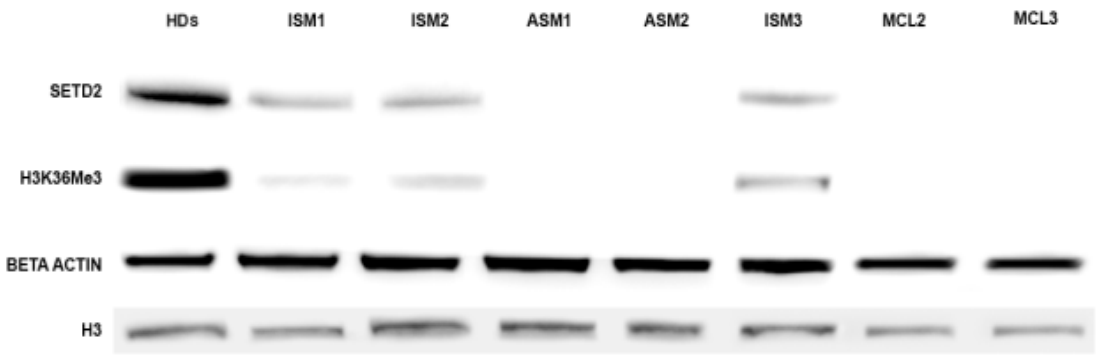

Figure 7: *SETD2 protein and H3K36Me3 deficiency in SM: WB results for SETD2 protein and H3K36Me3 levels in SM patients as compared to a pool of healthy donors (HDs)*

To confirm western blotting results, IHC with an anti-SETD2 antibody was performed on BM trephine biopsies of patients displaying various SETD2 protein levels. The intensity of nuclear staining and the percentage of immunostained atypical MCs varied among the cases and were consistent with SETD2 protein expression as assessed by western blotting (Figure 8). Internal positive controls (BM myeloid precursors and megakaryocytes) were present in each case and confirmed the specificity of the stain.

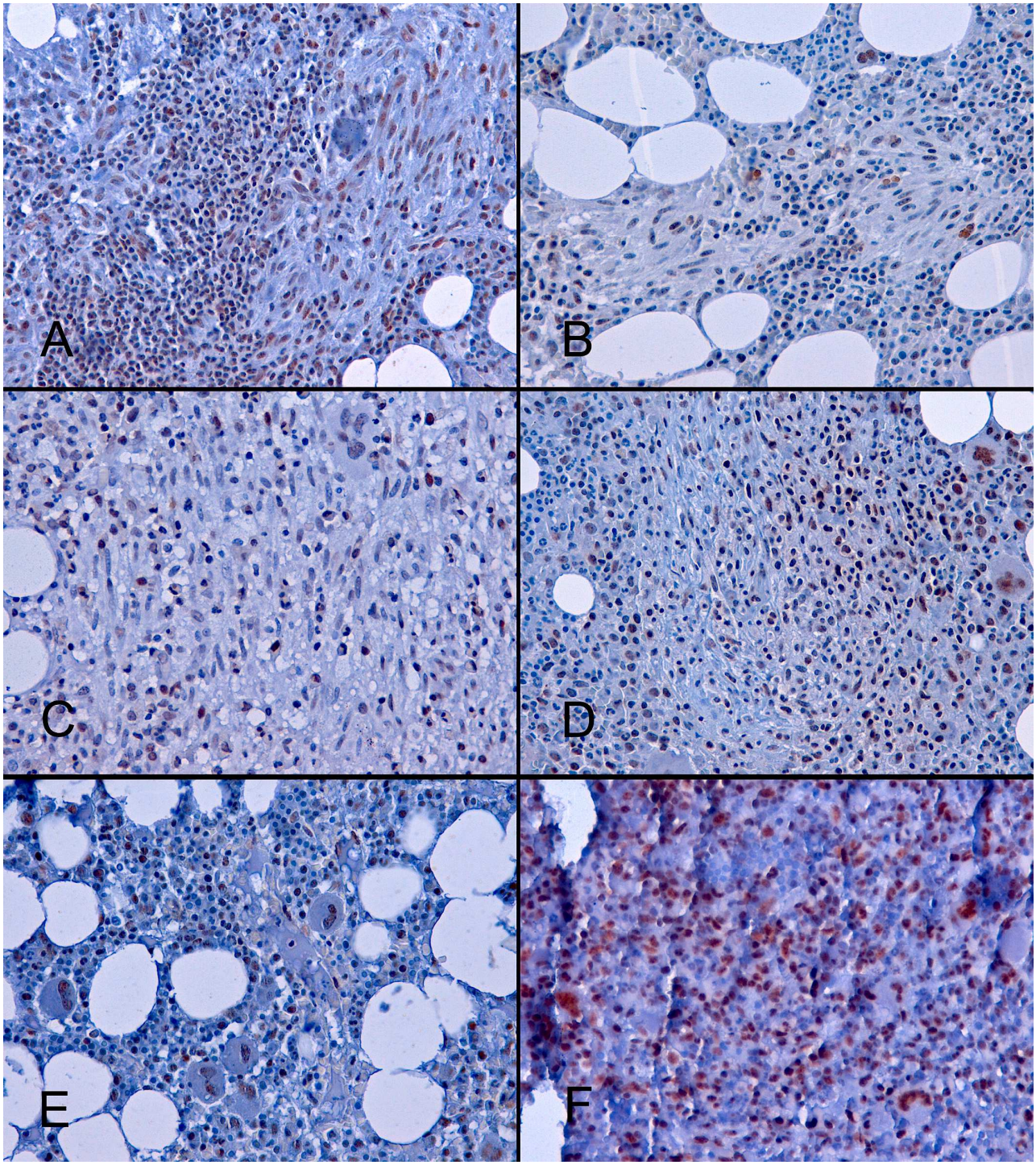

Figure 8. *IHC with anti-SETD2 antibody. 400x magnification.* ***(A)****patient ISM16 (SETD2 expression=0.926 by Western blotting). Densely packed aggregates of spindle-shaped MCs surrounded by reactive lymphocytes show diffuse and intense nuclear staining for SETD2.* ***(B-D)*** *patient ISM15 (SETD2 expression=0 by Western blotting), patient SSM1 (SETD2 expression=0 by Western blotting) and patient MCL10 (SETD2 expression=0.25 by Western blotting) show markedly*

reduced intensity of staining and reduced percentage of positive atypical MCs; ***(E)****SETD2 expression in normal BM myeloid precursors, megakaryocytes and sinusoidal endothelia;* ***(F)*** *chronic myelomonocytic leukemia showing intense SETD2 positivity in both myelo-monocytic components and megakaryocytes.*

Median SETD2 and H3K36Me3 levels, assessed by densitometric analysis of western blotting results were significantly correlated with each other (Spearman R = 0.91, P<0.001) and were lower in advanced SM (R = 0.57, P<0.001) (Figure 9). In particular, patients with MCL and ASM displayed significantly lower levels of SETD2 and H3K36Me3 as compared to ISM (SETD2: P = <0.001 and P = 0.002, respectively; H3K36Me3: P 0.001 and P = 0.004, respectively).

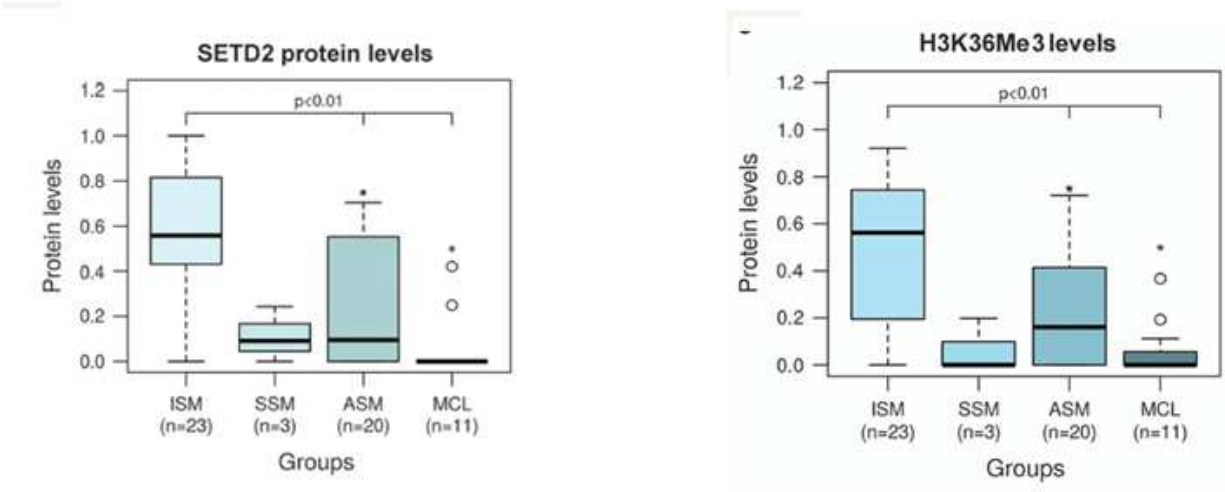

Figure 9. *Box and whiskers plots of SETD2 and H3K36Me3 level estimates obtained by densitometric analysis of western blots.*

There seemed to be no differences in SETD2 expression between advanced SM patients with (n = 8) or without (n = 26) AHN. There seemed to be no preferential association between SETD2 loss of

function and the presence or absence of specific additional mutations or mutation patterns in myeloid genes (for example, SF3B1, SRSF2, TET2, ASXL1 and so on; Table 6).

			SETD2 level	*KIT* mutation	Additional mutated genes
1	MCL2	MCL	0	D816H	*PTPN11*
2	MCL3	MCL	0	S476I	none
3	MCL4	MCL	0	D816V	*RUNX1; TET2; PHF6*
4	MCL5	MCL	0	D816V	NA
5	MCL6	MCL	0	none	NA
6	MCL7	MCL	0	D816V	*SF3B1*
7	MCL8	MCL	0	none	*SF3B1; NRAS; IKZF1*
8	MCL9	MCL	0.421	none	*SF3B1; TET2; MLL*
9	MCL10	MCL	0.25	none	NA
10	MCL11	MCL-AHN	0	D816H	*SRSF2*
11	MCL12	MCL-AHN	0	D816V	NA
12	ASM1	ASM	0	D816V	NA
13	ASM2	ASM	0	D816V	*SRSF2*
14	ASM3	ASM	0.594	D816V	NA
15	ASM4	ASM	0.704	D816V	*ASXL1; NRAS; BCORL1*
16	ASM5	ASM	0	D816V	none
17	ASM6	ASM	0.621	D816V	*RUNX1; ASXL1*
18	ASM7	ASM	0	D816V	NA
19	ASM8	ASM	0.299	D816V	none
20	ASM9	ASM	0.554	D816V	*DNMT3A*
21	ASM10	ASM	0.552	D816V	*CBL*
22	ASM11	ASM	0.594	D816V	none
23	ASM12	ASM	0.364	D816V	NA
24	ASM13	ASM	0.254	D816V	*TET2; NRAS*
25	ASM14	ASM	0	D816V	NA
26	ASM15	ASM	0	D816V	NA
27	ASM16	ASM	0	D816V	none
28	ASM17	ASM	0	D816V	*SRSF2; TET2*
29	ASM18	ASM-AHN	0.191	D816V	*SF3B1; ASXL1*
30	ASM19	ASM-AHN	0	D816V	*ASXL1; SRSF2*
31	ASM20	ASM-AHN	0	D816V	GATA2
32	SSM1	SSM	0	D816V	NA
33	SSM2	SSM	0.091	D816V	NA
34	SSM3	SSM	0.243	D816V	NA
35	ISM1	ISM	0.675	D816V	none
36	ISM2	ISM	0.561	D816V	none

37	ISM3	ISM	0.323	D816V	none
38	ISM4	ISM	0	D816V	none
39	ISM5	ISM	0	D816V	none
40	ISM6	ISM	0.437	D816V	NA
41	ISM7	ISM	0.496	D816V	NA
42	ISM8	ISM	0.521	D816V	none
43	ISM9	ISM	0.425	D816V	NA
44	ISM10	ISM	0.452	D816V	NA
45	ISM11	ISM	0.774	D816V	none
46	ISM12	ISM	0.668	D816V	none
47	ISM13	ISM	0.758	none	none
48	ISM14	ISM	0.905	D816V	none
49	ISM15	ISM	0	none	none
50	ISM16	ISM	0.924	D816V	none
51	ISM17	ISM	0.815	none	none
52	ISM18	ISM	0.918	D816V	*ASXL1*
53	ISM19	ISM	1	D816V	none
54	ISM20	ISM	0.815	D816V	none
55	ISM21	SM-AHN	0	D816V	none
56	ISM22	SM-AHN	0.542	D816V	*CBL*
57	ISM23	SM-AHN	0.998	none	*U2AF1*

Table 6. *Mutated genes additional to KIT in the patients of the validation cohort (NGS-Trusight Myeloid Sequencing Panel). The index MCL case (MCL), for whom WES data were available, was negative for mutations in any of the 54 genes of the panel. NA, not available.*

5.1.2 SETD2 loss of function in SM occurs at the post-translational level

The screening for mutations of *SETD2* gene by Sanger sequencing conducted on 11 MCL cases and the application of a high throughput approach (My Seq Instrument) on the remaining 46 samples of the validation cohort excluded the presence of *SETD2* mutations.

Deletions of the 3p21.3 region are a frequent and early event in the formation of lung, breast, kidney and other cancers[78], and the human SETD2 gene is located at the cytogenetic band p21.31, so the first attempt to explain its loss of function consisted to verify the LOH at this level. We thus examined the copy number status and searched for LOH at 3p21 in 13 cases of the validation cohort (eight MCL, four ASM, one ISM) thus extended the screen for LOH specifically at 3p21.3 in the remaining patients of the validation cohort. Overall, LOH was detected in 27/57 (47%) SM patients, namely in 8/11 (72%) MCL-, 11/20 (55%) ASM-, 1/3 SSM- and 7/23 (30%) ISM patients, but the patients with evidence of LOH at 3p21.3 did not always harbor lower SETD2 protein levels as compared to patients with no LOH. Thus, the biological significance of the recurrent 3p21.3 LOH events that can be observed in SM remains, at present, unclear.

We then assessed whether promoter hyper-methylation might be responsible for SETD2 protein deficiency, in the presence or absence of LOH. Analysis of the SETD2 promoter showed <1% methylated DNA in all the patients of the validation cohort. Methylation levels were not different from those of healthy donors. Other mechanisms of transcriptional down-regulation were excluded, since SETD2 mRNA levels were not significantly lower in the validation cohort as compared to healthy donors. To rule out the possibility that SETD2 loss of function might be another age-associated alteration in an epigenetic regulator, 80 healthy older adults with an age ranging from 65 to 95 years were screened for SETD2 mutations and for alterations in SETD2 protein expression or H3K36Me3[79-81]. No sequence variants other than the Pro1962Leu and the Asn1155Asn SNPs were detected. All the older adults did express SETD2; and densitometric analysis of western blots (done using a pool of 10 younger adults with an age ranging from 20 to 30 years as a calibrator, after having excluded inter-individual variations of expression) showed

comparable SETD2 and H3K36Me3 levels among individual older adults as well as between older and younger adults (Table 7).

N	Age	SETD2 level	H3K36Me3 level
1	65	1.121	0.996
2	65	1.248	1.077
3	65	0.997	0.999
4	65	1.173	1.073
5	65	1.174	0.962
6	65	1.233	1.117
7	65	0.999	0.887
8	66	1.101	1.211
9	66	1.049	1
10	66	1.013	1.022
11	67	1.154	1.103
12	67	0.911	1.199
13	67	1.003	1.000
14	67	0.799	0.998
15	67	1.150	1.296
16	67	0.800	0.800
17	68	1.023	1.058
18	68	0.983	1.015
19	68	0.816	0.897
20	69	0.974	1.141
21	69	0.832	1.099
22	69	1.222	1.117
23	70	1.245	1.267
24	70	1.005	1.000
25	70	0.804	0.799
26	71	0.888	0.896
27	71	0.941	0.888
28	71	1.111	0.975
29	71	1.211	0.969
30	72	1.115	1.210
31	72	1.256	1.201
32	73	1.000	0.921
33	73	0.822	0.799
34	73	1.101	1.122
35	74	0.887	0.799

36	74	0.955	0.888
37	74	0.876	0.850
38	74	0.9	0.9
39	74	0.966	0.899
40	74	1.120	1.010
41	75	1.222	1.000
42	75	1.111	1.144
43	75	1.265	1.201
44	75	0.944	0.886
45	76	1.246	1.001
46	76	1.000	0.969
47	76	1.268	1.010
48	76	0.879	0.856
49	77	1.203	1.151
50	77	1.040	0.998
51	77	0.832	0.819
52	78	1.000	1.000
53	78	1.200	1.210
54	78	1.215	1.110
55	78	0.904	0.799
56	78	0.888	0.996
57	79	0.841	0.8
58	79	1.000	0.966
59	80	1.115	1.000
60	80	1.122	1.100
61	81	1.133	1.000
62	81	1.200	1.200
63	81	0.885	0.885
64	82	0.876	0.821
65	83	0.999	0.990
66	83	0.991	0.991
67	84	0.955	0.915
68	84	1	1
69	84	1.230	1.244
70	84	1.001	1.000
71	85	1.224	1.004
72	86	1.155	1.113
73	86	0.852	0.850
74	87	1.178	1.111
75	87	1.009	0.877
76	88	1.124	1.100
77	90	0.898	0.896
78	91	0.910	0.899
79	93	0.996	0.888
80	95	1.100	1.000

Table 7. *SETD2 and H3K36Me3 levels in 80 healthy older adults with an age ranging from 65 to 95 years. Expression was assessed by densitometric analysis of Western blots.*

5.1.3 Characterization of HMC.1 and ROSA cell lines as “in vitro” models

SETD2 expression levels and activity were assessed in HMC-1 and ROSA cell lines by western blotting assay. Both HMC-1.1 and 1.2 clones displayed SETD2 and H3K36Me3 deficiency as our cohort of patients with advSM (Figure 10), while ROSA expressing KIT WT or mutated (D816V) showed SETD2 expression levels and activity superimposable to those of healthy donors (data not shown). Sequencing ruled out the presence of SETD2 gene mutations. Similarly to the patients of the validation cohort, both HMC-1.1 and HMC-1.2 cells were found to have no significant reduction in SETD2 transcript levels as compared to SETD2 wild-type cell lines and the gene promoter was found to have very low methylation levels (4.08% and 1.08% in HMC-1.1 and HMC-1.2, respectively). This suggested that similar mechanism(s) acting at the translational or post translational level underlie SETD2 deficiency in advanced SM patients and in HMC-1 cells.

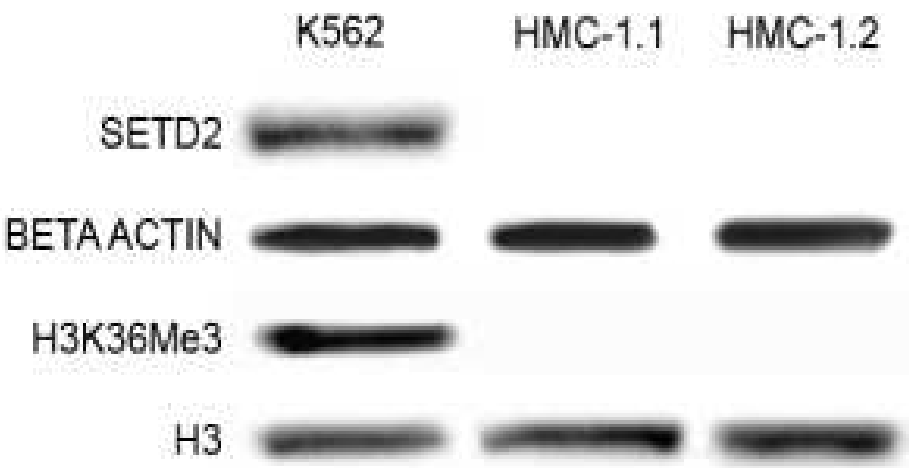

Figura 10: *SETD2 protein and H3K36Me3 levels in HMC-1.1 and -1.2 cell lines*

5.1.4 SETD2 deficiency results from enhanced proteasomal degradation

Once all the mechanisms of altered transcription were excluded, we proceed to investigate whether this down-modulation could be the result of an increased degradation of the protein. In HMC-1 cells, incubation with the proteasome inhibitor bortezomib at a concentration of 10 nM for 24 h, rescued SETD2 protein expression and restored H3K36Me3 levels (Figure 11), indicating that a functional SETD2 protein is regularly translated in neoplastic MCs, and that failure to detect it by western blotting is rather due to altered turnover and proteasomal degradation.

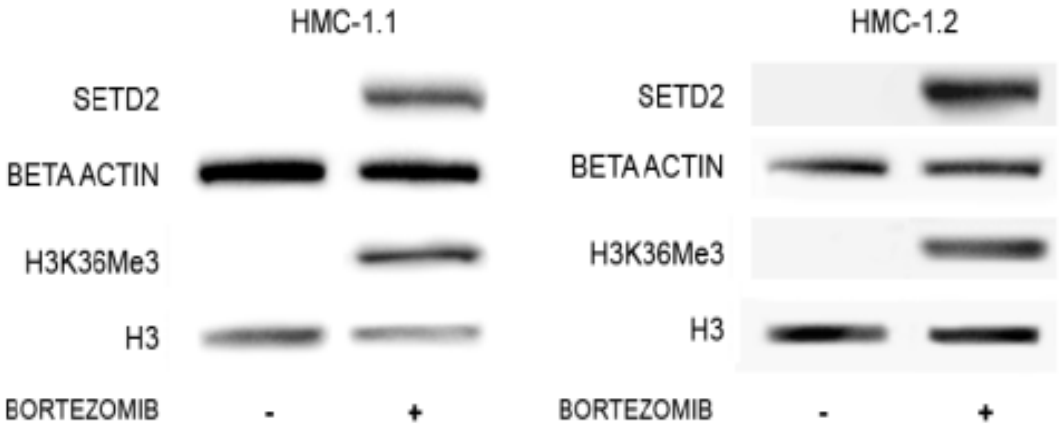

Figura 11. *SETD2 protein and H3K36Me3 levels in HMC-1.1 and -1.2 cell lines before and after inhibition of proteasome-mediated degradation by bortezomib*

To investigate the post-translational modifications underlying the altered turnover of the setd2 protein, after Bortezomib treatment, SETD2 was immunoprecipitated with a specific antibody able to recognize it and the immune-complex, loaded on gel and transferred onto a PVDF filter, it has been labeled with antibodies able to recognize the sumoylated and ubiquitinated epitopes of the protein. The results showed a protein accumulation in the sumoilated and ubiquitinated form of SETD2 protein, thus confirming the hypothesis that its down-modulation is mediated by instability mechanisms due to a dysregulation of the post-translational modifications. We therefore speculated that reduced or undetectable SETD2 expression in advanced SM patients might be accounted for by hyper-ubiquitination and -SUMOylation leading to proteasomal degradation (Figure 12).

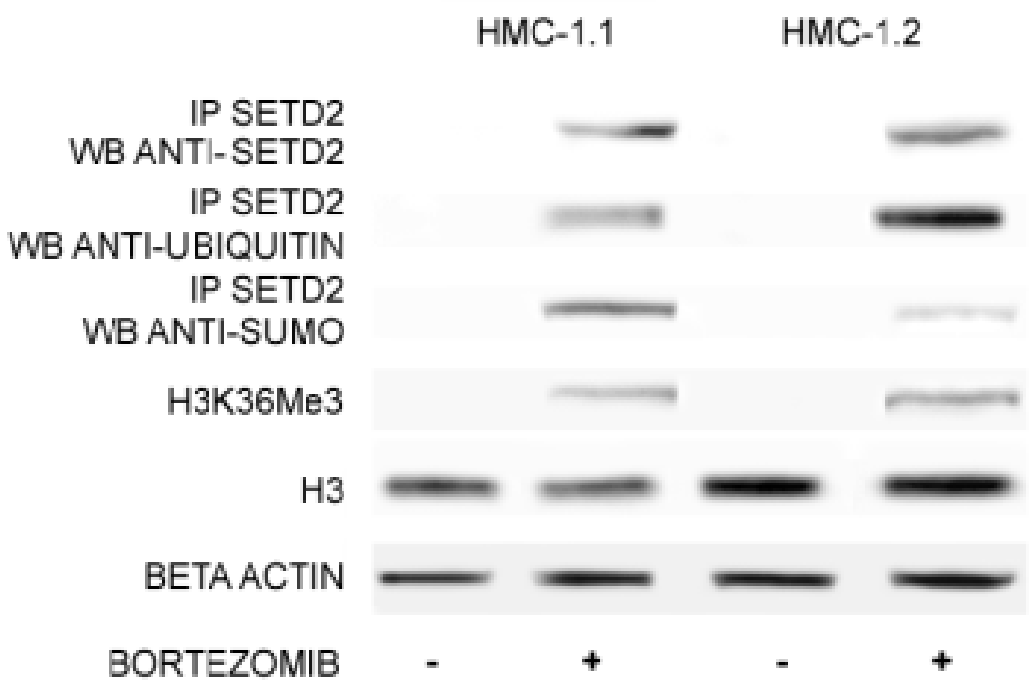

Figure 12. *Ubiquitinated and SUMOylated SETD2 after proteasome inhibition by bortezomib in HMC-1 cells*

We thus compared the effects of proteasome inhibition in malignant MCs from advanced SM patients displaying no SETD2 protein and from ISM patients with near-normal SETD2 levels. In contrast to SETD2-deficient patients, where results were superimposable to those obtained in HMC-1 cells, patients with near-normal SETD2 expression had similar levels of ubiquitinated and SUMOylated SETD2 protein (and similar H3K36Me3 levels) before and after the inhibition of proteasome-mediated degradation (Figure 13).

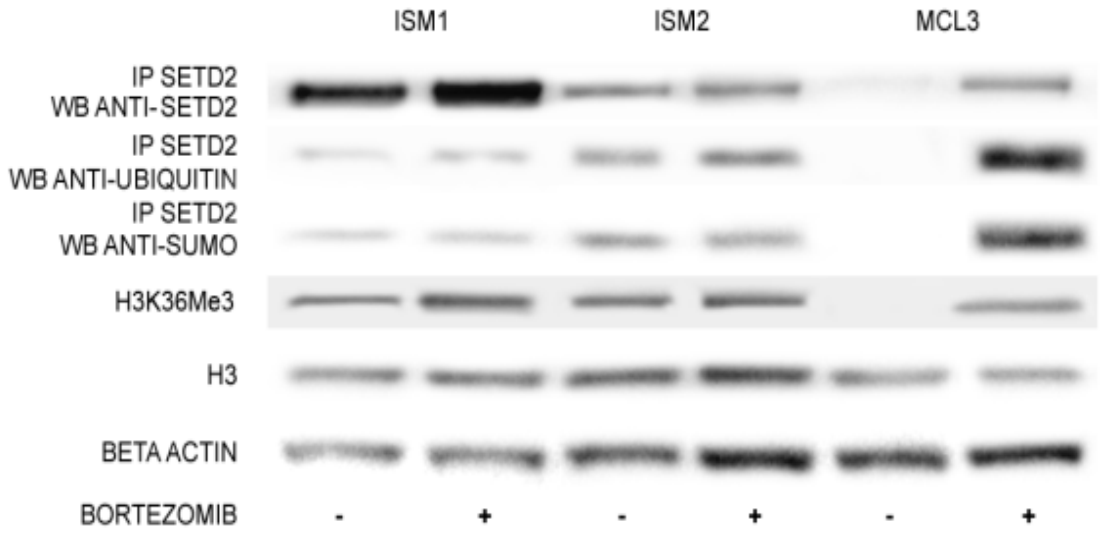

Figure 13. *Co-immunoprecipitation with an anti-SETD2 antibody and immunoblotting (western blotting) with anti-ubiquitin and anti-SUMO antibodies performed before and after bortezomib treatment (10 nM for 24 h)in two ISM patients and one MCL patient.*

Given the ability of bortezomib to rescue setd2 expression and H3K36Me3, we tested whether proteasome inhibition might be effective *in vitro* in HMC-1 cells. Bortezomib as single agent strikingly inhibited colony formation (LD50 in HMC-1.1 = 0.173 nM; LD50 in HMC-1.2 = 0.226 nM)(Figure 14).

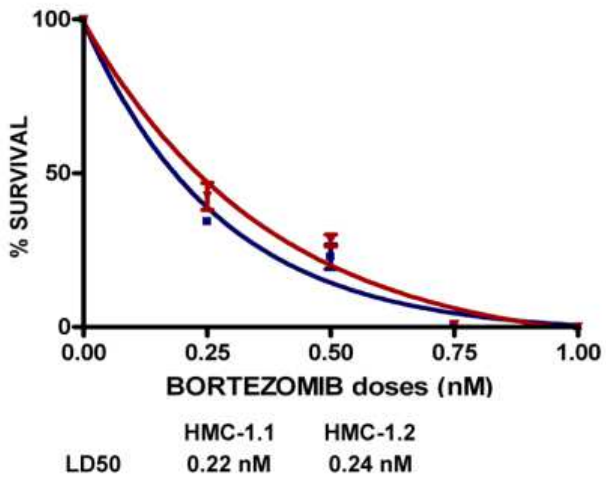

Figure 14. *Reduction of clonogenic growth in HMC-1.1 cells (red curve) and -1.2 cells (blue curve), in the presence of increasing doses of bortezomib (0.25–1 nM) used as single agent*

Moreover bortezomib reduce the clonogenic potential of setd2/H3K36Me3-deficient neoplastic MCs from two patients with MCL with no SETD2 expression (MCL3 and MCL7) and one patient with ASM (ASM18) with very low SETD2 expression (20% as compared to a pool of healthy donors). Bortezomib induced a marked dose dependent reduction in colony formation with LD50 ranging from 0.105 to 0.295 nM (Figure 15).

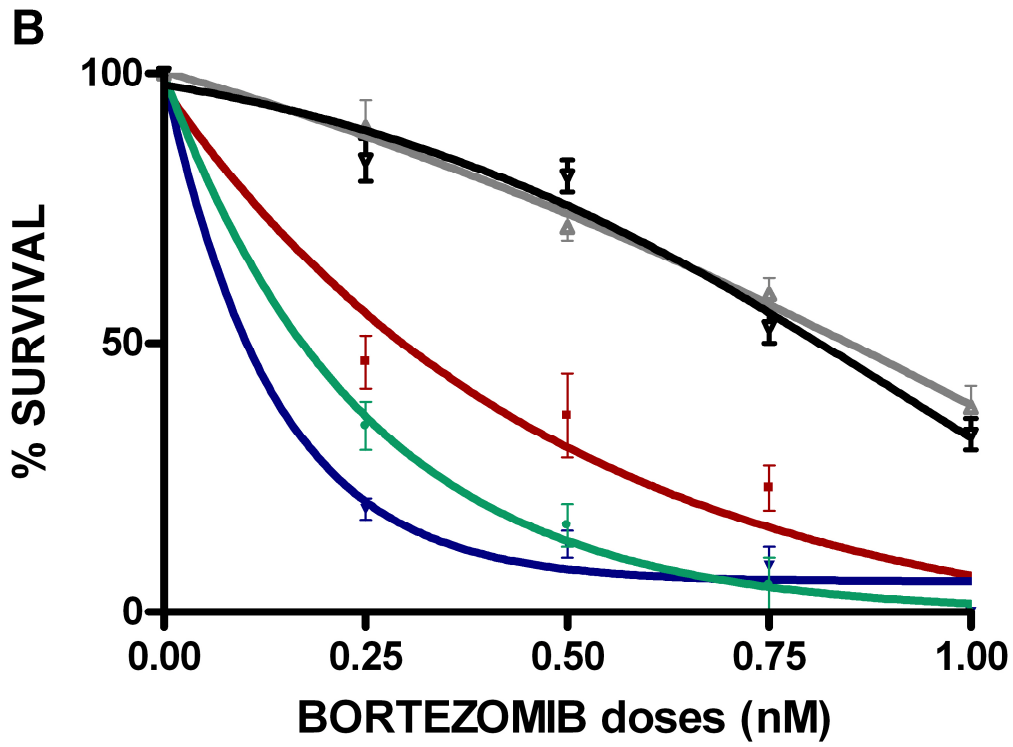

Figure 15.*Growth inhibition curves and LD50 values after Bortezomib treatment in cell*

5.1.5 Aurora Kinase A (AKA) and MDM2-mediated post-translational modifications contribute to SETD2 non genomic loss of function in Advanced SM

To investigate which were post-translational modifications affecting setd2 stability, we used an *"in silico"* approach and interrogated on-line databases (BioGRID) to identify candidate proteins with ubiquitin-ligase activity that could bind SETD2 and address it to proteasomal degradation. We found that SETD2 may bind the oncogene MDM2, which encodes an E3 ubiquitin ligase overexpressed in solid cancers (pancreatic cancer). We confirmed this observation through co-immunoprecipitation experiments after proteasome inhibition on HMC-1.1 and HMC-1.2 cells (Figure 16). Setd2 co-immunoprecipitation with MDM2 supported the interaction between the two proteins and MDM2 hyper-ubiquitination of setd2.

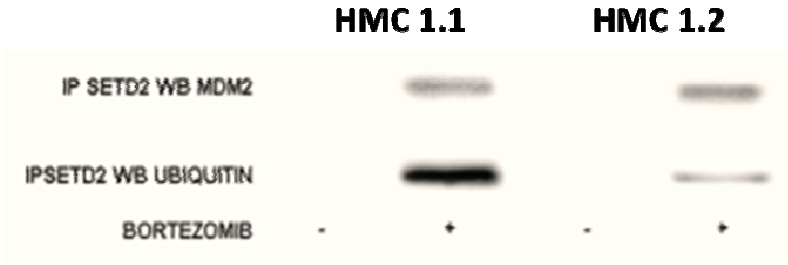

Figure 16. *After proteasome inhibition SETD2 levels restored and the interaction SETD2-MDM2 is revealed.*

To confirm our hypothesis, treatments with the MDM2 inhibitor SP-141 were performed: mdm2 inhibition rescued SETD2 expression and H3K36Me3, suggesting that mdm2 may play a role in SETD2 degradation in our *in vitro* models (Figure 17)[82]. Moreover, SP-141 treatment of HMC-1 cells at micromolar doses induced cytostatic but not cytotoxic effects as shown by cell growth curves. Clonogenic assays supported the cytostatic effects of SP141 in HMC-1.1 and -1.2 cells (Figure 18, 19). siRNA-mediated knock-down of MDM2 also rescued SETD2 expression and activity,

further supporting the hypothesis that SETD2 hyper-ubiquitination by MDM2 plays a role in SETD2 reduced stability and proteasomal degradation (data not shown).

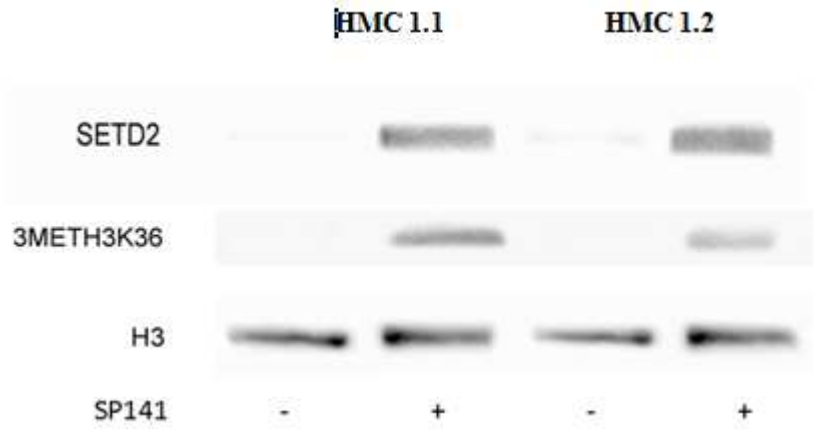

Figure 17. *Treatment of HMC-1.1 and HMC-1.2 with SP-141induce the restoration of normal SETD2 expression and activity.*

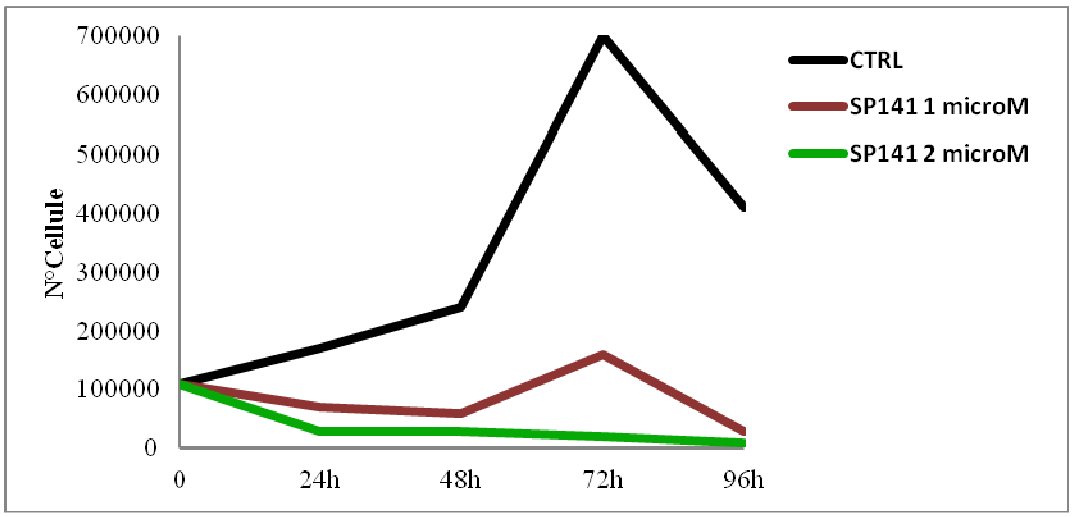

Figure 18. *Dose-survival curves of HMC 1.1 cell line treated with increasing dose of SP141 (96 h).*

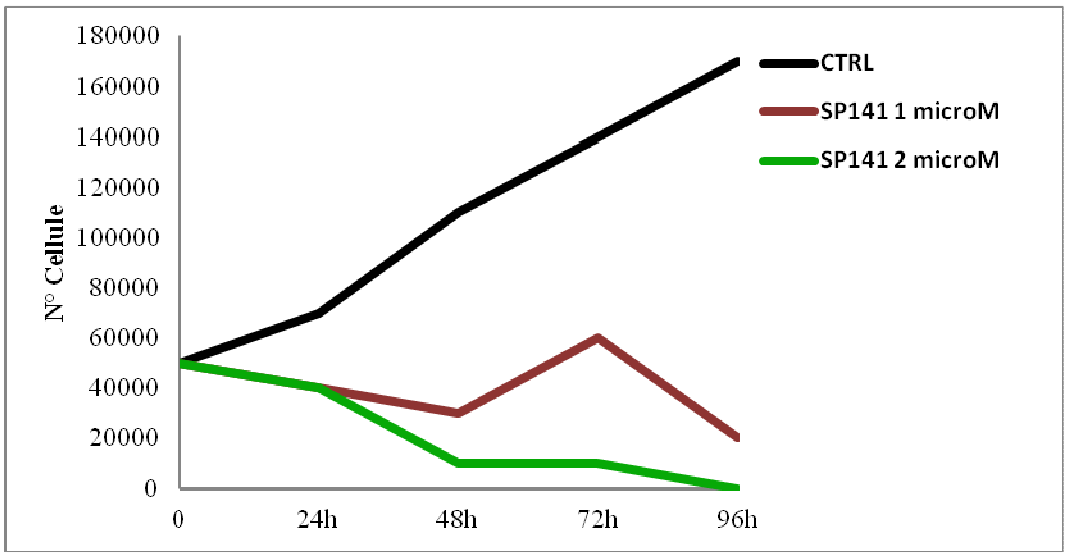

Figure 19. *Dose-survival curves of HMC 1.2 cell line treated with increasing dose of SP141 (96 h).*

Starting from the evidence that mdm2 inhibition did not result in cytotoxic effects we performed further *in silico* research to identify other possible setd2 ligands involved in its loss of stability.

The BioGRID database predicts that Aurora kinase A may also physically interact with SETD2. Accordingly, we found that activated Aurora A co-immunoprecipitates with SETD2 in the HMC-1 cell line after proteasome inhibition (Figure 20). We also found that Aurora A is aberrantly expressed and activated in advanced SM and this inversely correlates with setd2 expression (Figure 21). Both inhibition of kinase activity with Danusertib and down-modulation by siRNA rescued SETD2 expression (Figure 22). Taken together, these data suggest that phosphorylation by aberrantly expressed Aurora A may be one of the triggers of MDM-2 dependent SETD2

degradation and point to several druggable targets that are worth exploring in an attempt to rescue SETD2 expression.

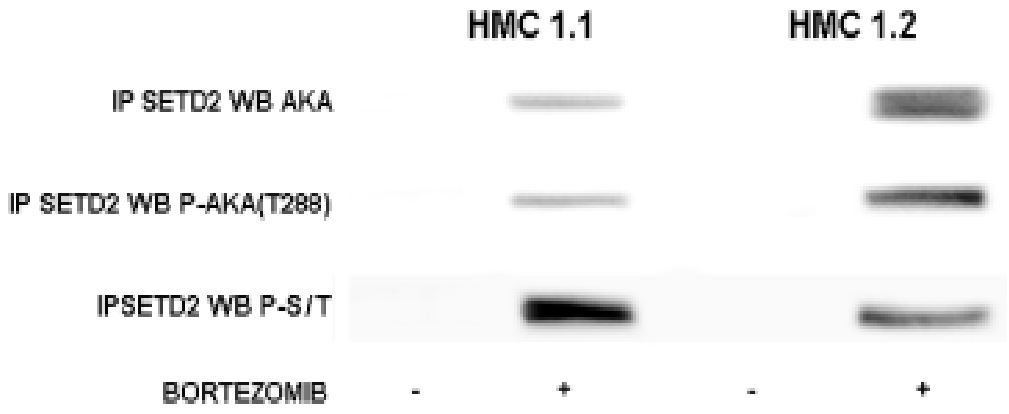

Figure 20. *Phosphorilation of SETD2 protein by AKA in HMC-1 cell lines.*

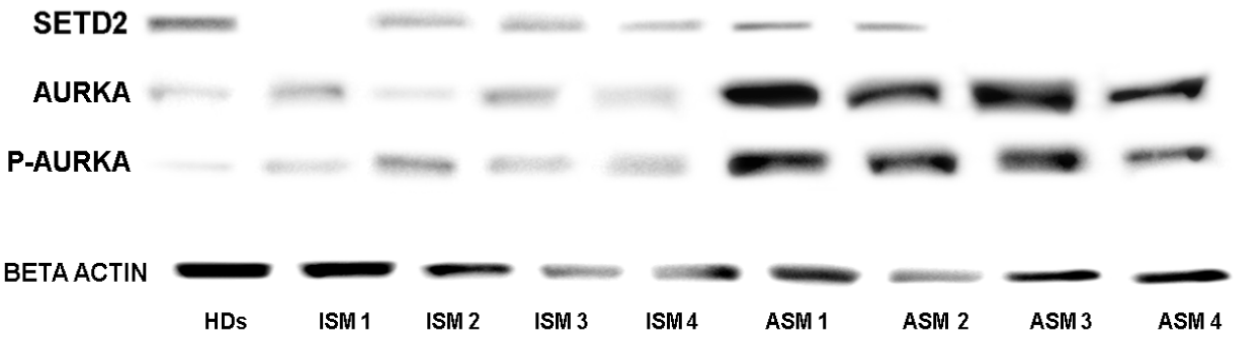

Figure 21. *Hyper-expression of AURKA in advanced forms of Systemic mastocytosis.*

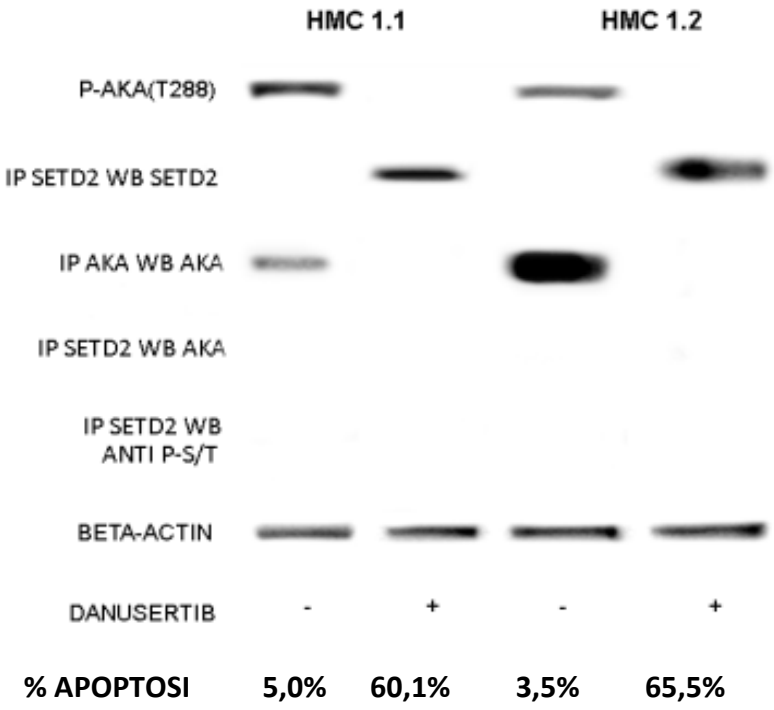

Figure 22. *Aurora A inhibition by danusertib correlates with Ser/thr unphoshorylated setd2 re-expression in HMC-1 cells..*

5.1.6 Setd2 non genomic loss of function induced p53 degradation, cell cycle and apoptosis deregulation

p53 is a transcription factor that plays a pivotal role in tumor suppression by directing cellular responses to diverse stresses including DNA damage and oncogene activation resulting in diverse biological effects. The wide range of p53's biological effects can in part be explained by its activation of expression of a number of target genes[83,84]. MDM2, a major ubiquitin E3 ligase for p53 and also the target of p53, plays an important role in down-regulating p53 activities. Recently, increasing amounts of data suggest that p53 stability and degradation are more complex than once thought[85].

In the present study, we identified SETD2 as an interacting protein of p53 *in vitro* through co-immunoprecipitation assay. SETD2 enhances the transcriptional activity of p53 and regulates expression of select p53 target genes. We also demonstrate that loss of SETD2 may affect the stability of p53 protein, by contrast rescue of SETD2 after proteasomal inhibition stabilized p53 and activated its target genes transcription (Figure 23).

In particular in HMC-1 cell line we confirmed what has been already reported in ccRCCs, p53 co-immunoprecipitates with setd2 after proteasome inhibition. Moreover, we observed that rescuing the interaction between setd2 and p53 with bortezomib stabilized p53 and up-regulated a subset of p53 targets including p21, p27, Bax and Gadd45a (Fig. 23). This restored inhibition of cell proliferation, block of the transition towards cell cycle checkpoints and consequent activation of apoptosis.

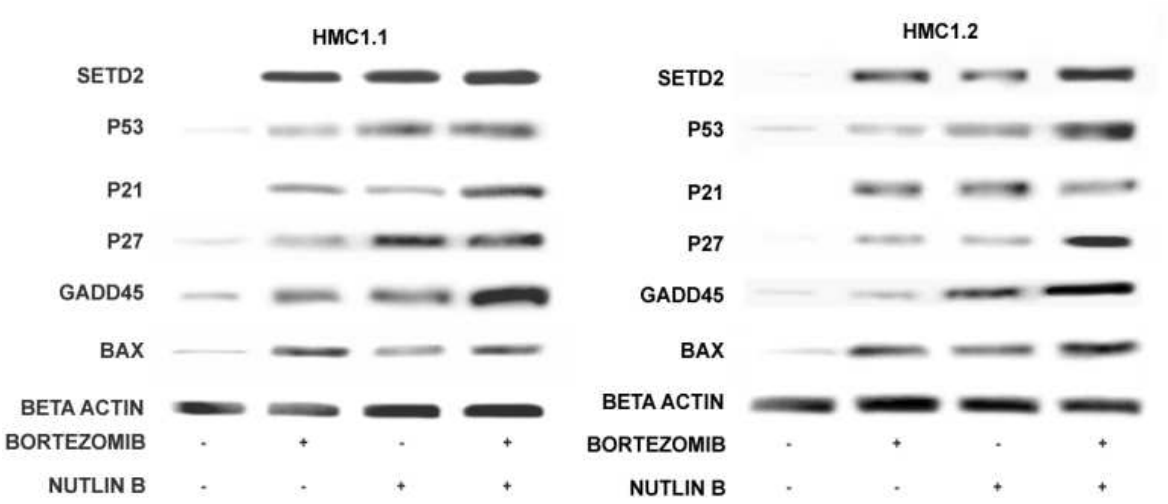

Figure 23. *WB showing the expression of p53-target genes after SETD2 re-expression by bortezomib in*

HMC-1cells.

5.1.7 Loss of SETD2 and H3K36Me3 is associated with increased DNA damage

Recent studies have established a role for SETD2 and H3K36 trimethylation in HR repair of double strand breaks (DSBs) in human cells (Pfister, Cell Rep 2014; Carvalho, Elife 2014). SETD2 was found to promote the formation of Rad51 foci, and SETD2 depletion generated a mutation signature with significantly increased deletions arising through microhomology-mediated end-joining. To investigate whether increased DNA damage and reduced HR proficiency can be observed also in SETD2/H3K36Me3-deficient SM, we used immunofluorescence to assess phosphorylated histone 2A.X (H2AX), which marks ongoing DNA damage signalling and DNA DSBs (Lukas, Nat Cell Biol 2011) and Rad51, which we used as a surrogate for active HR. With respect to cells from healthy controls, cells from SETD2- and H3K36Me3-deficient patients had significantly higher levels of H2AX (Figure 24). However, Rad51 levels in MCL cells were comparable to those of controls, suggesting the possibility that in SETD2/H3K36Me3-deficient SM enhanced DNA damage may less efficiently be addressed by HR repair mechanisms.

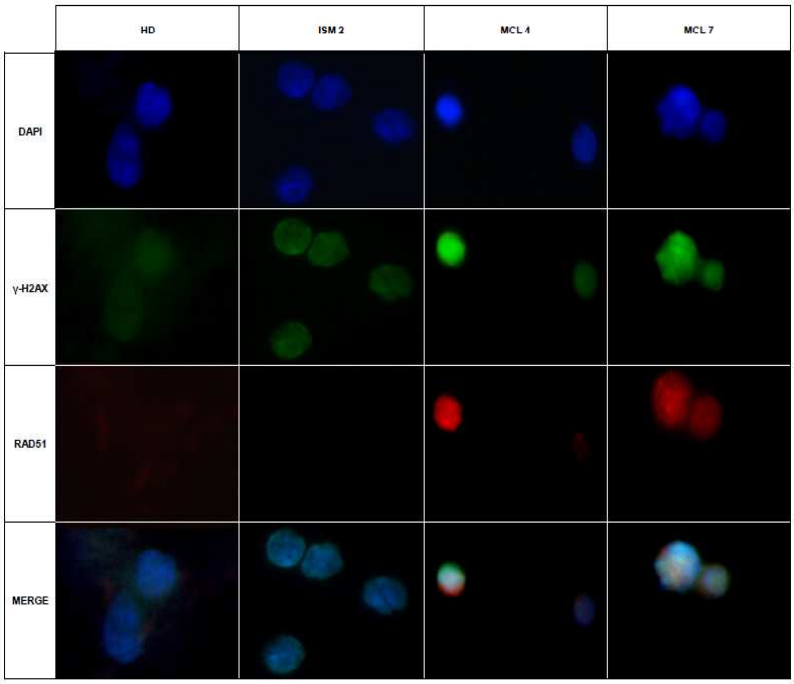

Figure 24. *Immunofluorescence analysis of H2AX phosphorilation (green) and Rad51 (red) expression in mononuclear cells from a HD, an ISM patient and two MCL patients. Nuclei were marked with DAPI (Blue).*

Next, to correlate setd2 loss of function and genomic instability in SM the ROSA^{D816V} cell line was used as in vitro model. ROSA^{D816V} cells display SETD2 and H3K36me3 levels superimposable to healthy donors, therefore were studied by WB and IF to assess γH2AX and Rad51 in steady state and after sub-lethal DNA damage by UV exposure. The same experiments were carried out after SETD2 silencing for 2 months. Cells with silenced SETD2 had significantly higher levels of γH2AX and were unable to activate the HR repair (Figure 25).

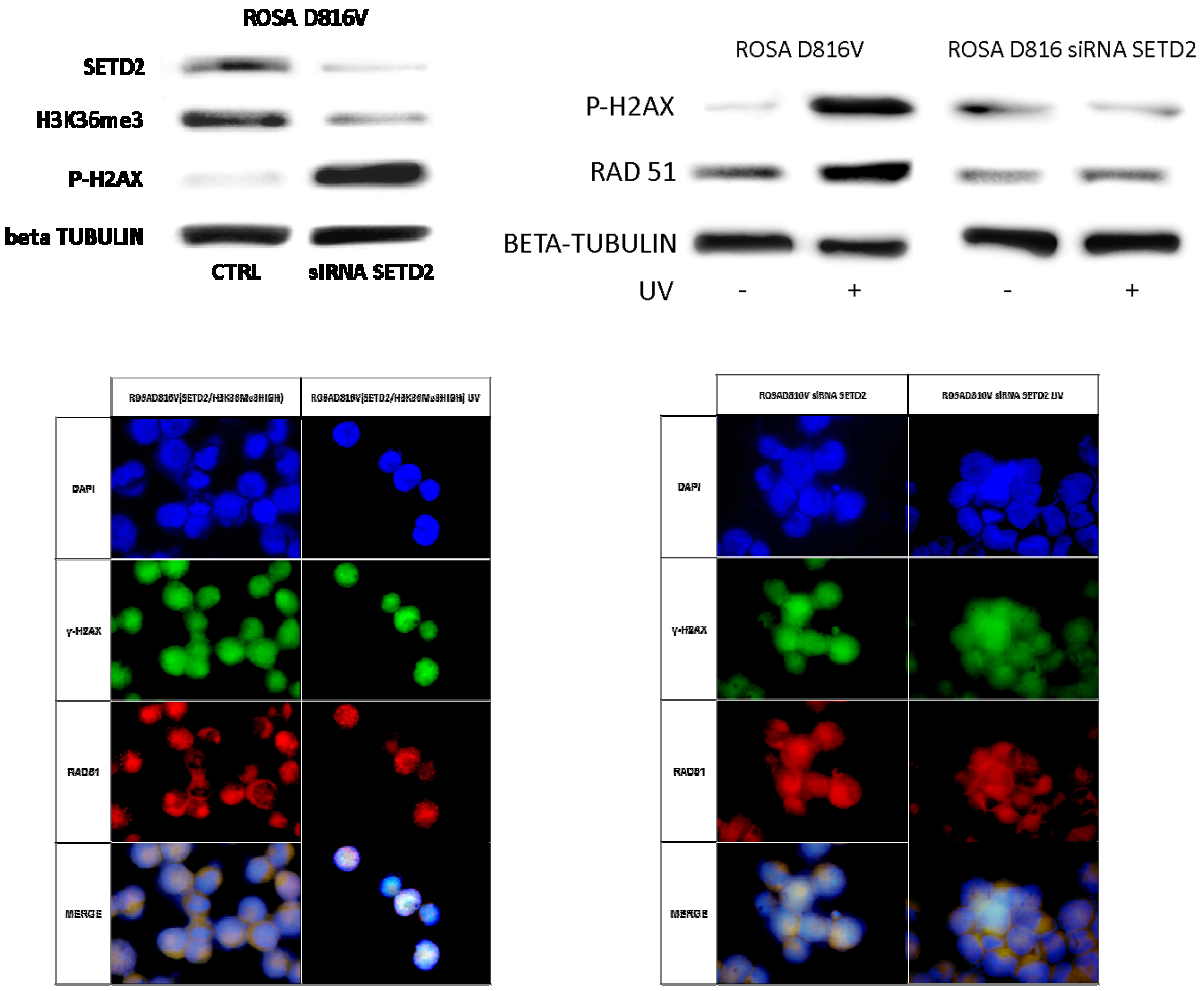

Figure 25. *Western blotting and immunofluorescence analysis of H2AX phosphorilation (green) and Rad51 (red) expression in parental ROSAD816V cell line and after setd2 silencing. Nuclei were marked with DAPI (Blue).*

5.1.8 Effects of midostaurin on MCs

On the basis of the observation that hyper-phosphorylation of Aurora Kinasi A in the advanced forms of SM and aware of the effects of the inhibitors on the cell lines tested *in vitro*, we decided to investigate the possibility of testing Midostaurin (PKC 412), in the same experimental setting. Midostaurin is a pan-inhibitor that has among its molecular targets: KIT (both wild-type and mutated D816V), FLT3, PDGFRA and PDGFRB, IGF1R, LYN, PDPK1, RET, SYK, TRKA, VEGFR2, and also AKA and AKB[41].

Therefore we investigated if midostaurin effects may be addressed to AKA inhibition and consequent SETD2/H3K36me3 rescue. To this purpose, HMC-1 cells were treated with 5 µM midostaurin for 24 h and AKA, SETD2 and H3K36me3 expression were evaluated by western blotting (Figure 26). Treatment with midostaurin was able to inhibit AKA activity by about 60%, partially restoring SETD2 expression and H3K36Me3. Moreover, midostaurin treatment of HMC-1 cells at micromolar doses induced cytostatic but not cytotoxic effects as shown by cell growth curves performed in liquid medium (Figure 27).

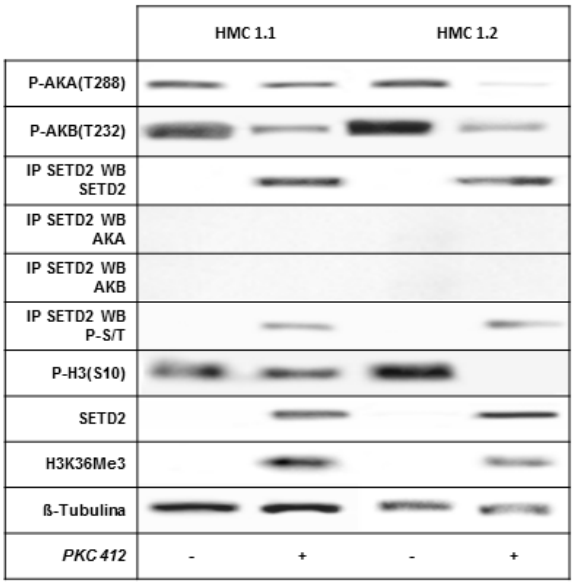

Figure 26. *Western blotting, immunoprecipitation and co-immunoprecipitation after Midostaurin treatment in HMC 1.1 and HMC 1.2.*

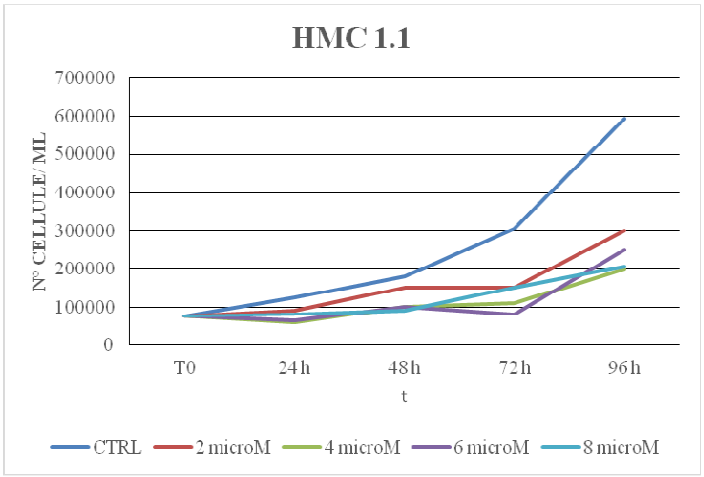

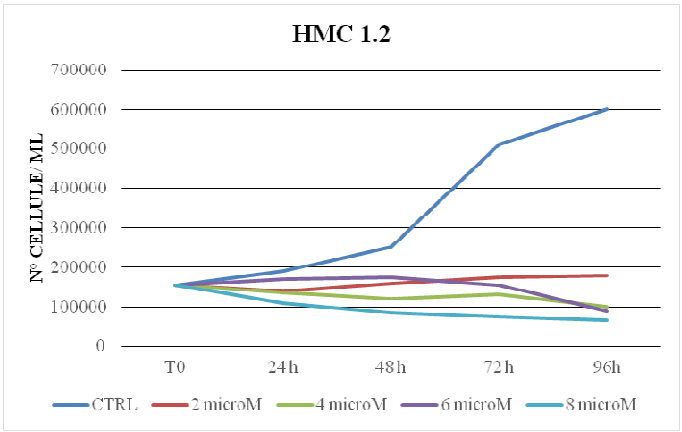

Figure 27*: Dose-survival curves of HMC 1.1 and 1.2 cell lines treated with increasing dose of Midostaurin.*

Our results suggest that AKA-mediated post-translational modifications contribute to SETD2 non-genomic loss of function in advSM. Inhibiting AKA and c-Kit activity by Midostaurin is a promising therapeutic strategy in patients with SETD2/H3K36Me3 deficiency.

Finally, our observations in cell lines were confirmed in neoplastic mast cells collected from three patients with advSM before and after three months of midostaurin treatment. Western blotting showed that midostaurin treatment *in vivo* indeed results in a rescue of SEDT2 expression and activity.

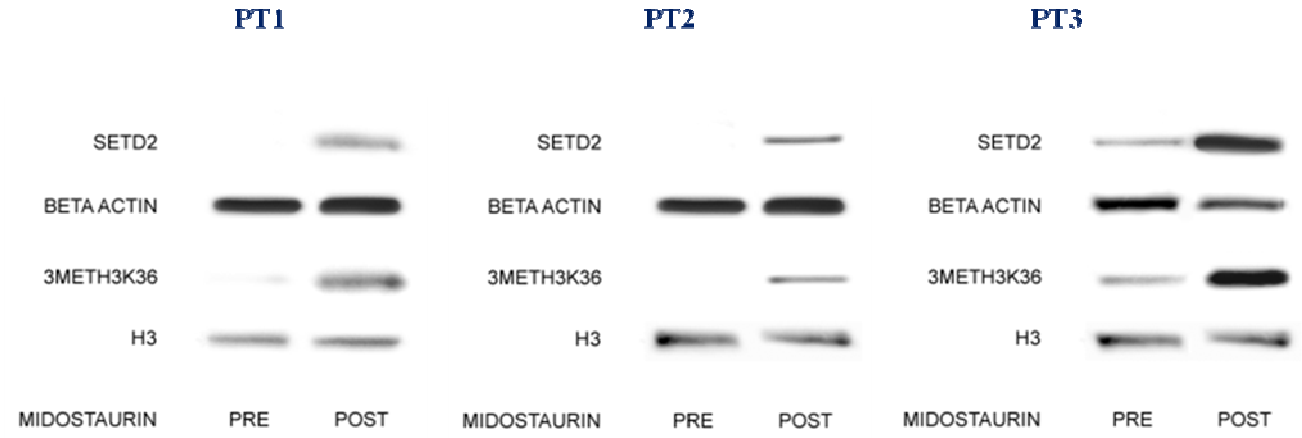

Figure 28. WB pre and post Midostaurin therapy in SM patients

5.2 AIM2: Clinical implication of SETD2 inactivation in SM

5.2.1 Patients and characteristics

The study included 88 patients with a median age of 58 years (range 19-78). The diagnosis were: ISM (n=44), SSM (n=5), SM-AHN (n= 10), including ISM-AHN (n=2, one associated with indolent non Hodgkin Lymphoma and one with myelodisplastic/myeloproliferative neoplasm unclassified), ASM-AHN (n=5 , two cases associated with Myelomonocytic leukemia, two cases associated with myelodisplastic syndrome, and one Acute myeloid leukemia), MCL-AHN (n=3, two cases

associated with a myelodisplastic syndrome and one with Acute Myeloid leukemia), ASM (n=17), MCL(n=12).

In the entire cohort, 56.3% were males, mostly represented in ISMs, as reported in [5, 16]. Median age at diagnosis was 58 years (range 19-78) and it was lower (50 years) in the ISMs group compared with all other subtypes ($p<0.001$). Clinically, in the entire cohort skin lesions were present in 48.9% of patients, with a higher prevalence among ISM and SSM subtypes ($p< 0.001$) whereas severe anaphylaxis reactions in 34.1%, again with higher percentages among ISM and SSM ($p<0.001$). Other mediator-related or systemic symptoms were present in 62.5%, with no significant association with WHO subtypes ($p=0.153$); osteoporosis was reported in 37.1% and osteopenia in 71.0%, without significant association with any WHO subtypes ($p = 0.203$ and $p= 0.282$ respectively); palpable splenomegaly in 29.1% with a very low prevalence (2.3%) in ISM subtype compared to the other WHO subtypes. Anemia defined by hemoglobin < 10 g/dL was present in 19.5% whereas platelet count below the limit of 100 x 109/L in 19.5%. For both these variables prevalence was particularly low for the ISM and the SSM WHO subtypes ($p<0.001$). No statistically significant differences were observed among the subtypes for WBC and Eosinophils count ($p=0.199$ and $p=0.203$); serum alkaline phosphatase (ALP) above the upper normal limit of the reference range (> 104 U/L) in 38.1%, with association with WHO subtype ($p<0.001$; different lactate dehydrogenase [LDH]value (U/L) resulted associated with WHO categories ($p=0.035$); serum tryptase level >200 ug/L was present in 21.8%, whereas serum tryptase level > 20 ug/L in 79.3% of patients, with lower levels in ISM compared to the other forms ($p<0.001$ and $p=0.003$ respectively). Table 8 lists clinical and laboratory characteristics at SM diagnosis.

The D816V KIT mutation result present in 81/88 patients. Four MCL resulted negative, and in 3 patients a diffrent mutation was detected: D816H in two patients (1 MCL and 1 SM.AHN), and mutation S476 in MCL.

Cytoreductive treatment in 30/37 patients with advSM included midostaurin (n = 9), cladribine (n = 6), cladribine following midostaurin or vice versa (n = 4), dasatinib (n = 3) or cladribine (n = 2) followed by intensive chemotherapy with (n = 1) or without (n = 4) allogeneic stem cell transplantation. Ten patients were treated with hydroxyurea (n = 2), imatinib then dasatinib (n=1), nilotinib (n = 2) or azacitidine (n = 1).

Characteristics	**All patients (n=88)**		**ASM (n=17)**		**ISM (n=44)**		**MCL (n=12)**		**SSM (n=5)**		**SM-AHN (n=10)**		**P**
	n	**%**	***n***	**%**	***n***	**%**	***n***	**%**	***n***	**%**	***n***	**%**	
Gender													
F	42	47.7	10	58.8	18	40.9	7	58.3	4	80.0	3	30.0	0.257
M	46	52.3	7	41.2	26	59.1	5	41.7	1	20.0	7	70.0	
Age (years): median (min-max)	58 (19 – 78)		63 (30-77)		50 (19-72)		64 (32-78)		61 (57-65)		69 (55-76)		**<0.001**
≤ 65	68	77.3	11	64.7	42	95.5	7	58.3	5	100.0	3	30.0	**<0.001**
> 65	20	22.7	6	35.3	2	4.5	5	41.7	0	0.0	7	70.0	
Hemoglobin (g/dl): median (min-max)†	13.4 (6.7 – 17.5)		11.7 (8.3-14.0)		14.5 (9.3-17.5)		10.1 (7.7-15.6)		12.5 (12.0-14.8)		10.3 (6.7-16.5)		**<0.001**
≥ 10	70	80.5	11	68.8	43	97.7	6	50.0	5	100.0	5	50.0	**<0.001**
< 10	17	19.5	5	31.3	1	2.3	6	50.0	0	0.0	5	50.0	
Leukocyte count (x 10^9/L): median (min-max)†	6.2 (1.9 – 76.0)		7.9 (3.4-21.6)		5.8 (3.0-76.0)		4.6 (2.9-54.6)		7.6 (4.7-9.1)		8.1 (1.9-63.9)		0.199
Platelet count (x 10^9/L): median (min-max)†	227.0 (13.0 – 979.0)		166.5 (42-470)		249 (113-366)		182 (53-464)		245 (208-355)		132 (13-979)		**0.001**
≥ 100	70	80.5	9	56.3	44	100.0	7	58.3	5	100.0	5	50.0	**<0.001**
< 100	17	19.5	7	43.8	0	0.0	5	41.7	0	0.0	5	50.0	
Serum tryptase (ug/L): median (min-max)†	52 (4.7 – 2250.0)		200 (26-1900)		28.6 (4.7-94.8)		287 (30.8-2250)		140 (18.8-250)		115 (14-1310)		**<0.001**
≤ 200	68	78.2	10	58.8	43	97.7	5	45.5	3	60.0	7	70.0	**<0.001**
> 200	19	21.8	7	41.2	1	2.3	6	54.5	2	40.0	3	30.0	
Serum tryptase (ug/L)†													
< 20	18	20.7	0	0.0	16	36.4	0	0.0	1	20.0	1	10.0	**0.003**
≥ 20	69	79.3	17	100.0	28	63.6	11	100.0	4	80.0	9	90.0	
Skin lesions													
No	45	51.1	11	64.7	14	31.8	10	83.3	2	40.0	8	80.0	**0.002**
Yes	43	48.9	6	35.3	30	68.2	2	16.7	3	60.0	2	20.0	
Mast cell mediator symptoms													

No	33	37.5	3	17.7	22	50.0	4	33.3	1	20.0	3	30.0	0.153
Yes	55	62.5	14	82.3	22	50.0	8	66.7	4	80.0	7	70.0	
Severe anaphylaxis reactions													
No	58	65.9	17	100.0	19	43.2	11	91.7	2	40.0	9	90.0	**<0.001**
Yes	30	34.1	0	0.0	25	56.8	1	8.3	3	60.0	1	10.0	
Palpable splenomegaly[†]													
No	61	70.9	5	32.3	43	97.7	6	54.6	2	40.0	5	50.0	**<0.001**
Yes	25	29.1	11	68.7	1	2.3	5	45.4	3	60.0	5	50.0	
Osteopenia[†]													
No	18	29.0	2	25.0	9	22.5	3	60.0	2	50.0	2	40.0	0.282
Yes	44	71.0	6	75.0	31	77.5	2	40.0	2	50.0	3	60.0	
Osteoporosis[†]													
No	39	62.9	3	37.5	27	67.5	3	60.0	4	100.0	2	40.0	0.203
Yes	23	37.1	5	62.5	13	32.5	2	40.0	0	0.0	3	60.0	
Serum ALP (U/L) [†]													
≤ 104	39	61.9	3	25.0	28	82.3	4	66.7	1	25.0	3	42.9	**0.001**
> 104	24	38.1	9	75.0	6	17.7	2	33.3	3	75.0	4	57.1	
Serum LDH (U/L): median (min-max)[†]	*186 (46 - 712)*		338 (113-564)		182.5 (90-384)		149 (117-290)		125.5 (46-189)		215 (130-712)		**0.035**
Follow-up (months): median (min-max)	3.4 (0.5-15.4)		7.6 (5.1-9.4)		2.5 (0.5-15.2)		1.6 (0.9-2.4)		8.2 (1.6-15.4)		3.2 (2.7-5.8)		
Deaths	29	33.3	10	62.5	2	4.6	10	83.3	0	0.0	7	70.0	**<0.001**
SETD2 protein levels: median (min-max)	0.42 (0.0-1.0)		0 (0.0-0.80)		0.69 (0.0-1.0)		0 (0.0-0.76)		0.24 (0.0-0.86)		0 (0.0-1.0)		**<0.001**
H3k36me3 protein levels: median (min-max)	0.33 (0.0-1.12)		0 (0.0-0.85)		0.69 (0.0-1.12)		0 (0.0-1.0)		0.17 (0.0-0.67)		0.16 (0.0-0.79)		**<0.001**

Table 8. *Comparison of the clinical characteristics of patients among WHO different subtypes*

5.2.2 SETD2 expression and H3K36Me value confirm their association with WHO subtype

With our previous results (Leukemia, 2018) we had showed that MCL and ASM had significantly lower levels of SETD2 protein ($p<0.001$ and $p=0.002$, respectively) and H3K36Me3 ($p<0.001$ and $p=0.004$, respectively) as compared to ISM. The updated analysis carried out on an extended series, including a higher number of non-advanced forms, confirms those results. The distribution of SETD2 and H3K36Me3 values was quite different among the WHO subtypes ($p<0.001$ in both cases)(Figure 29). In particular the median SETD2 values were 0 (range 0.0-0.80) in ASMs, 0 (range 0.00-0.76) in MCLs, and 0 (range 0.00-1.00) in SM-AHN 0.24 (range 0.0-0.86) in the SSMs, and 0.69 (range 0.00-1.00) in the ISMs. Similar results were obtained for the H3K36Me3 values ($p <0.001$),

(Figure30) median of 0 (range 0.0-0.85) in the ASMs, 0 (range 0.0-1.0) in the MCLs, 0.16 (range 0.0-0.79) in the SM-AHNs , 0.17 (range 0.0-0.67) in the SSM, 0.69 (range 0.0-1.12) in the ISMs.

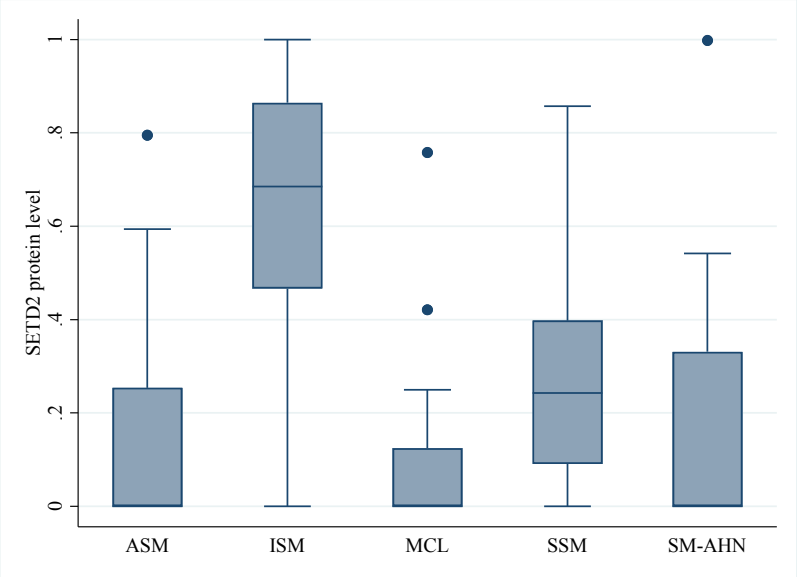

***Figure 29**. Boxplot of SETD2 values distribution among the WHO subtypes*

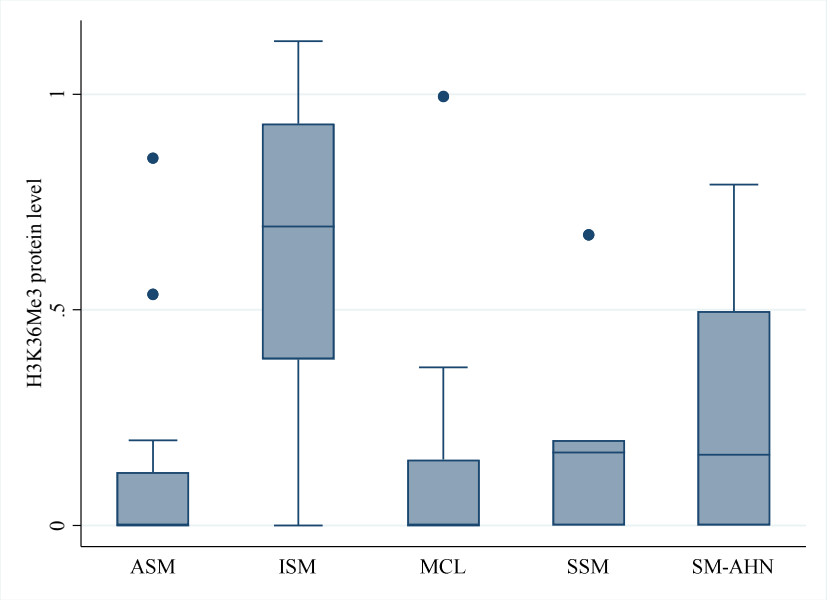

***Figure 30**. Boxplot of H3K36Me3 values distribution among the WHO subtypes*

5.2.3 Statistical correlation between SETD2 expression value and trimethylation

SETD2 is the only gene responsible for histone H3 trimethylation in Lisine 36, but the regulatory network controlling access to and modification of the H3K36 substrate remain complex and poorly understood, so we wondered if SETD2 expression and the related value of H3k36Me3 were two interchangeable measurements as they are thought to be. The correlation between SETD2 and trimethylation values was rather high (Pearson's coefficient of 0.897), although not perfect, meaning that there are probably many biological factors involved in the global process of DNA methylation in patients with mastocytosis, of any WHO subtype.

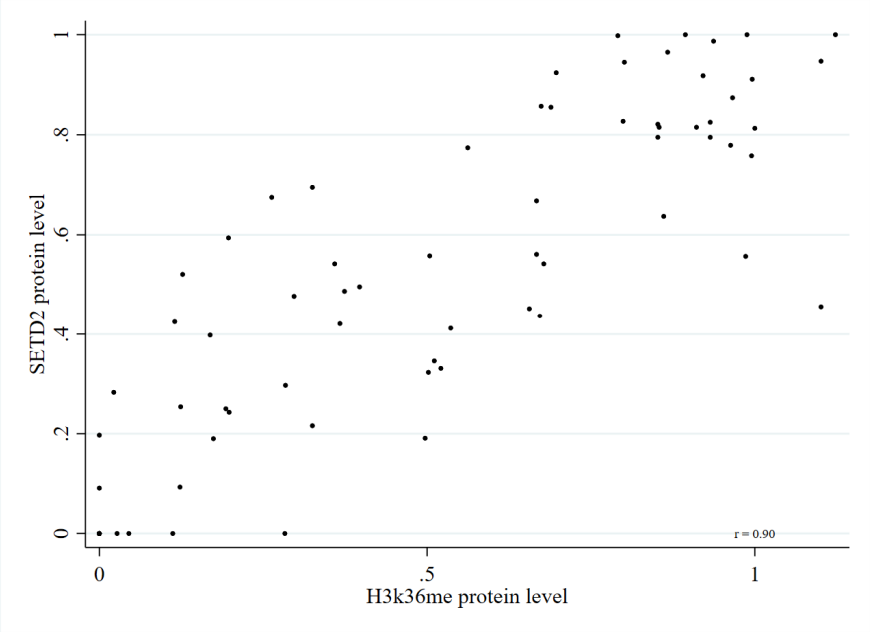

Figure 31. *Pearson's correlation between SETD2 and trimethylation valuesin 88 patients*

5.2.4 Identification of a threshold of SETD2 expression and H3K36Me3 level than can identified Indolent Systemic mastocytosis

In order to evaluate the diagnostic accuracy of SETD2 in distinguishing between forms of indolent mastocytosis, characterized by the absence of any sign of organ infiltration by the mast cells (absence of B-findings) from all others (thus also excluding the Smoldering forms), the ROC curve

was used. This analysis together with the use of some statistical methods, among which the Youden index, allowed to identify a cut-off for SETD2 corresponding to high levels of sensitivity and specificity. Through ROC curve analysis, we found that the SETD2 value of 0.425 discriminated ISM from other subtypes with a sensitivity of 84.09% and specificity of 86.36% (45 patients had a value <0.425, 43 patients ≥0.425). The area under the curve (AUC) was 0.87 (95% CI: 0.79-0.95). We also found that the H3K36Me3 value of 0.284 could discriminate quite well the two SM classes (ISM vs other subtypes). Associated sensitivity and specificity were of 86.36% and 79.55%, respectively (41 patients had a value <0.284, 47 patients ≥0.284). AUC was equal to 0.87 (95% CI: : 0.79-0.95).

5.2.5 Correlation between SETD2 expression, clinical phenotype and OS

Overall, 29 deaths were observed in this study. The median follow-up, computed only on censored patients, was 3.4 years (range 0.5-15.4). OS for each WHO subtype is reported in figure 32.

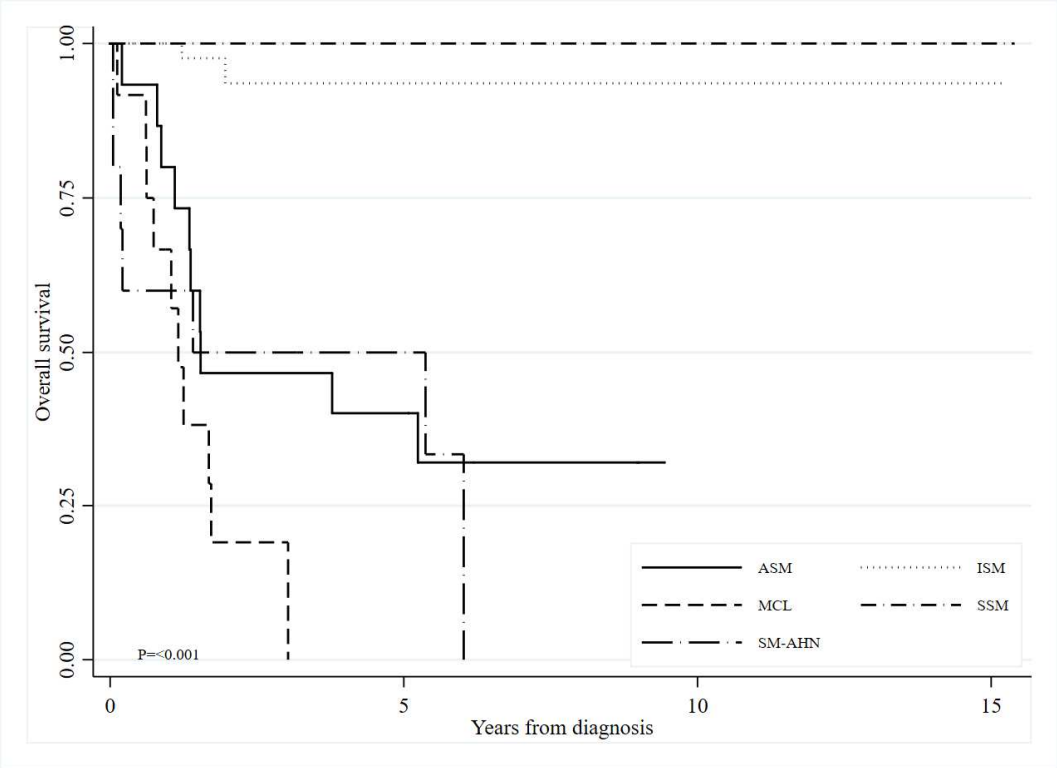

Figure 32. *Kaplan–Meier estimates of OS of patients depending on WHO category in 88 patients with SM*

The SETD2 expression assessed in terms of a binary variable using the ROC-based cut-off was significantly associated with OS (Figure 33). The same was observed for H3K36Me3 (Figure 34). For both markers, values above the cut-off were associated with longer OS. Median OS was not reached (NR) in patients with SETD2 value ≥0.425 whereas was equals to 3.0 (1.37 – NR) for those with lower values. With regard to H3K36Me, median OS was not reached for patients with values above the cutoff and equals to 3.78 (1.25-NR) for those with lower values.

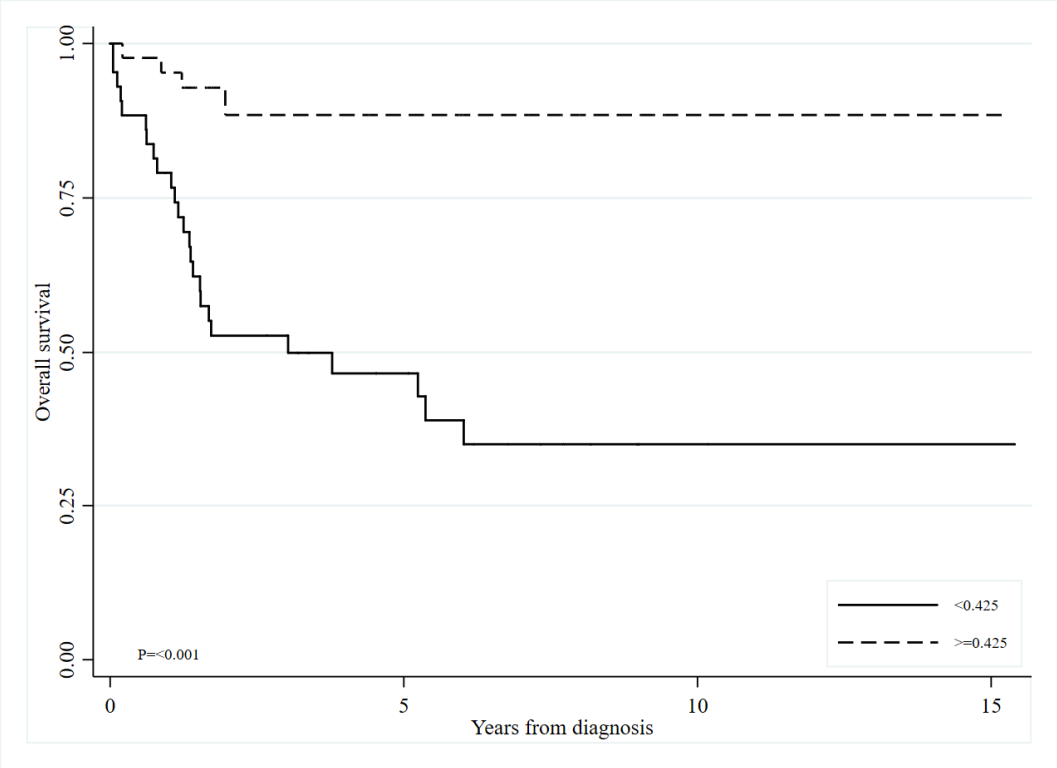

Figure 33: *Kaplan–Meier estimates of OS of patients depending on the SETD2 expression level by WB in 88 patients with SM*

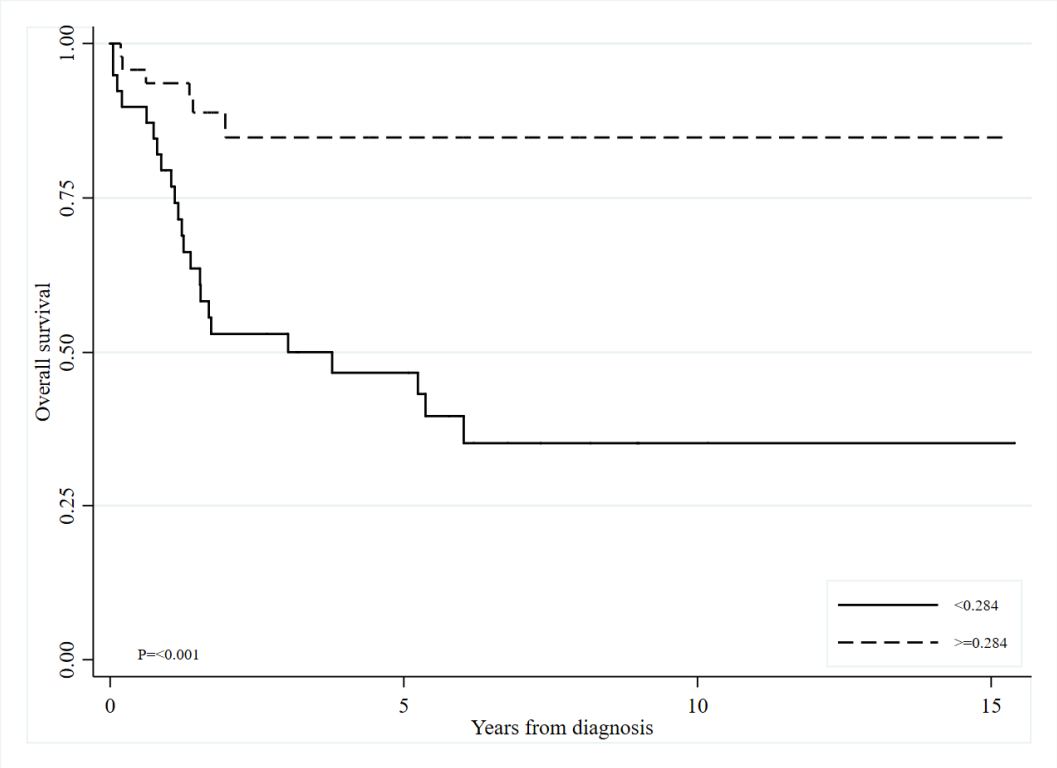

Figure 34. Kaplan–Meier estimates of OS of patients depending on the H3K36Me3 value by WB in 88 patients with SM

In ISM (n = 44, 50% of all patients), a SETD2 value <0.425 was observed in 7/44 patients (15.9%). In contrast, a SETD2 value ≥0.425 was present in 34/37 (91.9%) patients with AdvSM (ASM, ASM-AHN, MCL, MCL-AHN). The comparison between a SETD2 value <0.425 and a SETD2 value ≥0.425 revealed significant differences in almost all parameters, including age, Hb and Platelets level, serum alkaline phosphatase (ALP), serum tryptase and clinical parameters considered as the presence of skin lesions, severe anaphylaxis reactions, palpable splenomegaly (Table 8).

Characteristics	**All patients**		**SETD2 value**				**P**	**H3k36me value**				**P**
			<0.425 (n=45)		**≥0.425 (n=43)**			**<0.284 (n=41)**		**≥0.284 (n=47)**		
	n	**%**	***n***	**%**	***n***	**%**		***n***	**%**	***n***	**%**	
Gender												
F	42	47.7	26	57.8	16	37.2	0.053	23	56.1	19	40.4	0.142
M	46	52.3	19	42.2	27	62.8		18	43.9	28	59.6	

Age (years): median (min-max)	58 (19 – 78)		63 (31-78)		52 (19-71)		**<0.001**	63 (31-78)		53 (19-75)		**0.024**
≤ 65	68	77.3	28	62.2	40	93.0	**0.001**	27	65.9	41	87.2	**0.017**
> 65	20	22.7	17	37.8	3	7.0		14	34.2	6	12.8	
Hemoglobin (g/dl): median (min-max)[†]	13.4 (6.7 – 17.5)		11.6 (6.7-15.9)		14.4 (9.3-17.5)		**<0.001**	12 (6.7-14.8)		14.6 (7.9-17.5)		**<0.001**
≥ 10	70	80.5	28	63.6	42	97.7	**<0.001**	26	65.0	44	93.6	**0.001**
< 10	17	19.5	16	36.4	1	2.3		14	35.0	3	6.4	
Leukocyte count (x 10^9/L): median (min-max)[†]	6.2 (1.9 – 76.0)		7.0 (1.9-63.9)		5.8 (3.0-76.0)		0.306	6.6 (1.9-63.9)		6 (3-76)		0.586
Platelet count (x 10^9/L): median (min-max)[†]	227.0 (13.0 – 979.0)		191 (13-470)		248 (113-979)		**0.001**	191 (19-470)		242 (13-979)		**0.006**
≥ 100	70	80.5	27	61.4	43	100.0	**<0.001**	26	65.0	44	93.6	**0.001**
< 100	17	19.5	17	38.6	0	0.0		14	35.0	3	6.4	
Serum tryptase (ug/L): median (min-max)[†]	52 (4.7 – 2250.0)		171 (18.8-2250.0)		25.3 (52-4.7)		**<0.001**	152 (7.6-2250)		30.3 (4.7-2000)		**<0.001**
≤ 200	68	78.2	26	59.1	42	97.7	**<0.001**	25	62.5	43	91.5	**0.002**
> 200	19	21.8	18	40.9	1	2.3		15	37.5	4	8.5	
Serum tryptase (ug/L)[†]												
< 20	18	20.7	1	2.27	17	39.5	**<0.001**	2	5.0	16	34.0	**0.001**
≥ 20	69	79.3	43	97.7	26	60.5		38	95.0	31	66.0	
Skin lesions												
No	45	51.1	31	68.9	14	32.6	**0.001**	29	70.7	16	34.0	**0.001**
Yes	43	48.9	14	31.1	29	67.4		12	29.3	31	66.0	
Mast cell mediator symptoms												
No	33	37.5	14	31.1	19	44.2	0.205	13	31.7	20	42.6	0.294
Yes	55	62.5	31	68.9	24	55.8		28	68.3	27	57.5	
Severe anaphylaxis reactions												
No	58	65.9	38	84.4	20	46.5	**<0.001**	37	90.2	21	44.7	**<0.001**
Yes	30	34.1	7	15.6	23	53.5		4	9.8	26	55.3	
Palpable splenomegaly[†]												
No	61	70.9	23	53.5	38	88.4	**<0.001**	21	53.9	40	85.1	**0.001**
Yes	25	29.1	20	46.5	5	11.6		18	46.2	7	14.9	
Osteopenia[†]												
No	18	29.0	7	28.0	11	29.7	0.883	8	38.1	10	24.4	0.261
Yes	44	71.0	18	72.0	26	70.3		13	61.9	31	75.6	
Osteoporosis[†]												
No	39	62.9	15	60.0	24	64.9	0.697	13	61.9	26	63.4	0.907
Yes	23	37.1	10	40.0	13	35.1		8	38.1	15	36.6	
Serum ALP (U/L)[†]												
≤ 104	39	61.9	11	37.93	28	82.4	**<0.001**	5	21.7	34	85.0	**<0.001**
> 104	24	38.1	18	62.1	6	17.6		18	78.3	6	15.0	
Serum LDH (U/L): median (min-max)[†]	186 (46 - 712)		186 (46-712)		186 (90-395)		0.616	186 (46-712)		186 (90-576)		0.834
Follow-up (years): median (min-max)	3.4 (0.5-15.4)		5.6 (0.9-15.4)		2.0 (0.5-15.2)			6.1 (0.9-15.4)		2.0 (0.5-15.2)		
Deaths	29	33.3	25	56.8	4	9.3		23	57.5	6	12.8	

Table 8. *Comparison of the clinical characteristics of patients with a SETD2 value <0.425 and a SETD2 value ≥0.425 and with a H3K36Me3 value <0.284 and a H3K36Me3 value ≥0.284.*

The results of univariate analyses for multiple clinical and laboratory variables concerning OS were reported in table 10: age ≥65 years (HR 4.1 (1.9-9.0), P= 0.0002), hemoglobin < 10 g/dl, HR 5.52 (2.65-11.52), p<0.001, platelets < 100 × 10^9/L, HR 10.35 (4.91-21.75), P<0.001), markedly elevated serum tryptase (>200 µg/L, HR 3.6 (1.71–7.59), P = 0.001), palpable splenomegaly , HR 4 (1.87-8.57), P<0.001), high SETD2 value (≥0.425, HR 0.14 (0.05-0.40), P<0.001), and high value of H3K36Me3 (≥ 0.284, HR 0.20 (0.08-0.49).

Variables	HR	95% CI	P-value
Sex			
F	1		
M	0.70	0.34-1.47	0.356
Diagnosis		Diagnosis	
Others	1		
ISM	0.08	0.02-0.26	<0.001
Presence of Skin Lesions			
No	1		
Yes	0.20	0.08-0.50	0.001
Severe anaphylaxis reactions			
No	1		
Yes	0.17	0.05-0.56	0.004
Presence of Mediator Related Symphtoms			
No	1		
Yes	1.89	0.081-4.42	0.143
Osteopenia			
No	1		
Yes	0.55	0.18-1.69	0.299
Osteoporosis			
No	1		
Yes	2.63	0.86-8.06	0.089
Splenomegaly			
No	1		
Yes	4.00	1.87-8.57	<0.001
Hb value (g/dL)			
≥ 10	1		
< 10	5.52	2.65-11.52	<0.001
Platelet value (x 10^3)			
≥ 100	1		
< 100	10.35	4.91-21.75	<0.001
Serum Alkaline Phosphatase			
< 150	1		
≥ 150	2.22	0.86-5.73	0.101
Serum tryptase level (ug/L)			
< 200	1		
≥ 200	3.60	1.71-7.59	0.001
SETD2 level			
< 0.425	1		
≥ 0.425	0.14	0.05-0.40	<0.001
H3K36Me3 level			
< 0.284	1		

≥ 0.284	0.22	0.10-0.47	<0.001
Continuous variables			
Age	1.37	1.16-1.66	<0.001
Serum tryptase level	1.11	1.06-1.17	<0.001
Hemoglobin	0.58	0.48-0.70	<0.001
Platelets	0.43	0.29-0.67	<0.001
White blood cells	1.18	0.96-1.44	0.112
Eosinophils	1.51	1.09-2.08	0.012
Lactate	2.66	1.87-3.77	<0.001
Alkaline phosphatase	1.00	1.00-1.00	0.007
SETD2	0.06	0.01-0.25	<0.001
H3K36Me3	0.06	0.01-0.26	<0.001

Table 9. R*esults of univariate analyses for multiple clinical and laboratory variables (Cox model)*

The heat map reported in Figure 35 shows the tetrachoric correlation among the variables included in this study (all considered as binary) as well as the diagnostic category (ISM vs other class) defined by WHO criteria and the two categorized biomarkers, SETD2 ≥ 0.425 and H3K36Me3 ≥ 0.284.

Diagnosis of ISM is inversely correlated quite importantly with age (0: ≤65.1:> 65), triptase (0: ≤200.1:> 200), phosphatase (0: ≤150.1:> 150), platelets (0: ≥100, 1: <100), hemoglobin (0: ≥10, 1: <10), and splenomegaly (0: no, 1 : Yes). Patients with diagnosis of ISM are younger, have lower triptase, phosphatase, higher values for platelets and hemoglobin and have no splenomegaly. The same correlations are found considering a value of SETD2 ≥ 0.425 and H3K36Me3 ≥ 0.284 (even if with a slightly lower intensity). This is because the cut-off identified for SETD2 expression divides ISM patients fairly well from all others.

The presence of this strong correlation precludes the specification of a multivariable Cox model.

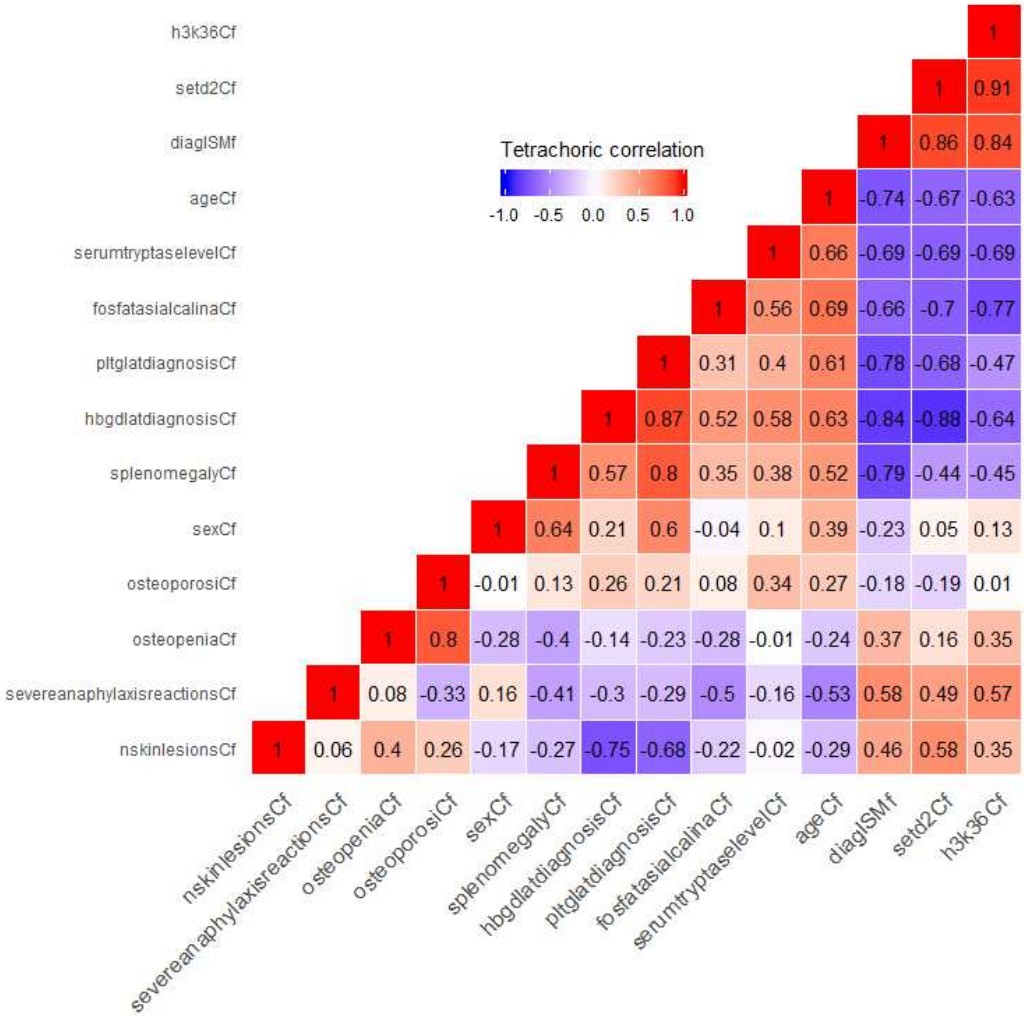

Figure 35. *The heat map displays correlations between two individual parameters. Colors were assigned on basis of the value of the correlation coefficient . For example, a strong positive correlation (the other variable has a tendency to increase, in red) was observed between platelet and hemoglobin while a strong negative correlation (the other variable has a tendency to decrease, in blue) was observed between platelets/hemoglobin and SETD2 elevated value, or ISM diagnosis. Cells that tend to white imply the almost absence of correlation.*

Due to the substantial correlation between clinical and laboratory factors and the diagnostic variable (ISM vs other) and of the very high correlation of the diagnostic variable and the two biomarkers, the multivariable analysis showed that only the diagnostic class defined by who

criteria predicted OS. This result was expected due to the correlation among the considered variables. The diagnostic classes per se contain/bring also the informative content of other clinical and laboratory parameters.

6. DISCUSSION

Systemic Mastocytosis (SM) is a myeloproliferative neoplasm that includes a heterogeneous spectrum of disease variants ranging from indolent forms having an almost normal life expectation, to aggressive forms with dismal outcome. The D816V activating KIT gene mutation, responsible for mast cell proliferation, represents a key diagnostic criterion and a pathogenetic hallmark of SM. However, the mutation is present in ≥90% of patients, therefore it cannot alone explain the phenotypical and clinical heterogeneity of the disease. Despite the (potentially) early acquisition of the KIT D816V mutation during ontogeny, the onset of clinical symptoms associated with advanced forms of SM often occurs at middle or late adulthood. Such observations suggest that continuous activation of the defective (i.e., D816V-mutated) SCF/KIT pathway in an early progenitor cell does not confer a malignant phenotype per se, whereas it might facilitate malignant transformation of the disease, either because of an increased susceptibility to acquire secondary “oncogenic” mutations and/or by cooperating with a particular (preexisting) genetic background. We here show for the first time that perturbation of the SETD2/H3K36Me3 axis can be detected in virtually all patients with advanced SM. We can speculate that SETD2 down modulation/absence and H3K36Me3 deficiency may cooperate with, and potentiate the effects of the constitutive activation of the KIT pathway to determine the phenotype of advanced SM.

The *SETD2* tumor suppressor, which encodes the only histone methyltransferase able to catalyze the trimethylation of histone H3 at Lysine 36, is implicated in the pathogenesis of several solid tumors (clear cell renal carcinoma [ccRCC] *in primis*) and of some acute leukemias via a variety of mechanisms including transcriptional and splicing defects, unfaithful homologous recombination repair and p53 inactivation[64,66] .

In ccRCCs, *SETD2* loss of function mainly results from large monoallelic deletions or CN-LOH at chromosome 3p followed by mutation of the remaining allele. In acute leukemias, it rather derives from biallelic missense or truncating mutations. In SM, inactivating (biallelic) mutations were found only in the index case. Anyway, reduced SETD2 protein expression to various extents was observed in all cases studied and, similarly to ccRCC, where lower SETD2 and H3K36Me3 levels as assessed by immunohistochemistry correlate with larger tumor burden, more advanced stage and worse prognosis[86], we found that very low or absent protein expression especially marked the cases with advanced SM. As expected, this was mirrored by similarly reduced, or totally abrogated, H3K36Me3.

We confirmed that SETD2 loss of function may play a pathogenetic role in SM. We observed that in SM, SETD2 loss of function correlates with increased DNA damage that might be responsible for the accumulation of additional molecular/cellular defects accounting for the phenotypic and clinical heterogeneity of the disease. Increased genetic instability may be result of the p53 checkpoint disruption as a consequence of SETD2 loss as well as the result of impaired double strand break recognition by the homologous recombination machinery as a consequence of H3K36 trimethylation deficiency.

Trying to delineate the mechanisms underlying SETD2 loss of function in SM, we uncovered a previously unreported non-genomic mechanism based on hyperubiquitination and enhanced

proteasome-mediated degradation. Intriguingly, inhibition of proteasome-mediated degradation by bortezomib rescued not only SETD2 expression but also H3K36Me trimethylation, indicating that this novel mechanism is reversible and that SETD2 loss of function in advSM is druggable. When tested in vitro in cell lines and primary patient cells, bortezomib was found to be strikingly effective (at subnanomolar concentrations) in inducing apoptosis and reducing clonogenic growth of neoplastic MCs. The mechanism through which proteasome inhibitors induce apoptosis in our *in vitro* and *ex vivo* models may involve an increase in levels of tumor suppressor SETD2, able to stabilize and activate p53 and a consequent increase in cell cycle regulators p27, p21 and gadd45a, as well as an increase in pro-apoptotic protein Bax. We further investigated the events upstream SETD2 hyperubiquitination in an attempt to find other druggable vulnerabilities, and identified two attractive targets: MDM2 and Aurora kinase A (AKA). The MDM2 oncogene is amplified and overexpressed in a number of human malignancies and encodes an E3 ubiquitin ligase known to be a negative regulator of the tumour suppressor p53. Based on the observation that SETD2 may interact with p53 in neoplastic MCs (similarly to what has been reported in ccRCCs)[85], we hypothesized that MDM2 may also target SETD2. Looking for the phosphorylation event capable to trigger SETD2 ubiquitination by MDM2, we focused our attention on AKA since it emerged from public databases of protein-protein interactions when we searched for SETD2-interacting kinases. AKA is a serine/threonine kinase that has been implicated in the regulation of mitosis and identified as a potential target in solid tumors and leukemias[87]. The AKA-targeting drug danusertib induces cell cycle arrest and apoptosis in various neoplastic cells. Here, we show for the first time that neoplastic MCs display overexpression and hyper-activation of AKA leading to an hyper-phosphorylation of SETD2 and a consequent hyper-ubiquitination by MDM2, driving SETD2 proteasomal degradation. Danusertib treatment rescued SETD2 expression and activity and

induced apoptosis in a dose-dependent manner and reduced clonogenic potential in neoplastic MCs. In contrast, MDM2 inhibition rescued SETD2 expression and activity but showed only cytostatic and not cytotoxic effects. Our findings open new therapeutic avenues in advSM. Cladribine, interferon, or the recently approved KIT inhibitor midostaurin are currently the main options for advanced SM patients, and hematopoietic stem cell transplant is also considered in younger patients. However, in many cases with advanced SM intensive therapy cannot be applied because of age or poor performance status. In addition, many patients relapse on therapy or have resistant disease to midostaurin. Thus, biomarkers of response to midostaurin, as well as other treatment options, are urgently needed. We found that by partially inhibiting AKA, midostaurin may increase SETD2 and H3K36 trimethylation levels. Our preliminary observations, worth testing in larger series of patients, indicate that SETD2 re-expression can be observed in patients who respond to midostaurin as early as after 3 months of treatment, whereas refractory patients do not show any significant increase in SETD2 levels. As far as alternative treatment options targeting the AKA/MDM2/proteasome axis, we focused on testing drugs (like bortezomib and danusertib) already approved or in advanced clinical development for other conditions, aware that repurposing of an existing drug may be much easier and faster than testing novel compounds starting from phase I trials, especially in a rare disease like SM.

In an initial cohort of SM patients (Leukemia, 2018) we had shown that MCL and ASM had significantly lower levels of SETD2 protein ($p<0.001$ and $p=0.002$, respectively) and H3K36Me3 ($p<0.001$ and $p =0.004$, respectively) as compared to ISM and SSM. The updated analysis carried out on an extended series, including a higher number of non-advanced forms, confirms those results. The statistical difference in levels ($p<0.001$) between each form is highly significant, and confirms the different clinical behavior of WHO subtypes (Figure 29). In particular, median SETD2

values were 0 (range, 0.00-0.76) in MCLs, 0 (range, 0.0-0.80) in ASMs, 0 (range, 0.00-1.00) in SM-AHN, 0.24 (range, 0.0-0.86) in SSMs, and 0.69 (range, 0.00-1.00) in ISMs. In the group of SM-AHN, SETD2 and H3K36Me3 values varied greatly. Nowadays the subset of SM-AHN is of particular interest, for their variable OS and for the detection of myeloid additional mutations in a large proportion of them[35,36]. Screening for additional 'myeloid' gene mutations (e.g., ASXL1, SRSF2, RUNX1, etc), performed on this group, showed some insights but they were not conclusive and no specific association of molecular alterations was identified[27,28]. In the future, further analysis of SETD2/H3K36 trimethylation levels, presence of specific additional myeloid mutations and outcome in a larger series of SM-AHN patients is warranted.

In order to evaluate the diagnostic accuracy of SETD2 in distinguishing between different clinical forms of SM, we tried to obtain the best ROC curve grouping the different subtypes. Indolent mastocytosis, characterized by the absence of any sign of organ infiltration by neoplastic MCs (absence of B-findings) were distiguished with great precision from all others (including the smoldering forms): a SETD2 value of 0.425 discriminated ISM from all other WHO subtypes with a sensitivity of 84.09% and a specificity of 86.36% (45 patients had a value <0.425, 43 patients ≥0.425). The area under the curve (AUC) was 0.87 (95% CI: 0.79-0.95). We also found that the H3K36Me3 value of 0.284 could discriminate quite well ISM from other subtypes. The impact of this observation is very important for the clinical practice, for example in the first approach to very symptomatic patients who can mimick an aggressive form for the presence of mediator-related symptoms, or to characterize the SM component in a case of SM-AHN. One of the major concerns about the clinical approach to SM-AHN is the choice of therapy, that depends on understanding which of the two pathologies is the most symptomatic for the patient. In this regard, we believe

that the evaluation of SETD2/H3K36Me3 status has the potential to become an important prognostic factor when assessed in larger series of SM-AHN.

On the basis of univariate analysis, we demonstrated that low SETD2 and H3K36Me3 values are strong adverse prognostic parameters for OS (Figure 33 and 34) in patient with SM. The close correspondence between this biological parameter and the clinical factors that are recognized as independent factors in the main survival scores recently validated in large series of patients (such as Hb level, platelet value and splenomegaly), makes it very intriguing. The presence of additional myeloid mutations has a prognostic value in the setting of AdvSMs, and recent data suggest that they might also influence the risk of progression of ISM, but the scenario is still complex and a possible role for SETD2/H3K36 trimethylation deficiency will have to be assessed.

A last consideration concerns the rare cases of MCL, that is considered the most aggressive subtype of SM. The KIT mutational status of a large cohort of patients with AdvSM was recently revised, and it has to be emphasized that 5-7% of patients tested negative for mutation of the KIT gene, in particular among MCL cases (8/31)[27]. In the same study, more than one third of patients who were wild-type for KIT mutation (37%) did not have any other detectable mutation, and this underlines the importance of the evaluation of SETD2 expression as a prognostic factor. MCL accounted for 17% of patients in our cohort, and, as reported in literature, they were largely negative for the KIT D16V mutation (4/15 tested negative when a highly sensitive digital PCR assay was used).

In conclusion, we show that non-genomic loss-of-function of SETD2 is a recurrent event in advanced SM. SETD2 and H3K36Me3 deficiency might cooperate with the ligand-independent activation of the KIT pathway to enhance leukemic transformation and progression and determine the phenotype of ASM and MCL. Targeting SETD2 down-modulation itself (with bortezomib or

second-generation proteasome inhibitors) and/or SETD2/KIT cooperation are promising therapeutic strategies to improve the outcome of AdvSM. SETD2/H3K36 trimethylation deficiency seems to be a prognostic factor predicting for poor OS and has the potential to be a biomarker of response to midostaurin. Additional studies are warranted to further explore its pathogenetic and clinical value.

7. BIBLIOGRAPHY

1. Metcalfe DD. Mast cells and mastocytosis. Blood. 2008;112(4):946-956.
2. Carter MC, Metcalfe DD, Komarow HD. Mastocytosis. Allergy Clin North Am. 2014 Feb;34(1):181-96.
3. Horny HP, Metcalfe DD, Bennett JM, et al. Mastocytosis. In: Swerdlow SH, Campo E, Harris NL, et al, eds. WHO Classification of Tumors of Hematopoietic and Lymphoid Tissues. 4th ed. Lyon: International Agency for Research and Cancer (IARC); 2008:54-63
4. Lim KH, Tefferi A, Lasho TL, et al. Systemic mastocytosis in 342 consecutive adults: survival studies and prognostic factors. Blood. 2009; 113(23):5727-5736.
5. Valent P, Sperr WR, Akin C. How I treat patients with advanced systemic mastocytosis. Blood. 2010;116(26):5812-5817.
6. Pardanani A, Lim KH, Lasho TL, Finke C, McClure RF, Li CY, Tefferi A. Prognostically relevant breakdown of 123 patients with systemic mastocytosis associated with other myeloid malignancies. Blood. 2009;114(18): 3769-3772.
7. Valent P, Horny HP, Escribano L, Longley BJ, Li CY, Schwartz LB, et al. Diagnostic criteria and classification of mastocytosis: a consensus proposal. Leuk Res 2001;25:603–25.
8. Valent P, Horny H-P, Li CY, Longley JB, Metcalfe DD, Parwaresch RM, et al. Mastocytosis (mast cell disease). In: World Health Organization (WHO) Classification of Tumours. Pathology & Genetics. Tumours of Haematopoietic and Lymphoid Tissues. Eds:Jaffe ES, Harris NL, Stein H, Vardiman JW. IARC PressLyon, France, 2001, pp291–302.

9. Brockow K Epidemiology, prognosis, and risk factors in mastocytosis. Immunol Allergy Clin North Am. 2014 May;34(2):283-95.
10. Kettelhut BV, Metcalfe DD. Pediatric mastocytosis. J Invest Dermatol 1991;96: 15S–8S.
11. Van Doormaal JJ, Arends S, Brunekreeft KL, et al. Prevalence of indolent systemic mastocytosis in a Dutch region. J Allergy Clin Immunol 2013;131: 1429–31
12. Lennert K, Parwaresch MR: Mast cells and mast cell neoplasia: a review. Histopathology 1979; 3: 349–65
13. Horny HP, Akin C, Metcalfe DD, Escribano L, Bennett JM, Valent P, et al. Mastocytosis (mast cell disease). In: Eds:Swerdlow SH, Campo E, Harris NL, Jaffe ES, Pileri SA, Stein H, et al. editors.World Health Organization (WHO) Classification of Tumours. Pathology & Genetics. Tumours of Haematopoietic and Lymphoid Tissues. Lyon, France:IARC Press; 2008. p.54–63.
14. Valent P, Akin C, Metcalfe DD: Mastocytosis: 2016 updated WHO classification and novel emerging treatment concepts. Blood 129:1420-1427, 2017
15. Hartmann K, Escribano L, Grattan C, Brockow K, Carter MC, AlvarezTwose I, et al. Cutaneous manifestations in patients with mastocytosis: Consensus report of the European Competence Network on Mastocytosis; the American Academy of Allergy, Asthma & Immunology; and the European Academy of Allergology and Clinical Immunology. J Allergy Clin Immunol 2016;137:35–45
16. Valent P, Akin C, Escribano L, Fodinger M, Hartmann K, Brockow K, et al. Standards and standardization in mastocytosis: consensus statements on diagnostics, treatment recommendations and response criteria. Eur J Clin Invest 2007;37:435–53.

17. Pardanani A. How I treat patients with indolent and smoldering mastocytosis (rare conditions but difficult to manage). Blood. 2013;121(16): 3085-3094.
18. Zanotti R, Bonadonna P, Bonifacio M, et al. Isolated bone marrow mastocytosis: an underestimated subvariant of indolent systemic mastocytosis. Haematologica 2011;96:482-484.
19. Escribano L, Alvarez-Twose I, Garcia-Montero A, et al. Indolent systemic mastocytosis without skin involvement vs. isolated bone marrow mastocytosis. Haematologica 2011;96:e26; author reply e28.
20. Pardanani A. Systemic mastocytosis in adults: 2013 update on diagnosis, risk stratification, and management. American journal of hematology 2013;88:612-624.
21. Valent P, Akin C, Arock M, et al. Definitions, criteria and global classification of mast cell disorders with special reference to mast cell activation syndromes: a consensus proposal. Int Arch Allergy Immunol 2012;157:215–25.
22. Lim KH, Tefferi A, Lasho TL, Finke C, Patnaik M, Butterfield JH et al. Systemic mastocytosis in 342 consecutive adults: survival studies and prognostic factors. Blood. 2009 Jun 4;113(23):5727-36.
23. Escribano L, Alvarez-Twose I, Sanchez-Munoz L, et al. Prognosis in adult indolent systemic mastocytosis: a long-term study of the Spanish Network on Mastocytosis in a series of 145 patients. J Allergy Clin Immunol 2009;124:514–21.
24. Munoz-González JI, Álvarez-Twose I, Jara-Acevedo M, Henriques A, Viñas E, Prieto C et al. Frequency and prognostic impact of KIT and other genetic variants in indolent systemic mastocytosis. Blood. 2019 Aug 1;134(5):456-468.

25. Jawhar M, Schwaab J, Hausmann D, et al. Splenomegaly, elevated alkaline phosphatase and mutations in the SRSF2/ASXL1/RUNX1 gene panel are strong adverse prognostic markers in patients with sistemic mastocytosis. Leukemia. 2016;30(12):2342-2350.
26. Pardanani A, Lasho T, Elala Y, et al. Next-generation sequencing in systemic mastocytosis: derivation of a mutation-augmented clinical prognostic model for survival. Am J Hematol. 2016;91(9):888-893.
27. Jawhar M, Schwaab J, Álvarez-Twose I, Shoumariyeh K, Naumann N, Lübke J,et al. MARS: Mutation-Adjusted Risk Score for Advanced Systemic Mastocytosis. J Clin Oncol. 2019 Sep 11:JCO1900640.
28. Pardanani A, Shah S, Mannelli F, Elala YC, Guglielmelli P, Lasho TL, et al. Mayo alliance prognostic system for mastocytosis: clinical and hybrid clinical-molecular models. Blood Adv. 2018 Nov 13;2(21):2964-2972.
29. Pardanani A, Lasho T, Elala Y, et al. Next-generation sequencing in systemic mastocytosis: derivation of a mutation-augmented clinical prognostic model for survival. Am J Hematol. 2016;91(9):888-893.
30. Arber DA, Orazi A, Hasserjian R, et al: The 2016 revision to the World Health Organization classification of myeloid neoplasms and acute leukemia. Blood 127: 2391-2405, 2016
31. Pardanani A: Systemic mastocytosis in adults: 2019 update on diagnosis, risk stratification and management. Am J Hematol 94:363-377, 2019
32. Valent P, Oude Elberink JNG, Gorska A, et al: The data registry of the European Competence Network on Mastocytosis (ECNM): Set up, projects, and perspectives. J Allergy Clin Immunol Pract 7:81-87, 2019

33. Jawhar M, Schwaab J, Meggendorfer M, et al: The clinical and molecular diversity of mast cell Leukemia with or without associated hematologic neoplasm. Haematologica 102:1035-1043, 2017

34. Valent P, Sperr WR, Akin C. How I treat patients with advanced systemic mastocytosis. Blood. 2010 Dec 23;116(26):5812-7.

35. Wang SA, Hutchinson L, Tang G, et al. Systemic mastocytosis with associated clonal hematological non-mast cell lineage disease: clinical significance and comparison of chomosomal abnormalities in SM and AHNMD components. Am J Hematol. 2013;88(3):219-224.

36. Jawhar M, Schwaab J, Schnittger S, et al: Molecular profiling of myeloid progenitor cells in multi-mutated advanced systemic mastocytosis identifies KIT D816V as a distinct and late event. Leukemia 29:1115-1122, 2015

37. Sotlar K, Colak S, Bache A, et al: Variable presence of KITD816V in clonal haematological non-mast cell lineage diseases associated with systemicmastocytosis (SM-AHNMD). J Pathol 220:586-595, 2010

38. Budnik J, Milano MT . A registry-based analysis of survival outcomes in mast cell leukemia. Leuk Res. 2019 Mar;78:24-28.

39. Valent P, Sotlar K, Sperr WR, Reiter A, Arock M, Horny HP. Chronic mast cell leukemia: a novel leukemia-variant with distinct morphological and clinical features. Leuk Res. 2015 Jan;39(1):1-5.

40. Ustun C, Arock M, Kluin-Nelemans HC, Reiter A, Sperr WR, George T, et al. Advanced systemic mastocytosis: from molecular and genetic progress to clinical practice. Haematologica. 2016 Oct;101(10):1133-1143.

41. Valent P, Akin C, Hartmann K, George TI, Sotlar K, Peter B, et al Midostaurin: a magic bullet that blocks mast cell expansion and activation. Ann Oncol. 2017 Oct 1;28(10):2367-2376.

42. Ustun C, Gotlib J, Popat U, Artz A, Litzow M, Reiter A, et al. Consensus Opinion on Allogeneic Hematopoietic Cell Transplantation in Advanced Systemic Mastocytosis. Biol Blood Marrow Transplant. 2016 Aug;22(8):1348-1356.

43. Gotlib J, Kluin-Nelemans HC, George TI, Akin C, Sotlar K, Hermine O, et al. Efficacy and Safety of Midostaurin in Advanced Systemic Mastocytosis. N Engl J Med. 2016 Jun 30;374(26):2530-41

44. Niedoszytko M, Oude Elberink JN, Bruinenberg M, et al. Gene expression profile, pathways, and transcriptional system regulation in indolent systemic mastocytosis. Allergy. 2011 Feb;66(2):229-37.

45. Garcia-Montero AC, Jara-Acevedo M, Teodosio C, et al. KIT mutation in mast cells and other bone marrow hematopoietic cell lineages in systemic mast cell disorders: a prospective study of the Spanish Network on Mastocytosis (REMA) in a series of 113 patients. Blood. 2006 Oct 1;108(7):2366-72.

46. Arock M, Sotlar K, Akin C, Broesby-Olsen S, Hoermann G, Escribano L, et al. KIT mutation analysis in mast cell neoplasms: recommendations of the European Competence Network on Mastocytosis. Leukemia 2015;29:1223–32

47. Feger F, Ribadeau-Dumas A, Leriche L, Valent P,Arock M. Kit and c-kit mutations in mastocytosis:a short overview with special reference to novel molecular and diagnostic concepts. *Int Arch Allergy Immunol.* 2002;127(2):110-114.

48. Miettinen M, Lasota J. KIT (CD117): A review on expression in normal and neoplastic tissues, and mutations and their clinicopathologic correlation. Appl Immunohistochem Mol Morphol 2005;13:205–220.

49. Nolen B, Taylor S, Ghosh G (2004) Regulation of protein kinases; controlling activity through activation segment conformation. Mol Cell 15: 661–675.

50. Longley BJ, Reguera MJ, Ma Y (2001) Classes of c-KIT activating mutations: proposed mechanisms of action and implications for disease classification and therapy. Leuk Res 25: 571–576.

51. Laine E, Chauvot de Beauche I, Perahia D, Auclair C, Tchertanov L (2011) Mutation D816V Alters the Internal Structure and Dynamics of c-KIT Receptor Cytoplasmic Region: Implications for Dimerization and Activation Mechanisms

52. Pardanani A. Systemic mastocytosis in adults: 2011 update on diagnosis, risk stratification, and management. Am J Hematol. 2011 Apr;86(4):362-71

53. Schwaab J, Schnittger S, Sotlar K, Walz C, Fabarius A, Pfirrmann M et al Comprehensive mutational profiling in advanced systemic mastocytosis. Blood. 2013 Oct 3;122(14):2460-6.

54. Wilson TM, Maric I, Simakova O, et al. Clonal analysis of NRAS activating mutations in KIT-D816V systemic mastocytosis. Haematologica. 2011;96(3): 459-463.

55. Jawhar M, Schwaab J, Schnittger S, et al. Additional mutations in SRSF2, ASXL1 and/or RUNX1 identify a high-risk group of patients with KIT D816V(1) advanced systemic mastocytosis. Leukemia. 2016;30(1):136-143

56. Cronin M, Ross JS. Comprehensive next-generation cancer genome sequencing in the era of targeted therapy and personalized oncology. Biomark Med. 2011 Jun;5(3):293-305.

57. Edmunds JW, Mahadevan LC, Clayton AL. Dynamic histone H3 methylation during gene induction: HYPB/Setd2 mediates all H3K36 trimethylation. EMBO J 2008;27(2):406-20.

58. Wagner EJ, Carpenter PB. Understanding the language of Lys36 methylation at histone H3. Nat Rev Mol Cell Biol 2012;13(2):115-26.

59. Kizer KO, Phatnani HP, Shibata Y, Hall H, Greenleaf AL, Strahl BD. A novel domain in Set2 mediates RNA polymerase II interaction and couples histone H3 K36 methylation with transcript elongation. Mol Cell Biol 2005;25(8):3305-16.

60. Yuan W, Xie J, Long C, Erdjument-Bromage H, Ding X, Zheng Y, et al. Heterogeneous nuclear ribonucleoprotein L Is a subunit of human KMT3a/Set2 complex required for H3 Lys-36 trimethylation activity in vivo. J Biol Chem 2009;284(23):15701-7.

61. Pfister SX, Ahrabi S, Zalmas LP, Sarkar S, Aymard F, Bachrati CZ, et al. SETD2-dependent histone H3K36 trimethylation is required for homologous recombination repair and genome stability. Cell Rep 2014;7(6):2006-18.

62. Carvalho S, Vitor AC, Sridhara SC, Martins FB, Raposo AC, Desterro JM, et al. SETD2 is required for DNA double-strand break repair and activation of the p53-mediated checkpoint. Elife 2014;3:e02482.

63. Xie P, Tian C, An L, Nie J, Lu K, Xing G, et al. Histone methyltransferase protein SETD2 interacts with p53 and selectively regulates its downstream genes. Cell Signal 2008;20(9):1671-8.

64. Dalgliesh GL, Furge K, Greenman C, Chen L, Bignell G, Butler A et al. Systematic sequencing of renal carcinoma reveals inactivation of histone modifying genes. Nature 2010; 21: 360–363.

65. Li J, Duns G, Westers H, Sijmons R, van den Berg A, Kok K. SETD2: an epigenetic modifier with tumor suppressor functionality. Oncotarget 2016; 7: 50719–50734.

66. Zhu X, He F, Zeng H, Ling S, Chen A, Wang Y et al. Identification of functional cooperative mutations of SETD2 in human acute leukemia. Nat Genet 2014; 46: 287–293.

67. Mar BG, Bullinger LB, McLean KM, Grauman PV, Harris MH, Stevenson K et al. Mutations in epigenetic regulators including SETD2 are gained during relapse in paediatric acute lymphoblastic leukaemia. Nat Commun 2014; 5: 3469.

68. Fontebasso AM, Schwartzentruber J, Khuong-Quang DA, Liu XY, Sturm D, Korshunov A et al. Mutations in SETD2 and genes affecting histone H3K36 methylation target hemispheric high-grade gliomas. Acta Neuropathol 2013; 125: 659–669

69. Ho TH, Park IY, Zhao H, Tong P, Champion M, Yan H, Monzon F, Hoang A, Tamboli P, Parker AS, Joseph RW, Qiao W, Dykema K, et al. High-resolution profiling of histone H3 lysine 36 trimethylation in metastatic renal cell carcinoma. Oncogene. 2015; 35: 1565-74.

70. Gerlinger M, Rowan AJ, Horswell S, Larkin J, Endesfelder D, Gronroos E, Martinez P, Matthews N, Stewart A, Tarpey P. Intratumor heterogeneity and branched evolution revealed by multiregion sequencing. N Engl J Med. 2012; 366: 883-92.

71. Baylin SB, Jones PA. A decade of exploring the cancer epigenome—biological and translational implications. Nat Rev Cancer 2011; 11: 726–734.

72. Gleixner KV, Mayerhofer M, Aichberger KJ, Derdak S, Sonneck K, Böhm A, et al. PKC412 inhibits in vitro growth of neoplastic human mast cells expressing the D816V-mutated variant of KIT: comparison with AMN107, imatinib, and cladribine (2CdA) and evaluation of cooperative drug effects. Blood. 2006; 107:752–759.

73. Akin C, Brockow K, D'Ambrosio C, Kirshenbaum AS, Ma Y, Longley BJ, et al. Effects of tyrosine kinase inhibitor STI571 on human mast cells bearing wild-type or mutated c-kit. Exp Hematol. 2003; 31:686–692.

74. Butterfield JH, Weiler D, Dewald G, Gleich GJ. Establishment of an immature mast cell line from a patient with mast cell leukemia. Leuk Res. 1988; 12:345–355.

75. Saleh R , Wedeh G, Herrmann H , Bibi S et al A new human mast cell line expressing a functional IgE receptor converts to tumorigenic growth by KIT D816V transfection Blood (2014) 124 (1): 111-120.

76. Martinelli G, Mancini M, De Benedittis C, Rondoni M, Papayannidis C, Manfrini SETD2 and histone H3 lysine 36 methylation deficiency in advanced systemic mastocytosis. Leukemia. 2018 Jan;32(1):139-148.

77. Duns G, van den Berg E, van Duivenbode I, et al. Histone methyltransferase gene SETD2 is a novel tumor suppressor gene in clear cell renal cell carcinoma. Cancer Res 2010;70:4287-91.

78. Hesson LB, Cooper WN, Latif F. Evaluation of the 3p21.3 tumour-suppressor gene cluster. Oncogene 2007; 26: 7283–7301.

79. Genovese G, Kahler AK, Handsaker RE, Lindberg J, Rose SA, Bakhoum SF et al. Clonal hematopoiesis and blood-cancer risk inferred from blood DNA sequence. N Engl J Med 2014; 371: 2477–2487.

80. Jaiswal S, Fontanillas P, Flannick J, Manning A, Grauman PV, Mar BG et al. Agerelated clonal hematopoiesis associated with adverse outcomes. N Engl J Med 2014; 371: 2488–2498.

81. Xie M, Lu C, Wang J, McLellan MD, Johnson KJ, Wendl MC et al. Age-related mutations associated with clonal hematopoietic expansion and malignancies. Nat Med 2014; 20: 1472–1478.

82. Wang W, Qin JJ, Voruganti S, Wang MH, Sharma H, Patil S, Zhou J, Wang H, Mukhopadhyay D, Buolamwini JK, Zhang R. Identification of a new class of MDM2 inhibitor that inhibits growth of orthotopic pancreatic tumors in mice. Gastroenterology. 2014 Oct;147(4):893-902.e2.

83. Levine AJ. p53, the cellular gatekeeper for growth and division. Cell. 1997 Feb 7;88(3):323-31.

84. Vogelstein B, Lane D, Levine AJ. Surfing the p53 network. Nature. 2000 Nov 16;408(6810):307-10.

85. Moll UM, Petrenko O. The MDM2-p53 interaction. Mol Cancer Res. 2003 Dec;1(14):1001-8

86. Liu W, Fu Q, An H, Chang Y, Zhang W, Zhu Y, Xu L, Xu J. Decreased Expression of SETD2 Predicts Unfavorable Prognosis in Patients With Nonmetastatic Clear-Cell Renal Cell Carcinoma. Medicine (Baltimore). 2015 Nov;94(45):e2004.

87. Warner SL, Bearss DJ, Han H. Targeting Aurora-2 kinase in cancer. Mol Cancer Ther 2003;2:589–95.